AEROSOL AND OZONE SENSITIVITY ANALYSIS WITH THE COMMUNITY MULTI-SCALE AIR QUALITY (CMAQ) MODEL FOR THE PACIFIC NORTHWEST

By

JACK CHI-MOU CHEN

A thesis submitted in partial fulfillment of
the requirements for the degree of

MASTER OF SCIENCE IN ENVIRONMENTAL ENGINEERING

WASHINGTON STATE UNIVERSITY
Department of Civil and Environmental Engineering

DECEMBER 2002

To the Faculty of Washington State University:

The members of the Committee appointed to examine the thesis of JACK CHI-MOU CHEN find it satisfactory and recommend that it be accepted.

_____
Chair

_____

_____

ACKNOWLEDGMENTS

I would like to acknowledge all of those who have aided me throughout the time I have spent here at Washington State University. I could not have accomplished any of this without their guidance and assistance. I would especially like to thank my advisor, Dr Brian Lamb, for his encouragements, patience and trusts. He showed me the door to the fascinating world of air quality models and gave me the chance to 'play' with several high-end computer systems. I would also like to thank Dr Hal Westberg and Dr Candis Claiborn for being on my Master's Committee. Their guidance and direction was beneficial to my education here at WSU.

Through the project, I get the chance to work with a large group of people each with passions to improve the air quality of this beautiful Pacific Northwest. I like to thank Sally Otterson, Clint Bowman, Cristiana Figueroa, and Mike Boyer of Washington Department of Ecology for helping with emissions inventory in this and other projects. I also thank Rob Wilson of EPA-R10 for hosting the monthly Northwest Regional Modeling Center (NWRMC) conference call that put knowledgeable people together to collaborate on various projects. Thank also goes to all the participants of the NWRMC for their patience and interest in this study.

I appreciate the assistance I received from the CE department front office. Thank you, Tom, Maureen, Kathy, and Vicki.

I like to express my appreciation to my fellow graduate students and friends. They are the ones that made my student life a fun and enjoyable one. Thank to the "Goddesses" of LAR: Susan, Shelley and Tara, for making Dana 334 the homiest office in WSU, and welcoming this "Lucky Guy" to be a part of your Lair. I will always remember the fun, stressful, and dreadful times we have spent together. I also like to thank Guangfeng Jiang and Joe Vaughan for helping me in various computing and modeling problems.

Last but not least, I thank my wife, Maggie, for her love, encouragement and determination to study with me in this little town called Pullman.

AEROSOL AND OZONE SENSITIVITY ANALYSIS WITH THE COMMUNITY MULTI-SCALE AIR QUALITY (CMAQ) MODEL FOR THE PACIFIC NORTHWEST

Abstract

by Jack Chi-Mou Chen, M.S.
Washington State University
December 2002

Chair: Brian K. Lamb

The CMAQ model was applied to investigate the sensitivity of PM2.5 and ozone to changes in precursor emissions in the Pacific Northwest.

The simulation results showed that different regions responded differently to changes in emissions species. For PM2.5 changes with precursor emissions, the responses were explained by the region's total ammonia to sulfate molar ratio. Enumclaw, WA, had a high ratio, its PM2.5 concentrations were highly sensitive to NOx and NH3 emissions, but insensitive to SO2 emissions change. In areas that had low ratios, such as, Carus, OR and the Columbia River Gorge, OR, PM2.5 concentrations were highly sensitive to changes in SO2 emissions, but insensitive to NOx and NH3 changes.

The results also demonstrated the coupled chemistry between aerosol and ozone in the atmosphere. High ozone concentrations led to higher atmospheric oxidant production, which in turn, increased aerosol formation. These interactions led to decreases in PM2.5 formation with increased in NOx emission, as ozone was titrated by the increased NO emissions.

In terms of ozone sensitivity towards VOC and NOx emissions changes, ozone changed linearly in all areas with combined NOx and VOC (NOx&VOC), anthropogenic VOCs and biogenic VOCs. The sensitivity was stronger in urban regions than rural sites. However, when NOx emission was changed alone, ozone changed non-linearly in urban regions, but linearly in rural sites. The degrees of ozone sensitivity towards NOx or VOC emissions were correlated

with base-case H_2O_2/HNO_3 concentration ratio. This ratio appears to be a good indicator for regions that were sensitive to either NOx or VOC emissions changes, where a large ratio suggests a higher degree of ozone response to changes in precursor emissions.

TABLE OF CONTENTS

LIST OF TABLES

LIST OF FIGURES

CHAPTER 2

ATTRIBUTION

This dissertation consists of three chapters. Chapter 1 is an overview of the research and a literature review. Chapters 2 contains an independent manuscript, and Chapter 3 contains a summary and conclusion of this research. While I am the primary author of the entire dissertation, I received much help from my advisor and colleagues. In Chapter 2, Dr. Brian Lamb assisted in the development of the manuscript and provided editorial comments, and Dr. Susan O'Neill provided the initial, parent-domain CMAQ simulation. I also received help from the Washington Department of Ecology for providing the base-case anthropogenic emission inventory.

CHAPTER 1
INTRODUCTION

1.1 Research Overview

Ozone and fine particulate matter (PM) in the troposphere are atmospheric pollutants. Ozone is a secondary pollutant that forms from chemical reactions between nitrogen oxides (NO + NO2 = NOx) and volatile organic compounds (VOC) in the presence of sunlight. It is a strong oxidant that directly damages human, animal and plant tissues (Wark et al., 1998). Particulate matter or aerosols are emitted directly as primary pollutants or formed from precursor gases as secondary pollutants. Aerosols in the atmosphere deteriorate visibility and have various adverse effects on human health, including lung and heart diseases. In protecting people's health and welfare, the US Environmental Protection Agency (EPA) established the National Ambient Air Quality Standards (NAAQS) for six criteria pollutants. Both ozone and particulate matter with aerodynamic diameter less than 10μm (PM10) are regulated (Table 1a). In 1997 EPA promulgated more stringent levels for ozone and PM10, and added PM2.5 to the criteria pollutant list. Table 1b lists these new standards. In order to attain and maintain clean air through the implementation of cost effective control strategies, it is important to understand the formation and transport of these secondary pollutants and their response to changes in precursor emissions.

Table 1a-b: National Ambient Air Quality Standards for six criteria pollutants (NAAQS).

1a: National Ambient Air Quality Standards (NAAQS) for six criteria pollutants.

Pollutant	Concentration	Units	Averaging Period
Ozone	120	ppbv	1-hour
SO2	30	ppbv	1-year
NO2	50	ppbv	1-year
PM10	260	$\mu g/m^3$	24-hour
CO	9	ppmv	8-hour
Lead	1.5	$\mu g/m^3$	Quarterly

1b: Revised National Ambient Air Quality Standards (NAAQS) Promulgated in 1997

Pollutant	Concentration	Units	Averaging Period
Ozone	80	ppbv	8-hour
PM10	50	$\mu g/m^3$	1-year
PM10	150	$\mu g/m^3$	24-hour
PM2.5	15	$\mu g/m^3$	1-year
PM2.5	65	$\mu g/m^3$	24-hour

In this research, the Community Multi-scale Air Quality (CMAQ) model (U.S. EPA, 1999) is implemented to study the sensitivity of ozone and PM2.5 to changes in anthropogenic and biogenic emissions over the Pacific Northwest region. CMAQ represents the latest state-of-the-science in regional air quality models (Byun and Ching, 1999; Dennis et al., 1996; Malm and Day, 2000). It was developed by EPA as a part of a modeling system aimed at a one-world modeling approach where a single model could be used to treat all of the various types of air quality issues that occur on urban to regional scales. The model simulates chemical, photochemical and physical processes that are important for understanding atmospheric aerosol and trace gas transformations and distributions.

This research was a continuation to the Northwest Regional Modeling Center (NWRMC) CMAQ demonstration project funded by EPA. In the demonstration project, CMAQ was applied for the first time to the Pacific Northwest region to simulate ozone and particulate matter formation (O'Neill et al., 2002). In the work described herein, the CMAQ model was utilized to investigate the changes in ozone and aerosol formation due to changes in anthropogenic and biogenic emissions.

A number of recent air quality studies using numerical models have been performed over the Pacific Northwest region. Barna et al. (2000), Jiang et al. (2001) and O'Neill and Lamb (2002) used the CALGRID photochemical grid model to study ozone formation chemistry. In the work by O'Neill and Lamb (2002), results from CALGRID were compared with results from CMAQ applied to the I-5 corridor stretching from Vancouver, BC through Puget Sound to Portland, OR. In all of these simulations, the focus was only on gas-phase ozone chemistry. Both Barna et al. (2001) and Jiang et al. (2001) performed ozone sensitivity analyses using the CALGRID model to study the response of ozone predictions to changes in anthropogenic and biogenic emissions. However in their studies, they did not take aerosol chemistry into account. It is important to take aerosol formation chemistry into account when performing ozone sensitivity analyses since standard ozone control strategies can have unexpected results on the

secondary formation of PM (Meng et al., 1997). This research presents the first application of both aerosol and ozone sensitivity analysis for the Pacific Northwest. The objective of this work is to obtain better insight into the relationship between emissions of gaseous pollutants such as NOx, SO2, NH3 and VOCs, and the corresponding secondary pollutant concentrations of ozone and PM in the Pacific Northwest.

In the remainder of this chapter, recent results from the literature are reviewed to place this research in perspective, and details of the CMAQ modeling system are described. In Chapter 2, a manuscript describes the modeling approach and presents the sensitivity analysis results. The analyses are divided into two main parts. The first part covers the sensitivity of PM2.5 concentrations to changes in precursor emissions, while the second half of the paper is focused on the sensitivity of ozone concentrations for different locations in the model domain due to changes in precursor emissions. The final chapter provides a summary of results and recommendations for future work.

1.2 Literature Review

An air quality model is the collection of mathematical relationships and computer algorithms that calculates the behavior of various pollutants over time and space. It is based on theoretical approaches describing our general understanding of the chemistry, photochemistry and physical transport of pollutants in the atmosphere. In recent years, air quality models have increased significantly in complexities and capabilities in line with improvements in our understanding, the need to incorporate aerosol dynamics, and the rapid growth of computer technology. Some of the earlier models were based on a Lagrangian framework using well-mixed air masses carried along specific trajectories. These models, although computationally inexpensive, can have significantly large errors in predicting the transport and pollutant concentrations over long simulation scenarios (Russell and Dennis, 2000). Nowadays most of the photochemical models are three-dimensional grid models based on the Eulerian framework. Although these models are computationally expensive to operate, they are the most powerful

with least-restrictive assumptions. These models are well suited to simulate chemical transformation and transport processes over a larger area and longer timescale (Russell and Dennis, 2000; Seigneur, 2001; Seigneur et al., 1999). This review will concentrate on the Eulerian grid models that treat both gas-phase chemistry and organic and inorganic aerosol production.

Recently Russell and Dennis (2000) published a comprehensive review on Eulerian air quality models for troposphere ozone. Many of these models are now equipped with aerosol modules that solve secondary aerosol formation and aerosol dynamics. Table 2 lists some of these air quality models that have capability of modeling both gas-phase chemistry and aerosol formation. The table lists the name and the types of modules used to treat gas-phase chemistry, organic and inorganic aerosol formations.

Among the models in Table 2, CIT, SAQM-AERO and UAM-AERO are considered as urban-scale since they have upper limits on model vertical height of up to the planetary boundary layer or the lower free troposphere. For the rest of the models, DAQM, GATOR, Models-3/CMAQ, and EURAD are considered as urban to regional scale models, since they can simulate transports from the ground surface up to at least 5km, including the free troposphere. Transport at the higher elevation is more important for regional scale models that cover a larger area.

Although the models have significant differences, each model shares similarities in the types of processes treated. These include horizontal and vertical advection and turbulent diffusion, gas phase chemical transformations, secondary aerosol formation from gas phase precursors, aerosol dynamics including aerosol growth mechanisms, and deposition of gas and aerosol pollutants. In some cases, treatment of aqueous phase cloud chemistry is also included. In the following, details concerning the gas phase chemistry and aerosol formation and growth are described.

Table 2: Eulerian photochemical air quality models that have both gas-phase chemistry and aerosol modules.

AQM Model	**Gas-Phase Chemistry**	**Inorganic Aerosol**	**Organic Aerosol**	**Spatial Scale**	**References**
CIT[1]	CACM	SCAPE2	Absorption and Dissolution	Urban	[*Griffin et al.*, 2002b] [*Pun et al.*, 2002] [*Griffin et al.*, 2002a]
DAQM[2]	RADM2	MARS	Vapor Saturation	Urban to Regional	[*Middleton*, 1997]
GATOR[3]	CB-IV	EQUISOLV	Vapor Saturation	Urban to Regional	[*Jacobson et al.*, 1996] [*Jacobson*, 1997]
Models-3/CMAQ[4]	CB-IV	MARS	Vapor Saturation	Urban to Regional	[*Byun and Chang*, 1999] [Saxena, Hudischewskyj, et al. 1986]
Models-3/CMAQ	RADM2	MARS	Vapor Saturation	Urban to Regional	[*Byun and Chang*, 1999]
SAQM-AERO[5]	CB-IV	SEQUILIB	Vapor Saturation	Urban	[*Dabdub et al.*, 1998] [*Pai et al.*, 2000]
UAM-AERO[6]	SAPRAC-97	SEQUILIB	Vapor Saturation	Urban	[*Wexler et al.*, 1994] [*Lurmann et al.*, 1997]
UAM-AERO	SAPRAC-97	ISORROPIA	Vapor Saturation	Urban	[*Nenes et al.*, 1999]
EURAD[7]	RADM2	MARS	Absorption	Urban to Regional	[*Ackermann et al.*, 1998] [*Schell et al.*, 2001]

[1] California Institute of Technology
[2] Denver Air Quality Model
[3] Gas Aerosol, Transport, and Radiation air quality model
[4] Community Multi-scale Air Quality System
[5] SARMAP Air Quality Model with Aerosol module
[6] Urban Airshed Model-IV with Aerosol module
[7] European Air Pollution Dispersion model system

1.2.1 Gas-phase Chemistry

Each model includes a detailed gas-phase mechanism that represents the gas-phase, aqueous-phase and photolytic reactions that occur in the atmosphere. The mechanism includes the reaction steps and kinetics for different reactions tracked by the model. Due to the complexity of gas-phase chemistry in the atmosphere, simplifications are necessary to reduce the number of chemical species in the mechanisms. For the air quality models in Table 2, most models adopt the CB-IV, RADM2 or the SAPRAC mechanisms. CIT is the only model that uses the recently developed Caltech Atmospheric Chemical Mechanism (CACM) mechanism.

SAPRAC-97 (Carter and Atkinson, 1996) and RADM2 (Stockwell et al., 1997) use the lumped-molecule approach to simplify the modeled species. In this method, organic molecules with similar reactivities and functional groups are lumped together to represent similar organics. The CB-IV mechanism employs a lumped-structure approach to simplify the modeled chemical species. In the lumped-structure method, organic molecules are divided into smaller reaction elements based on the type of carbon bonds the molecules have, and the reactivities are then represented by the sum of the molecules' reaction elements.

Although these mechanisms have different approaches for representing organic chemical species, they all have very similar inorganic species and reactions. This is because inorganic chemistry is simpler and reasonably well understood (Dodge, 2000; Stockwell et al., 1997). For predicting ozone formation, Dodge (2000) compiled results in many mechanism inter-comparison studies and concluded that most of these modules are able to predict ozone to within 10% of each other but can have considerable differences in predicting other intermediate oxidants and radical species.

In terms of aerosol formation, all three mechanisms include algorithms for forming condensable inorganics such as H_2SO_4, HNO_3, NH_4^+ and some condensable organics. These condensable species are precursors to secondary PM in the air, and are formed via the oxidization of SO_2, NOx and VOC gases. When condensable species are formed, they are

passed to the inorganic and organic aerosol modules (discussed below) for partitioning between gas/aerosol phases to determine the final formation of PM in the air. In all mechanisms, species such as NH_3, NaCl, and other crustal compounds, if included, are treated as inert gaseous species that do not undergo any gaseous reactions. These inert species are passed directly into the aerosol modules for inorganic aerosol reactions and phase partitioning calculations.

The CACM gas-phase chemical mechanism used in the CIT model was recently developed (Griffin et al., 2002b). It is the first detailed atmospheric chemical mechanism that is directed toward explicit prediction of formation of semi-volatile organics for the formation of secondary organic aerosol (SOA). This mechanism has the most complex organic chemistry among the current mechanisms. It uses the lumped-molecule approach similar to RADM2 and SAPRAC-97. However, the CACM mechanism tracks many more modeled species and reactions compared to the other mechanisms. CACM has a total of 191 model species and 361 reactions compared to only 57 species, 158 reactions in RADM2 and 36 species, 93 reactions in CB-IV. The 191 model species in CACM are categorized by molecule size, structural characteristics (e.g., branched versus cyclic), functionalities, reactivity and SOA forming potential. The mechanism uses the updated SAPRAC-97 inorganic chemistry. Unlike other mechanisms that track only first order VOC oxidation, this mechanism explicitly predicts more VOC species and tracks their secondary and tertiary oxidation products. This new gas-chemistry mechanism in CIT has been applied to simulate the ozone formation in the South Coast Air Basin of California. It was found that the predicted mixing ratios of inorganic gas-phase species (O_3, NO, and NO_2) are statistically comparable to those predicted by other mechanisms. The improvement in predicting SOA will be discussed in the organic aerosol module section. However, because the mechanism tracks large number of chemical species, the model framework requires very long computation time and is thus limited to modeling smaller urban regions.

1.2.2 Inorganic Aerosol Formation

Secondary formation of inorganic PM is a significant source of aerosol in the atmosphere. Gaseous pollutants such as NOx, SO_2 and NH_3 correspond to formation of major inorganic aerosol in the form of ammonium nitrate (NH_4NO_3) and ammonium sulfate ($(NH_4)_2SO_4$) salts. Crustal species and sea-salt also contribute to inorganic aerosol formation by increasing concentrations of available cations (K^+, Ca^{2+}, Mg^{2+}, Na^+) (Jacobson, 1999; Kim and Seinfeld, 1995). Inorganic aerosols comprised roughly 25-50% of fine particle mass (Gary et al., 1986), and the nitrate and sulfate aerosols can be responsible for 49% reduction in visibility in the Pacific Northwest, and up to 80% visibility reduction in the Eastern U.S. (Ames and Malm, 2001).

In modeling inorganic aerosol formation, a thermodynamic module performs equilibrium calculations to determine the partitioning of condensable species between gas/particulate and aqueous phases depending on the relative humidity (RH) and temperature. Mass transport of volatile and condensable species between phases is driven by the differences between ambient and equilibrium concentrations and governed by the equilibrium constants. Each modeled species can undergo several equilibrium reactions with species of opposite charge. The complexity of the module and the computing efficiency depends on the number of equilibrium reactions and the number of modeled species. In the inorganic modules solving these thermodynamic equilibrium equations takes up the most processor time in the air quality models (Jacobson et al., 1996; Nenes et al., 1998).

Several thermodynamic inorganic equilibrium modules have been developed and inter-compared to simulate the gas/aerosol partitioning and the total mass and chemical composition of inorganic aerosols (Zhang et al., 1999; Zhang et al., 2000; Ansari and Pandis, 1999b; Saxena et al., 1986). However, not all modules have been integrated with air quality transport models. For example, the Gibb's Free Energy Minimization (GFEMN) module (Ansari and Pandis, 1999a; Ansari and Pandis, 2000; Moya et al., 2001) and the Multicomponent Aerosol Dynamics Model (MADM) module (Pilinis et al., 2000) are standalone thermodynamic models developed recently.

The GFEMN model is formulated based on the minimization of Gibbs free energy and not by equilibrium calculations, and the MADM uses the first fully dynamic mass transfer method for aerosol size fraction without simplifications on the representations of solid particles formation. These two models have the least simplifying set of assumptions and provide very accurate solutions (Moya et al., 2001; Ansari and Pandis, 2000; Seigneur, 2001). However due to their complexity, they are not easily incorporated in Eulerian air quality models. They are highly computationally demanding and are appropriate only for box and one-dimensional trajectory models.

Table 2 lists some of the popular inorganic aerosol modules that are used in the current air quality models, and Table 3 summarizes the general features and methods used by these modules. All the modules in the table assume particles in the modeled size range are internally mixed, such that all particles in the same size bin have the same chemical composition. Among the models, SCAPE2 is the most computationally intensive because of the number of reactions and number of chemical species it computes. It is also the only module that has extensive crustal species, K^+, Ca_2^+, Mg^+, and the carbonate CO_3^{-2} chemistry. Jacobson (1999) and Moya et al. (2001) showed that including explicit cation species provides better model performance for the nitrate aerosols because crustal elements can influence the partitioning of total nitrate. Meng et al. (1995) suggested that including the alkaline carbonate chemistry could better represent the pH, water content and cloud condensation nuclei (CCN) potentials of dust particles. The EQUISOLV module was recently updated to EQUISOLV-II (Jacobson, 1999), which includes the same number of species as that of SCAPE2 and an improved iteration technique of solving equilibrium equations, however at this time, the EQUISOLV-II has not yet been integrated and applied with the air quality model.

Table 3: General features and methods used in inorganic aerosol modules.

Module:	SCAPE2	MARS	EQUISOLV	SEQUILIB	ISORROPIA
Chemical species in thermodynamic equilibrium calculation	SO_4^{2-}, NO_3^-, NH_4^+, Cl^-, Na^+, K^+, Ca_2^+, Mg^+, CO_3^{-2}, H_2O	SO_4^{2-}, NO_3^-, NH_4^+, H_2O	SO_4^{2-}, NO_3^-, NH_4^+, Cl^-, Na^+, H_2O	SO_4^{2-}, NO_3^-, NH_4^+, Cl^-, H_2O	SO_4^{2-}, NO_3^-, NH_4^+, Cl^-, Na^+, H_2O
Number of Reactions	36	7	21	14	15
Method for Activity Coefficient	Binary Activity: Kusik-Meissner method Multi-component Activity: Bromley or Kusik-Meissner or Pitzer method	Binary Activity: Pitzer method Multi-component Acivity: Bromley method	Binary Activity: Pitzer method Multi-component Acivity: Bromley method	Binary Activity: Pitzer method Multi-component Acivity: Bromley method	Binary Activity: Kusik-Meissner method. Multi-component Acivity: Bromley method
Temperature Dependence	Equilibrium constants, DRH	Equilibrium constants	Equilibrium constants, DRH and activity coefficients	Equilibrium constants	Equilibrium constants, MDRH
Assume Instantaneous Thermodynamic Equilibrium	No	Yes	No	Yes	Yes
Water Activity	ZSR	ZSR	ZSR	ZSR	ZSR
Size distribution	Sectional	Modal	Sectional	Sectional	Sectional
Aerosol Size Dynamic	Nucleation, condensation	Nucleation, condensation, coagulation	Nucleation, condensation, coagulation	Nucleation, condensation	Nucleation, condensation

The EQUISOLV, SEQUILB and ISORROPIA modules have sea salt chemistry but no explicit crustal species. Moya et al. (2001) showed that increasing concentration of Na^+ could be used as equivalent for crustal elements. This compensation technique for crustal element improves model performance in areas where cation contributions are high.

MARS is the only module that does not have chemical treatment for sea salt and crustal species due to its simplifications for regional modeling. In the comprehensive review by Zhang et al. (2000) and comparative study by Saxena et al. (1986), they showed that even though MARS has the simplest chemistry, its results were comparable to those predicted by other complicated modules. Its formulation efficiency is suitable for large-scale models, however, since it does not have sea salt chemistry, it must be used with caution in areas where sea-salt contribution is important.

In solving the phase partition between gas and aerosol species, equilibrium calculations are performed by the modules iteratively for different modeled species. Among these modules two methods are used to establish thermodynamic equilibrium between the phases. MARS, SEQUILIB and ISORROPIA assume that thermodynamic equilibrium exists instantly between the gas and the particulate phase of all sizes, whereas SCAPE2 and EQUISOLV assume equilibrium between phases is variable and depends on the aerosol size range and chemical composition. The first method is called the thermodynamic equilibrium approach where thermodynamic calculations are performed on the bulk aerosol population regardless of size range, and assume all particle sizes have the same chemical composition. The second method is called the dynamic mass transfer approach. In this method, each aerosol size section between gas and aerosol phase equilibrium is treated independently, and each particle sizes bin is equilibrated with the gas phase at different time scales.

The instantaneous thermodynamic equilibrium approach is used most widely, but for cases where equilibrium time scale is long relative to the residence time of particles, this approach may introduce errors (Meng et al., 1998). This is because large particles with smaller

surface area to volume ratio may require much longer time to establish equilibrium with the gas phase than smaller size aerosols. Meng and Seinfeld (1996) have analyzed the equilibrium time scales for ammonium nitrate. They found that nitrate aerosols with sub-micrometer size range reach equilibrium with the gas-phase species within seconds, however for aerosol size greater than 1μm, the equilibrium time scale can extend to the order of an hour or more. The dynamic mass transfer approach is therefore, theoretically more accurate. However, since each aerosol size range is tracked independently in the module, solving the equilibrium concentrations in each size range and tracking each particle size and composition become very heavy overheads for air quality models. Due to this reason most commonly used inorganic aerosol modules implement the thermodynamic equilibrium approach. Furthermore, the thermodynamic equilibrium assumption has been experimentally confirmed to be valid for smaller particles and warmer temperature where reaction rates are faster (Nguyen and Dabdub, 2002).

In quantifying the gas/aerosol species concentration after thermodynamic equilibrium, all of the modules calculate the composition of the atmospheric aerosol by solving sets of algebraic equations based on reversible reactions derived from thermodynamic equilibriums (Kim et al., 1993a).

For example, in solving the partitioning of ammonium sulfate, the reaction:

$$(NH_4)_2SO_{4(s)} \Leftrightarrow 2NH_4^+{}_{(aq)} + SO_4^{2-}{}_{(aq)} \qquad (1)$$

is solved base on the equilibrium calculation:

$$\left[NH_4^+\right]^2\left[SO_4^{2-}\right]\cdot\gamma_{NH_4^+}^2\gamma_{SO_4^{2-}} = K \qquad (2)$$

where $[NH_4^+]$ and $[SO_4^{2-}]$ are aqueous concentrations of ammonium and sulfate; $\gamma_{NH_4^+}$ and $\gamma_{SO_4^{2-}}$ are binary activity coefficient of NH_4^+ and SO_4^{2-} respectively, and K is the equilibrium

constant for this reaction. Both the activity coefficients and the equilibrium constants are functions of temperature and reactions and are solved in the modules. In calculating the temperature dependence of K, thermodynamic equations are used with tables of standard molar Gibbs free energy (ΔG_f^o), molar enthalpy of formation (ΔH_f^o) and molar heat capacity at constant pressure (C_P^o) for different compounds. It is important for modules to have updated thermodynamic data, since it can significantly influence the model results in terms of calculating equilibrium concentrations of chemical species (Kim et al., 1993a; Zhang et al., 2000). In solving the binary and multicomponent activity coefficients, the modules use parameterized methods and lookup tables. Different modules use different parameterization methods. Kim et al. (1993a; 1993b) have reviewed many methods available and concluded that the Bromley and Kusik-Meissner methods are similar in predicting accurate activities with differences of less than 2%, and the Pitzer method, derived from the definition of the excess Gibbs free energy, is accurate for solutions with low ionic concentration ranges.

In addition to equilibrium concentrations, water activity and water aerosol content are also important in determine aerosol growth and specie concentrations in different RH conditions. All the modules use the ZSR (Zdanovskii-Stokes-Robinson) method although there are other methods for estimating water activity. The ZSR method is the popular choice because it is easy to use and provides accurate results (Kim et al., 1993a). The method is based on the correlation:

$$\sum_i \frac{m_i}{m_{oi}(RH)} = 1 \qquad (3)$$

where m_i is the molality of ith electrolyte in the multicomponent solution and $m_{oi}(RH)$ is the molality of an aqueous solution of pure species *i* at a specific RH (expressed in fractions as water activity) (kg/mol water). By definition, molality is

$$m_i = M_i / W \qquad (4)$$

where W is the mass concentration of water in the aerosol (kg water /m^3 air) and M_i is the molar concentration of aerosol species i in the air (mol/m^3 air). Thus, by combining and rearranging the equations, the water aerosol content for different inorganic aerosol species is expressed as:

$$W = \sum_i \frac{M_i}{m_i(\mathrm{RH})} \qquad (5)$$

In terms of determining partitioning between aqueous and solid phases, SCAPE2, EQISOLV and SEQUILIB assume the deliquescence aerosol behavior for both increases and decreases of RH. By definition, deliquescence is the uptake of water by a solid particle to produce an aqueous solution as RH increases. In this assumption, the multicomponent particle does not transform into an aqueous solution until RH in the atmosphere exceeds the threshold deliquescence relative humidity specific for the particle (DRH). The DRH changes with temperature and composition. This aerosol deliquescence phenomenon occurs in nature and the DRH has been determined experimentally for many multicomponent aerosols (Cruz and Pandis, 2000). SCAPE2 and EQISOLV adjust the DRH in the model as a function of temperature, and SEQUILIB uses DRH at constant temperature of 298.15K.

The ISORROPIA module uses a method similar to SCAPE2 but base on a more recent finding by Potukuchi and Wexler, (1995). In their study, they found that a salt mixture has a lower DRH than the minimum DRH of individual salt components in a closed system, such that:

$$\mathrm{MDRH} = \mathrm{DRH}(\text{salt-1, salt-2} \ldots \text{salt-n}) < \min\{\mathrm{DRH}_{\text{salt-1}}, \mathrm{DRH}_{\text{salt-2}} \ldots \mathrm{DRH}_{\text{salt-n}}\} \qquad (6)$$

This DRH of the salt mixture is known as the Mutual Deliquescence Relative Humidity (MDRH). This MDRH is a function of the mixture composition and temperature. When atmospheric RH is equal to MDRH, the aqueous phase is saturated with respect to all the salts and aqueous solution can coexist with a precipitate composed of all aerosol salts. When RH is below the MDRH, the RH is too low to sustain the aqueous phase, and all salts exist in solid phase. Using

this method, Nenes et al. (1998) suggested that neglecting the mutual deliquescence may leads to erroneous over prediction of dry aerosol for cases when RH is above MDRH and below the minimum DRH of the salts. This RH region is called the Mutual Deliquescence Region. This is because the aerosol does not actually crystallize until a lower RH since it exists as a salt mixture. In another study, Nenes et al. (1999) performed module comparison between ISORROPIA and SEQUILIB. They found that the MDRH approach in ISORROPIA to be accurate and suitable to be incorporated in urban and regional air quality models. Having the MDRH limits for the combined salt compounds, the module can break down the RH domain into sub-domains and increase the computer efficiency. In the ISORROPIA module, the MDRH values are compiled from experiments or estimated from other closely related salts. The module also adjusts the MDRH and DRH values according to temperature.

In the MARS module, the aqueous and solid phase partitioning method is again different. Since MARS was designed to be incorporated in regional air quality models, the computation efficiency was a crucial consideration. MARS simplified the approach by breaking the RH into fixed regions and calculating the chemical equilibrium concentrations in the sub-RH domains accordingly. In this method, each domain contains fewer species than the entire concentration domain and the number of equilibrium calculations is greatly reduced. In the module, it assumes all salts exist in solid phase when RH < 40% and exist in aqueous phase when RH > 80% (Saxena et al., 1986).

For aerosol dynamics regarding particle size distribution and mass transfer between sizes, two approaches are adopted by the current inorganic aerosol modules. Most of the modules use the sectional approach and only MARS uses the modal approach. The sectional approach distributes particles sizes into discrete sections, and models aerosol dynamics by these sections, assuming particle properties are constant over each section. The aerosol sizes are then represented by the mean size of each section. In each section, the model keeps track of the aerosol mass concentrations for each chemical species and calculates the mass transfer

between bins as particles grow during coagulation, or shrink during evaporation. When particles grow or reduce out of size margin of the current bin, they are added to the upper or lower size bin and removed from the current size bin. The total number of variables the model calculates equals the total number of chemicals multiplied by number of size bins. The more sections the higher the size distribution resolution, but this also increases computing cost. In most of the size bin selections, usually only 8 bins are used for sizes between 0.04μm to 10μm diameter.

MARS is the only module to use the modal approach. This is again due to computational efficiency considerations for regional models. In this method, the particle size distribution is approximated by a small number of super-positioned lognormal sub-distributions called modes. The MARS module has three modes: Aitken nuclei mode, Accumulation mode, and Coarse mode. The particle properties are assumed to be uniform in each mode. Mass transfer between modes is similar as in the size bin methods, however, since only three modes are calculated instead of 8 size bins, this type of formulation allows much faster solution.

In comparison between the two size-distribution approaches, Zhang and co-workers (1999) showed that the accuracy of the sectional representation was strongly dependent on the total number of size bins tracked. The higher the number of bins, the better the resolution and the model performance. However, for the modal approach, the solutions are more accurate in modeling coagulation and condensation growth particles when the modal standard deviations for different modes were not fixed.

1.2.3 Organic Aerosol Formation

Modeling secondary organic aerosol formation and thermodynamics is more difficult compared to that of inorganic aerosols. This is mainly because of the limited knowledge about the chemistry and physics of organic aerosol formation, and the difficulties in measuring the primary and secondary contributions of ambient organic aerosol with direct chemical analysis methods (Turpin et al., 2000; Seigneur, 2001). Despite these difficulties, air quality models can include an organic aerosol module to account for SOA formation. Treatment of SOA is

important since visibility degradation by organic carbon is significant, especially for areas with high biogenic VOC emissions. Biogenic VOCs are more abundant and have higher aerosol forming potential than anthropogenic VOCs (Fuentes et al., 2000; Griffin et al., 1999b). Griffin et al. (1999c) estimated global biogenic secondary aerosol formation of 18.5Tg per year from biogenic VOC precursors. Light extinction from organic carbon is the highest in the Western US where organic carbon could contribute up to 40% of visibility degradation (Malm et al., 1994). Organic aerosol can be emitted directly (primary organic aerosol) or formed from oxidation of reactive organic carbons (secondary organic aerosol). It is estimated that the secondary organic carbon formed in the atmosphere can comprise from 15-50% or more of total organic mass (Pandis et al., 1993).

In modeling organic aerosols, most modules focus on formation of secondary organic aerosol and do not treat primary organic aerosol. In the current air quality models, primary organic aerosols from the emission inventory are treated only in terms of transport and deposition; they do not undergo any chemical reactions or phase changes. The primary aerosols and are assumed to always remain in the particulate phase. The principle functions of organic aerosol modules are to process the condensable organic species from the gas-phase mechanisms and determine the fraction of these oxidized organics to partition into the aerosol phase. Turpin et al. (2000) and Seigneur (2001) have recently published reviews on the formulations of these organic aerosols modules. In their reviews, they grouped the SOA partitioning methods into four general categories: vapor saturation, adsorption, absorption and dissolution. Most of these methods are formulated with empirical gas/aerosol partitioning data from smoke chamber experiments, and all four methods have been found to participate in determining the gas/aerosol phase changes. They suggested that the more advanced the organic aerosol module, the more approaches it will attempt to include to provide better representations of the phase partitioning for the condensable organics. In current air quality

models, none of the organic aerosol modules contain all four approaches. In the modules listed in Table 2, none of them use the adsorption method as suggested.

Vapor saturation is the method used by most of the current air quality models. This is the simplest approach. It is based on the finding by Pandis et al. (1992) that organic compounds will condense if gas-phase concentrations exceed their organic saturation vapor pressure. Using this relationship, aerosol yields for various VOCs were determined in smoke chambers as they undergo gaseous oxidation by ozone (O_3), nitrate radical (NO_3) and hydroxyl radical ($OH^{\cdot}$). The aerosol yields measure the fraction of SOA formed from oxidation of specific VOC precursors. In the current organic aerosol modules, these yields are provided as constants specified by oxidized VOCs. In CMAQ and UAM, only six modeled VOCs are considered as SOA precursors, while in GATOR, ten modeled VOC species are taken into account. The difference is largely due to the representation of VOC in their respective gas-phase mechanisms. Most of these modeled VOC species are identified as long chain carbon molecules and large aromatics such as C8 or higher alkanes, large internal alkenes, toluene, xylene, cresol and terpenes. These are the only modeled species that produce low volatile organics after oxidation. The major disadvantages of using this method are that aerosol yields were experimentally determined, it is very chemical-specific, and the models do not take into account the actual kinetics during the formation of the secondary and tertiary oxidized species. The method also does not have treatment of aerosol dynamics as absorption, adsorption, or dissolution once SOA are formed. Seigneur (2001) suggests that this approach is applicable for compounds that have a low vapor pressure, but likely to be inaccurate for compounds with high vapor pressure.

The EURD air quality model uses the more recent absorption approach to model SOA formation. It is based on the finding of Pankow (1994) that suggested absorption to be one of the major driving forces for partitioning condensable organics into the aerosol phase. He reasoned that once the organics begin to condense, they form an organic layer on the particles,

and the organic layer enhances partitioning of organic gases. Thus, condensable products whose gas-phase concentrations are below their saturation concentrations will also partition a portion of their mass onto the condensed organic phase. As more organics condense, more can serve as a medium onto which the gas-phase species can absorb. Therefore the final aerosol yields of the condensable gases are determined by the interactions between the condensable organics and the absorbed chemical species, as well as the total mass of absorbing material available. Several researchers have demonstrated this phenomenon for various reactive organic gases in smoke chamber experiments (Odum et al., 1996; Hoffmann et al., 1997; Hoffmann et al., 1997; Griffin et al., 1999a). They found that organic aerosol yield increases with increase of the mass of organic aerosol initially present in the chamber, and the relationship between condensable organic and the absorbed chemical species can be quantified by partitioning coefficients determined empirically. A Lagrangian version of the EURD aerosol module was applied by (Schell et al., 2001). They found significant impact on the final SOA formation, since the saturation concentrations of the SOA compounds depend on the composition of the SOA and the amount of absorbing material present. They also concluded that the accuracy of each SOA precursor emissions could have significant impact on the total simulated SOA.

As mentioned in the previous section, the CIT air quality model applies a new CACM gas-phase chemical mechanism that explicitly predicts the formation of semi-volatile organics that could constitute observed SOA. In its organic aerosol module, it accounts for gas/aerosol partitioning using the combined adsorption and the dissolution approach (Pun et al., 2002). The adsorption approach was the same as that of the EURD model described previously, except that more aerosol yield calculations are carried out in the CIT organic aerosol module. The dissolution approach is described further in this section. This approach is based on the finding by Saxena and Hildemann (1997). They concluded organic compounds contain functional groups, such as carbonyl, hydroxyl and acid groups, which favor their solubility in water. As the

solubility of these organic compounds increase, they become more favorable to partitioning in the aqueous phase. This method suggested the foundation of simulating organic dissolution in aqueous particle is similar to that of inorganic aerosols where phase-partition occurs in both solid and aqueous phases and the concentrations depend on equilibrium calculations. Since water solubility of the semi-volatile organic is specie-specific and tied with the atmospheric conditions, its gas/particle partition fraction is a function of the effective Henry's law constant for the organic compound and the liquid water content of the aerosols. Unlike other organic aerosol modules, CIT is the only module that accounts for partitioning of organic aerosols into both solid and aqueous phases. Using the same approach as inorganic modules, CIT assumes instantaneous equilibrium between the gas-phase and a condensed aerosol phase organics to solve the equilibrium calculations. CIT-CACM and its secondary organic aerosol component were applied to simulate aerosol formation in the South Coast Air Basin of California (SoCAB) for the summer of 1993 (Griffin et al., 2002a). The model results were compared with observed concentrations of SOA. The comparison showed the predicted temporal behavior of the total mass of compounds available to partition to SOA tracks well with the pattern observed for ambient SOA. They concluded that uncertainty lies in the rate constants, the product yields, and the mechanisms of degradation of second-, third-, and further generation products.

The last method that is not adopted in any of the current air quality model (Table 2) is the adsorption approach. This method is based on the finding of Pankow, (1987), who suggested adsorption of organic species on particle surface is a significant process in the gas/aerosol phase partition of organic species. This process is very similar to the absorption approach where condensable organics partition on surface of particles through either physical or chemical processes. However, in this approach, the amount adsorbed is proportional to the surface area of particles rather than the total organic PM concentration in the absorption approach. He found that the SOA yield for different organic gases is a function of a temperature-dependent adsorption equilibrium parameter and the total particle surface area.

This approach has been used in box models to simulate partitioning of semi-volatile organics such as Polycyclic Aromatic Hydrocarbons (PAHs) and Polychlorinated Biphenyls (PCBs), but has not been adopted in the air quality models.

1.2.4 Model Sensitivity Studies

Although currently there are several air quality models with treatments for aerosol formation calculations, not many of them have been used to study the sensitivity of pollutants to changes in precursor emissions. This section discusses some of the available model sensitivity analyses.

One of the first aerosol sensitivity analyses was performed by Meng et al. (1995) for an episode in South Coast Air Basin of California (SoCAB). They used an older version of the CIT and SCAPE2 model to study the effects of ozone control strategies on inorganic aerosol formation. They found that controlling VOC and NOx emissions does not lead to proportional reductions in secondary formation of aerosols, and in some cases, it causes undesirable increases in PM formation. In their study, a reduction in VOC emissions with fixed NOx emissions caused big decrease in ozone formation, but also caused increases in nitrate PM2.5 and total PM2.5. On the other hand, reductions in NOx without changing VOC caused less than equal reduction in ozone and total PM2.5 concentrations.

Lurmann et al. (1997) also studied the PM sensitivity over the same SoCAB area with the UAM-AERO model. In the study, they changed domain wide NOx, VOC, NH3, SO2 or primary PM emissions to observe changes in various inorganic PM2.5 concentrations. They found that reduction in NOx emissions reduces nitrate aerosol by only a small amount in areas with low NH3 concentration but by a much larger amount in areas with low NOx concentrations. In addition, reductions in NH3 emissions can effectively reduce ammonium aerosol in areas with low NH3 emissions, but the strategy is not effective when NOx concentrations in the area are low. For the most effective total PM2.5 control strategy, they found that lowering ammonia emissions could reduce the total PM2.5 by the greatest amount. This is because the SoCAB

domain is generally low in NH3 emissions, and reducing NH3 lowers both nitrate and ammonium aerosol by the greatest amount. In terms of PM sensitivity to VOC emission changes, they found direct reduction in organic aerosol from lowering VOC, but the effect is less obvious for inorganic aerosols.

The Denver Air Quality Model (DAQM) was also applied to study visibility improvements over the state of Colorado for the winter season (Middleton, 1997). Unlike other studies that focused on PM responses to changes in emissions, this study concentrated on developing emission control strategies that are attainable and can provide the most effective improvement in visibility. Several scenarios were analyzed and compared with the base-case predictions. It was found that the biggest visibility improvement occurred when combined woodstoves/fireplace emissions were lowered by 90% together with major point source emissions by 80 to 90% and mobile exhaust emissions by 10% to 20%. When emissions from these source categories were reduced by the given percentages the DAQM model predicted a large 30% decrease in aerosol concentrations and 25% improvement in visibility. The improvement was largely due to decreases in VOC and primary PM from woodstove and fireplaces. The VOC compounds from wood burning have very high SOA forming potential. Reducing VOC from these sources directly reduced SOA in the atmosphere and improved the visibility in the area.

One of the most recent aerosol sensitivity analyses was by Nguyen and Dabdub (2002). They used the CIT model to study changes in inorganic aerosol from incremental changes in NOx, VOC and NH3 emissions over the SoCAB domain. Through a series of scenario runs they generated several isopleths to illustrate the predicted PM2.5 aerosol concentrations at different combinations of precursor emission adjustments. One of the major focuses is the analysis of aerosol formation from the coupling of ozone and aerosol chemistry. They found that the highest concentrations of PM occur at the highest emissions rates of VOC and NOx, and the 24-hour average PM concentration depends nonlinearly on NOx and VOC concentrations. The model predicted cases where increase in NOx emissions can lead to

decreases in the maximum 24-hour average PM concentrations in some regions. They also concluded that the quantitative effects of lowering NOx and VOC on controlling PM formation are not substantial for parts of the SoCAB area. When VOC emissions were changed by ±20% at 20% lowered NOx level, there were no substantial effects on 24-hour maximum PM formation, and when ammonia is reduced by20%, the changes in NOx emissions have no effect in PM level. Similar to other studies conducted over the SoCAB area, the authors suggested that the bigger change in 24-hour PM concentration is through ammonia emission reductions. The model predicted a 20% reduction in 24-hour maximum PM when ammonia emissions is set to zero.

Compared to all of the studies of gas-phase chemistry and ozone sensitivity studies, there are far fewer aerosol formation sensitivity analyses using three-dimenstional air quality models. For the available aerosol sensitivity studies, most of the model scenarios were applied to the Southwestern regions of US. The findings from these studies cannot be applied directly to other regions due to differences in chemistry and physical transport conditions. The manuscript in the following chapter describes the procedure and results of an ozone and aerosol sensitivity study covering the Pacific Northwest. The research used the Models-3/CMAQ model, with RADM2 gas-phase chemistry module to determine the changes in aerosol and ozone concentrations from percentage changes in both biogenic and anthropogenic emissions. Although several ozone sensitivity studies have been performed over this area, this is the first study to take ozone and aerosol chemistry into account. Since ozone control strategies can have unexpected impacts on secondary aerosol formation depending on the transport and chemistry in a region, it is important to understand what effects relative emission changes have on both ozone and PM concentrations. This sensitivity approach is the first of its kind for the Pacific Northwest. The results from this research can improve our understanding in the relationship of ozone and PM formation with their precursor emissions.

References

Ames, R. B. and W. C. Malm, Chemical Species' Contributions to the Upper Extremes of Aerosol Fine Mass, *Atmospheric Environment*, 35, 5193-5204, 2001.

Ansari, A. S. and S. N. Pandis, Prediction of Multicomponent Inorganic Atmospheric Aerosol Behavior, *Atmospheric Environment*, 33, 745-757, 1999a.

Ansari, A. S. and S. N. Pandis, An Analysis of Four Models Predicting the Partitioning of Semivolatile Inorganic Aerosol Components, *Aerosol Science and Technology*, 31, 129-153, 1999b.

Ansari, A. S. and S. N. Pandis, The Effect of Metastable Equilibrium States on the Partitioning of Nitrate Between the Gas and Aerosol Phases, *Atmospheric Environment*, 34, 157-168, 2000.

Barna, M., B. Lamb, S. O'neill, H. Westberg, C. Figueroa-Kaminsky, S. Otterson, C. Bowman, and J. Demay, Modeling Ozone Formation and Transport in the Cascadia Region of the Pacific Northwest, *Journal of Applied Meteorology*, 39, 349-366, 2000.

Barna, M., B. Lamb, and H. Westberg, Modeling the Effects of VOC/NOx Emissions on Ozone Synthesis in the Cascadia Airshed of the Pacific Northwest, *Journal of the Air & Waste Management Association*, 51, 1021-1034, 2001.

Byun, D. W. and Ching, J. K. S. Science Algorithms of the EPA Models-3 Community Multiscale Air Quality (CMAQ) Modeling System. 1999. Office of Research and Development Washington DC, U.S. Environmental Protection Agency.

Carter, W. P. L. and R. Atkinson, Development and Evaluation of a Detailed Mechanism for the Atmospheric Reactions of Isoprene and Nox, *International Journal of Chemical Kinetics*, 28, 497-530, 1996.

Cruz, C. N. and S. N. Pandis, Deliquescence and Hygroscopic Growth of Mixed Inorganic-Organic Atmospheric Aerosol, *Environmental Science & Technology*, 34, 4313-4319, 2000.

Dennis, R. L., D. W. Byun, J. H. Novak, K. J. Galluppi, C. J. Coats, and M. A. Vouk, The next generation of integrated air quality modeling: EPA's Models-3, *Atmospheric Environment*, 30, 1925-1938, 1996.

Dodge, M. C., Chemical Oxidant Mechanisms for Air Quality Modeling: Critical Review, *Atmospheric Environment*, 34, 2103-2130, 2000.

Fuentes, J. D., M. Lerdau, R. Atkinson, D. Baldocchi, J. W. Bottenheim, P. Ciccioli, B. Lamb, C. Geron, L. Gu, A. Guenther, T. D. Sharkey, and W. Stockwell, Biogenic Hydrocarbons in the Atmospheric Boundary Layer: a Review, *Bulletin of the American Meteorological Society*, 81, 1537-1575, 2000.

Gary, H. A., G. R. Cass, J. J. Huntzicker, E. K. Heyerdahl, and J. A. Rau, Characteristics of atmospheric organic and elemental carbon particle concentrations in Los Angeles, *Environmental Science & Technology*, 20, 580-589, 1986.

Griffin, R. J., D. R. Cocker, R. C. Flagan, and J. H. Seinfeld, Organic Aerosol Formation From the Oxidation of Biogenic Hydrocarbons, *Journal of Geophysical Research-Atmospheres*, 104, 3555-3567, 1999a.

Griffin, R. J., D. R. Cocker, and J. H. Seinfeld, Incremental Aerosol Reactivity: Application to Aromatic and Biogenic Hydrocarbons, *Environmental Science & Technology*, 33, 2403-2408, 1999b.

Griffin, R. J., D. R. Cocker, J. H. Seinfeld, and D. Dabdub, Estimate of Global Atmospheric Organic Aerosol From Oxidation of Biogenic Hydrocarbons, *Geophysical Research Letters*, 26, 2721-2724, 1999c.

Griffin, R. J., D. Dabdub, Kleeman J.K., P. M. Fraser, G. R. Cass, and J. H. Seinfeld, Secondary organic aerosol: III. Urban/regional scale model of size- and composition-resolved aerosols, *Journal of*

Geophysical Research, 107, 2002a.

Griffin, R. J., D. Dabdub, and J. H. Seinfeld, Secondary organic aerosol: I. Atmospheric chemical mechanism for production of molecular constituents, *Journal of Geophysical Research*, 107, 2002b.

Hoffmann, T., J. R. Odum, F. Bowman, D. Collins, D. Klockow, R. C. Flagan, and J. H. Seinfeld, Formation of Organic Aerosols From the Oxidation of Biogenic Hydrocarbons, *Journal of Atmospheric Chemistry*, 26, 189-222, 1997.

Jacobson, M. Z., Studying the Effects of Calcium and Magnesium on Size- Distributed Nitrate and Ammonium With Equisolv-II, *Atmospheric Environment*, 33, 3635-3649, 1999.

Jacobson, M. Z., A. Tabazadeh, and R. P. Turco, Simulating Equilibrium Within Aerosols and Nonequilibrium Between Gases and Aerosols, *Journal of Geophysical Research-Atmospheres*, 101, 9079-9091, 1996.

Jiang, G., Potochemical air quality modeling in the Puget Sound region, Ph.D. thesis, Washington State University, Department of Chemistry, Pullman, WA, 2001.

Kim, Y. P. and J. H. Seinfeld, Atmospheric Gas-Aerosol Equilibrium 3: Thermodynamics of Crustal Elements Ca2+, K+, and Mg2+, *Aerosol Science and Technology*, 22, 93-110, 1995.

Kim, Y. P., J. H. Seinfeld, and P. Saxena, Atmospheric Gas Aerosol Equilibrium 1: Thermodynamic Model, *Aerosol Science and Technology*, 19, 157-181, 1993a.

Kim, Y. P., J. H. Seinfeld, and P. Saxena, Atmospheric Gas-Aerosol Equilibrium 2: Analysis of Common Approximations and Activity-Coefficient Calculation Methods, *Aerosol Science and Technology*, 19, 182-198, 1993b.

Malm, W. C. and D. E. Day, Optical Properties of Aerosols at Grand Canyon National Park, *Atmospheric Environment*, 34, 3373-3391, 2000.

Malm, W. C., J. F. Sisler, D. Huffman, R. A. Eldred, and T. A. Cahill, Spatial and Seasonal Trends in Particle Concentration and Optical Extinction in the United-States, *Journal of Geophysical Research-Atmospheres*, 99, 1347-1370, 1994.

Meng, Z., D. Dabdub, and J. H. Seinfeld, Chemical Coupling Between Atmospheric Ozone and Particulate Matter, *Science*, 277, 116-119, 1997.

Meng, Z. Y., D. Dabdub, and J. H. Seinfeld, Size-Resolved and Chemically Resolved Model of Atmospheric Aerosol Dynamics, *Journal of Geophysical Research-Atmospheres*, 103, 3419-3435, 1998.

Meng, Z. Y. and J. H. Seinfeld, Time Scales to Achieve Atmospheric Gas-Aerosol Equilibrium for Volatile Species, *Atmospheric Environment*, 30, 2889-2900, 1996.

Meng, Z. Y., J. H. Seinfeld, P. Saxena, and Y. P. Kim, Atmospheric Gas-Aerosol Equilibrium .4. Thermodynamics of Carbonates, *Aerosol Science and Technology*, 23, 131-154, 1995.

Middleton, P., Daqm-Simulated Spatial and Temporal Differences Among Visibility, Pm, and Other Air Quality Concerns Under Realistic Emission Change Scenarios, *Journal of the Air & Waste Management Association*, 47, 302-316, 1997.

Moya, M., A. S. Ansari, and S. N. Pandis, Partitioning of Nitrate and Ammonium Between the Gas and Particulate Phases During the 1997 Imada-Aver Study in Mexico City, *Atmospheric Environment*, 35, 1791-1804, 2001.

Nenes, A., S. N. Pandis, and C. Pilinis, Isorropia: a New Thermodynamic Equilibrium Model for Multiphase Multicomponent Inorganic Aerosols, *Aquatic Geochemistry*, 4, 123-152, 1998.

Nenes, A., S. N. Pandis, and C. Pilinis, Continued Development and Testing of a New Thermodynamic Aerosol Module for Urban and Regional Air Quality Models, *Atmospheric Environment*, 33, 1553-1560, 1999.

Nguyen, K. and D. Dabdub, NOx and VOC Control and Its Effects on the Formation of Aerosols, *Aerosol Science and Technology*, 36, 560-572, 2002.

O'Neill, Susan M. and Lamb, Brian K. Intercomparison of the Community Multi-scale Air Quality (CMAQ) Model and CALGRID using Process Analysis. 2002.

Odum, J. R., T. Hoffmann, F. Bowman, D. Collins, R. C. Flagan, and J. H. Seinfeld, Gas/Particle Partitioning and Secondary Organic Aerosol Yields, *Environmental Science & Technology*, 30, 2580-2585, 1996.

Pandis, S. N., R. A. Harley, G. R. Cass, and J. H. Seinfeld, Secondary Organic Aerosol Formation and Transport, *Atmospheric Environment Part a-General Topics*, 26, 2269-2282, 1992.

Pandis, S. N., A. S. Wexler, and J. H. Seinfeld, Secondary Organic Aerosol Formation and Transport .2. Predicting the Ambient Secondary Organic Aerosol-Size Distribution, *Atmospheric Environment Part a-General Topics*, 27, 2403-2416, 1993.

Pankow, J. F., Review and Comparative Analysis of the Theories on Partitioning between the Gas and Aerosol Particulate Phases in the Atmosphere, *Atmospheric Environment*, 21, 2275-2283, 1987.

Pankow, J. F., An Absorption-Model of Gas-Particle Partitioning of Organic- Compounds in the Atmosphere, *Atmospheric Environment*, 28, 185-188, 1994.

Pilinis, C., K. P. Capaldo, A. Nenes, and S. N. Pandis, Madm - a New Multicomponent Aerosol Dynamics Model, *Aerosol Science and Technology*, 32, 482-502, 2000.

Potukuchi, S. and A. S. Wexler, Identifying Solid-Aqueous Phase-Transitions in Atmospheric Aerosols .1. Neutral-Acidity Solutions, *Atmospheric Environment*, 29, 1663-1676, 1995.

Pun, B. K., R. J. Griffin, C. Seigneur, and J. H. Seinfeld, Secondary organic aerosol: II. Thermodynamic model for gas/particle partitioning of molecular constituents, *Journal of Reophysical Research*, 107, 2002.

Russell, A. and R. Dennis, Narsto Critical Review of Photochemical Models and Modeling, *Atmospheric Environment*, 34, 2283-2324, 2000.

Saxena, P. and L. M. Hildemann, Water Absorption by Organics: Survey of Laboratory Evidence and Evaluation of Unifac for Estimating Water Activity, *Environmental Science & Technology*, 31, 3318-3324, 1997.

Saxena, P., A. B. Hudischewskyj, C. Seigneur, and H. J. Seinfeld, A comparative study of equilibrium approaches to the chemical characterization of secondary aerosols, *Atmospheric Environment*, 20, 1471-1483, 1986.

Schell, B., I. J. Ackermann, H. Hass, F. S. Binkowski, and A. Ebel, Modeling the Formation of Secondary Organic Aerosol Within a Comprehensive Air Quality Model System, *Journal of Geophysical Research-Atmospheres*, 106, 28275-28293, 2001.

Seigneur, C., Current Status of Air Quality Models for Particulate Matter, *Journal of the Air & Waste Management Association*, 51, 1508-1521, 2001.

Seigneur, C., P. Pai, P. K. Hopke, and D. Grosjean, Modeling Atmospheric: Particulate Matter, *Environmental Science & Technology*, 33, 80A-86A, 1999.

Stockwell, W. R., F. Kirchner, M. Kuhn, and S. Seefeld, A New Mechanism for Regional Atmospheric Chemistry Modeling, *Journal of Geophysical Research-Atmospheres*, 102, 25847-25879, 1997.

Turpin, B. J., P. Saxena, and E. Andrews, Measuring and Simulating Particulate Organics in the Atmosphere: Problems and Prospects, *Atmospheric Environment*, 34, 2983-3013, 2000.

U.S. Environmental Protection Agency. Community Multi-scale Air Quality (CMAQ) modeling system. Available online: http://www.epa.gov/asmdnerl/models3/cmaq.html

Wark, K., C. F. Warner, and W. T. Davis, Air pollution: its origin and control, Addison-Wesley, Menlo Park, Califonia. 1998.

Zhang, Y., C. Seigneur, J. H. Seinfeld, M. Jacobson, S. L. Clegg, and F. S. Binkowski, A Comparative Review of Inorganic Aerosol Thermodynamic Equilibrium Modules: Similarities, Differences, and Their Likely Causes, *Atmospheric Environment*, 34, 117-137, 2000.

Zhang, Y., C. Seigneur, J. H. Seinfeld, M. Z. Jacobson, and F. S. Binkowski, Simulation of Aerosol Dynamics: a Comparative Review of Algorithms Used in Air Quality Models, *Aerosol Science and Technology*, 31, 487-514, 1999.

CHAPTER 2

AEROSOL AND OZONE SENSITIVITY ANALYSIS WITH THE COMMUNITY MULTI-SCALE AIR QUALITY (CMAQ) MODEL FOR THE PACIFIC NORTHWEST

Jack Chen, Brian K. Lamb, Susan M. O'Neill

Laboratory for Atmosphere Research

Department of Civil and Environmental Engineering

Washington State University, Pullman, WA 99164-2910

ABSTRACT

The Community Multi-scale Air Quality (CMAQ) model was employed to perform a sensitivity analysis of aerosol and ozone concentrations to changes in precursor emissions in the Pacific Northwest. The simulations covered a three-day period with elevated ozone concentrations from July 13 to 15, 1996. The base-case had a complete set of biogenic and anthropogenic emission inventories, while the sensitivity runs had step-wise adjustments in anthropogenic NH3, NOx, VOCs, SO2 and biogenic VOCs emissions. The adjustments were made at ±100%, ±50% and ±25% of the base-case emissions.

Sensitivity results for PM2.5 were analyzed for selected regions in the domain. The results showed that secondary aerosol and ozone chemistry are closely tied to each other. Higher atmospheric oxidants often led to higher aerosol formation due to increases in sulfate and secondary organic aerosol formation. In addition, the coupled chemistry caused non-linear change in secondary aerosol concentration with precursor NOx emissions. The PM2.5 sensitivity also depends on the individual concentrations of NOx, SO2 and NH3 in local areas. In places with high ammonia to sulfate concentration ratios, PM2.5 was highly sensitive to NOx and NH3 emissions changes, but PM2.5 was insensitive to changes in SO2 emissions. At low ammonia to sulfate concentration ratios, PM2.5 concentrations were highly sensitive to changes in SO2 emissions but rather insensitive to changes in NOx and NH3 emissions.

Ozone sensitivity to precursor anthropogenic NOx, VOC and biogenic VOC emissions were also analyzed for selected regions in the domain. It was found that ozone changes linearly with changes in either biogenic or anthropogenic VOC emissions. Anthropogenic VOC emissions caused larger changes in large urban areas, while biogenic VOC emissions caused larger changes in smaller urban and rural areas. For NOx emission changes, ozone exhibited negative sensitivity in large urban regions where high levels of NO titrate ambient ozone. However, in smaller urban regions and rural areas, ozone changes linearly with NOx. This is

due to low NOx concentrations with respect to VOC concentrations in these regions. Sensitivity simulation results for ozone were correlated with the base-case HNO_3/H_2O_2 concentration ratio. It was found that the ratio is a good indicator for regions that are sensitive to either NOx or VOC emissions changes. In addition, the ratio suggests the degree of ozone response to changes in precursor emissions. Regions with a higher ratio have a higher degree of NOx and VOC emission sensitivity than regions with a lower indicator ratio.

2.1 Introduction

Tropospheric ozone (O_3) and fine aerosols have significant impact on the quality of life on Earth. Ozone is a secondary pollutant that forms from chemical reactions between NOx ($NOx=NO+NO_2$) and volatile organic compounds (VOCs) in the presence of sunlight. It is a strong oxidant that directly damages human, animal and plant tissues (National Research Council, 1991). Aerosols are airborne microscopic solid and/or liquid particles of various chemical compositions. Aerosols are both primary and secondary pollutants that are introduced directly to the atmosphere or formed chemically from precursor gases. Fine aerosols can be suspended in the air for a long period of time (days to weeks) and scatter light. High levels of fine aerosols contribute to reduced visibility and various adverse health effects on humans and animals (Wark et al., 1998). In protecting people's health and welfare, the US Environmental Protection Agency (EPA) established the National Ambient Air Quality Standards (NAAQS) for six criteria pollutants including ozone and particulate matter (PM). In 1997 the standards for ozone and PM were promulgated to more stringent levels. In this new standard, ozone was set to 80 parts per billion by volume (ppbv) over an 8 hour averaging period, and PM with aerodynamic diameter less than 2.5μm (PM2.5) was set to 15μg/m^3 annually and 65μg/m^3 over a 24-hour average. It has been shown that the new standards can put more areas in violation with the NAAQS (Chameides et al., 1997; Chock et al., 1999; Saylor et al., 1999). In order to implement cost effective control strategies for both pollutants, it is important to understand the formation and transport of these pollutants and their responses to changes in precursor emissions.

Three-dimensional air quality models have been used to study the dynamics of air pollutants over regional to urban scales (Barna et al., 2000; Pai et al., 2000; Russell and Dennis, 2000). These models incorporate comprehensive sets of physical and chemical processes to track the formation, transport and removal of various air pollutants with inputs of appropriate

meteorology and emissions. These numerical models are the best tools for analyzing different control strategies for atmospheric pollutants (Milford et al., 1989).

Reducing the amount of precursors emitted can often limit the formation of secondary pollutants. However the reductions are often non-linear and can sometimes produce opposite results where decreases in precursors can cause increases in pollutant concentrations. Several studies have used air quality models to study the effectiveness of different emission scenarios in controlling the secondary pollutants. Barna et al. (2001) and Jiang, et al. (2001) studied ozone responses due to changes in biogenic and anthropogenic NOx and VOC emissions in the Pacific Northwest; Meng et al. (1997) presented one of the first aerosol and ozone coupling sensitivity analysis over the South Coast Air Basin of California (SoCAB) and addressed the non-linearities between gas-phase and particle-phase chemistry; Middleton (1997) applied the Denver Air Quality Model (DAQM) to study visibility improvements in Colorado from combinations of attainable emission control strategies; and recently Nguyen and Dabdub (2002) reported the effects on aerosol formation from changing NOx and VOC emissions for the South Coast of California.

In the Pacific Northwest, the Northwest Regional Modeling Center (NWRMC) was established as a virtual modeling center to provide and share tools, resources, and capabilities for the benefit of air quality stakeholders in the region. As a first step for the NWRMC, O'Neill and co-workers (2002) employed the Community Multi-scale Air Quality (CMAQ) model in the Pacific Northwest to investigate ozone and particulate formation on a regional basis for the period of July 1 to 15, 1996. In their study, two different emission inventories were used, and the results were compared. First, the EPA National Emissions Trends (NET96) emission inventory was interpolated from the 36 km grid scale to a 12 km grid scale for a domain encompassing Idaho, Oregon, Washington, and significant portion of southern Canada. Second, a more detailed inventory was compiled with 12 km grid resolution with additional input from each state agency (NWRMC inventory). O'Neill et al. (2002) found that differences in the

emission inventory had significant effects on both ozone and PM formation, but the effects were different in different parts of the domain. In this work, we continued this investigation in terms of understanding the sensitivities of aerosol and ozone formation due to changes in emissions. We carried out the emissions sensitivity study using CMAQ with the 12 km gridded NWRMC inventory. To minimize computer time, the period from July 13 to 14, 1996 was simulated and a smaller domain was employed. In this sensitivity analysis, we examine the changes in ozone and PM2.5 concentrations at different urban and rural regions due to domain-wide changes in precursor emissions at various levels. This is one of the first assessments of aerosol sensitivity over the Pacific Northwest region using a three-dimensional air quality model.

The CMAQ modeling system used in this study represents the latest state-of-the-science in regional air quality models (Byun et al., 1998; Byun and Ching, 1999). It was developed by the EPA as a part of a modeling system using the 'one-world' modeling approach (Dennis et al., 1996). The model simulates chemical, photochemical and physical processes that are important for atmospheric pollutants including inorganic and organic aerosols and tropospheric ozone. The CMAQ modeling system has gained wide use by other researchers to simulate various atmospheric pollutants (Bullock and Brehme, 2002; Chandrasekar et al., 2002; Pagowski et al., 2002; Pun and Seigneur, 2001).

The purpose of this paper is to provide an initial analysis of how PM2.5 and ozone concentrations respond to changes in precursor emissions and to relate these changes to local area characteristics. This work will thus provide a foundation for further analysis of potential control strategies related to regional haze and urban area elevated pollutant levels. In Section 2 of this paper, we describe the model framework, emissions inventory and the CMAQ science algorithms. Section 3 gives a brief overview of general aerosol and ozone formation chemistry in the troposphere. Section 4 contains results and discussions for the sensitivity analysis in regard to secondary aerosol and ozone formation and section 5 gives a comparison of sensitivity results with observational data. Finally, concluding remarks are provided in the last section.

2.2 Description of Modeling System

2.2.1 Model Domain

In this study, a 'nested' modeling technique was implemented to reduce computing time while taking into account transport processes over a larger area. The nesting technique incorporates the analysis domain inside a larger parent domain. Figure 1 shows the coverage of the parent domain and contour plot of the region as employed by O'Neill et al. (2002). In this study, we focus on the sensitivity of the sub-domain depicted in Figure 2. The domain covers the states of Washington, Oregon, Idaho and parts of western Montana. This sub-domain includes several points of interest in terms of ozone and PM pollution. Seattle, WA and Portland, OR are two large metropolitan areas that have histories of ozone episodes and also have a legacy of elevated PM concentrations. The Columbia River Gorge at the boarder of Oregon and Washington is a National Class I scenic area, and the Craters of the Moon to the east of Boise, ID, is a National Monument. Both of these sites are important with regards to visibility degradation from primary and secondary PM2.5.

The grid resolutions for both the parent and the nested domain were at 12-km with 16 vertical layers. The vertical layers were distributed unevenly with 10 layers in the lower 1,000 meters and 6 more layers up to the tropopause (10,000 m). Higher vertical resolution at the ground surface ensured better model performance through the evolution of the planetary boundary layer (PBL). The high extent of the top model layer was required to better characterize transport over the regional scale.

Figure 1: CMAQ Parent domain and topographical contour map.

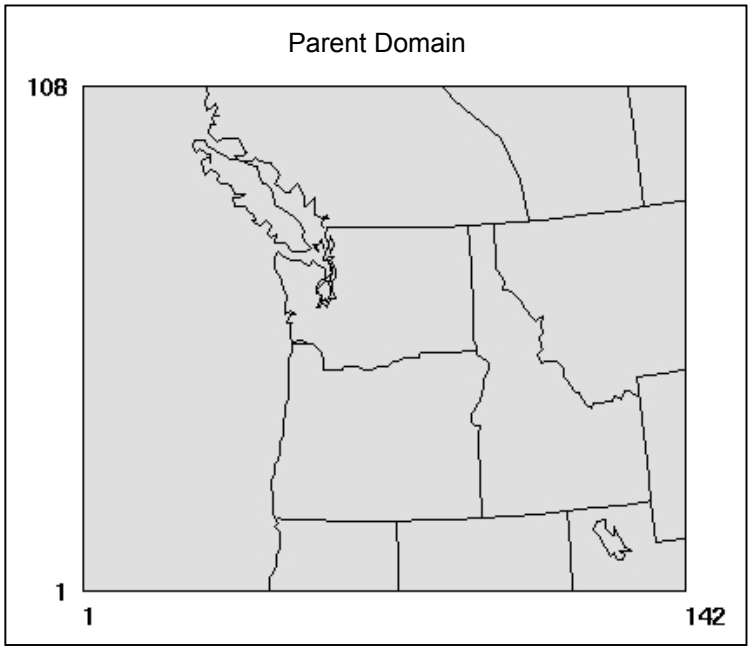

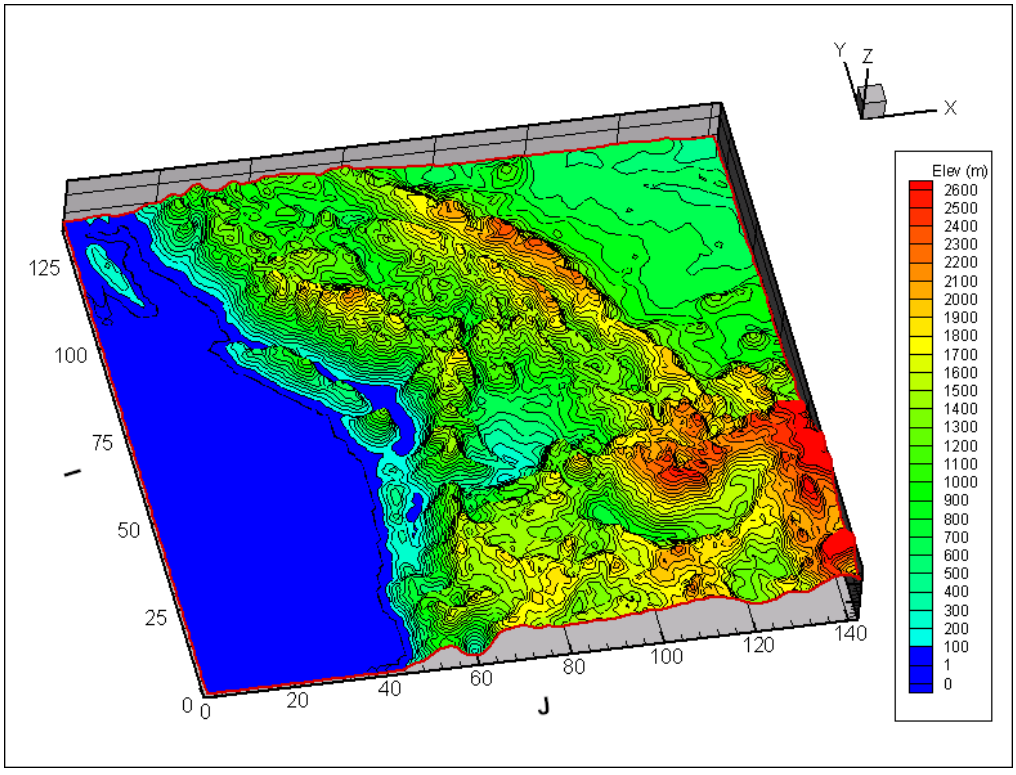

Figure 2: CMAQ Sensitivity domain and topographical contour map.

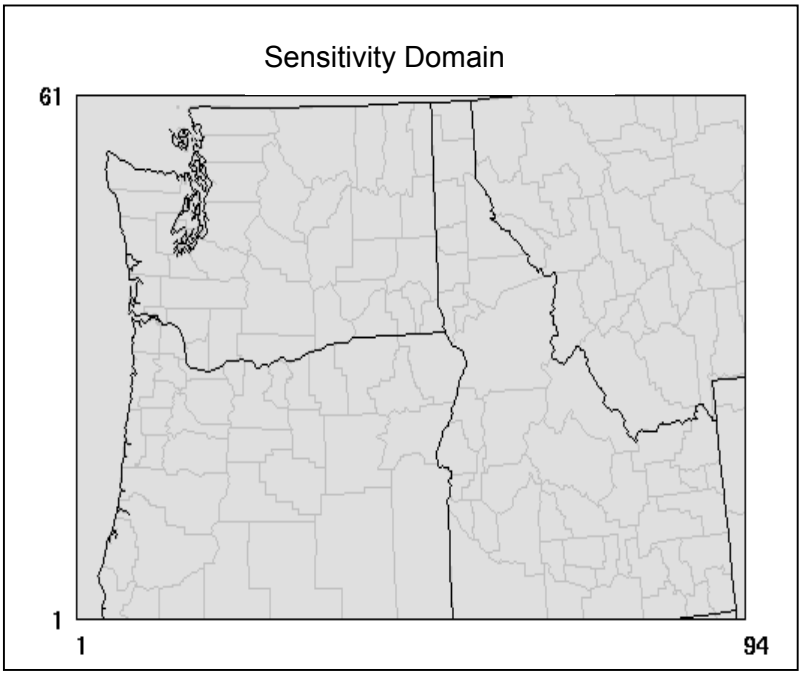

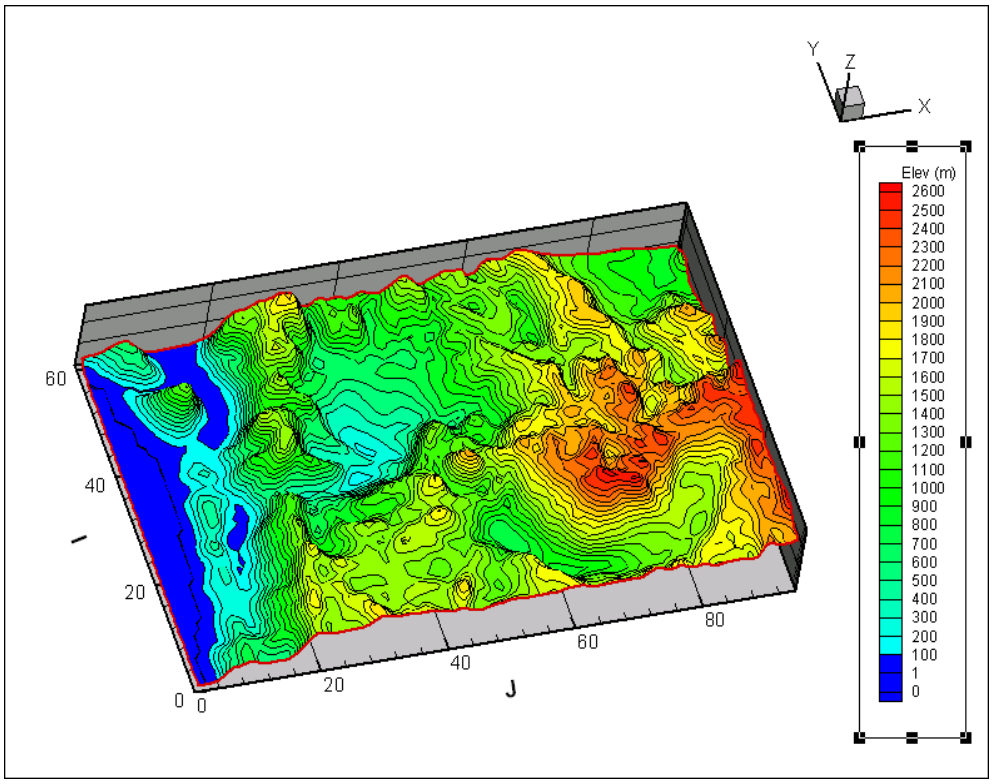

In performing the nested domain simulations, the parent domain was used to perform a base-case simulation for the first time. This base-case simulation was part of a fifteen-day simulation by O'Neill et al. (2002). Model spin-ups to equilibrate initial conditions were performed prior to the start of the modeling period. The solutions from the parent domain simulation were processed to extract the initial conditions and boundary conditions for the subsequent sub-domain sensitivity simulations. The sub-domain boundary conditions were thus time dependent outputs from the solution of the parent domain. This set of initial and boundary conditions remained unchanged for all sensitivity simulations. The sensitivity model period spans 3 days, from July 13 to 15, 1996.

This nested modeling method reduced the computational time by calculating a smaller area while taking into account transport and meteorological influences of a larger parent domain. Using this method, more simulations could be performed within a reasonable time frame. Each layer of the parent domain was made up of 142 by 136 grid cells, while in the sensitivity sub-domain each layer had only 94 by 61 cells. The smaller modeling area shortened the processing time by one-third to 20 minutes per simulation hour using a single processor COMPAQ/Dec Alpha ES40 workstation.

2.2.2 Model Framework

The entire model system consisted of models and software that pre- and post-process data to and from the main CMAQ model. Figure 3 shows the schematic for the model framework adopted in this study. CMAQ was the primary processor that performed the pollutant chemistry and transport modeling. The two most important inputs into any air quality model, including CMAQ, are the meteorological fields and the gridded emissions inventory. In this study, the 1996 Northwest Regional Modeling Center (NWRMC) emissions inventory was selected as the base-case emissions (Washington State Department of Ecology et al., 2002). The inventory contained both anthropogenic and biogenic emissions. Meteorological data for

the CMAQ model were generated from the MM5 meteorological model. The following sections describe the modeling framework in further detail.

2.2.2.1 Anthropogenic Emissions

Anthropogenic emissions are from sources such as automobiles, residential areas and industries. The NWRMC anthropogenic emissions were based on activities and emission factors for the year 1996 and compiled by the Washington Department of Ecology with assistance from the corresponding Idaho and Oregon state agencies. The NWRMC inventory contained area, point and mobile sources. The mobile sources included both off-road and on-road categories. The off-road emissions were from ships, aircrafts and non-highway vehicles and the on-road emissions were from highways and major roadway vehicles. Table 1 shows the sources and pollutants included in this anthropogenic emissions inventory. PM10 and PM2.5 in the table were primary aerosols emitted by the specific sources.

The SMOKE processor (Houyoux and Vukovich, 1999; Houyoux et al., 2000) was used to process the anthropogenic emissions into a gridded, hourly allocated and chemically speciated format used by CMAQ. VOC and PM emission categories were also speciated to the CMAQ final chemical mechanism (RADM2) species. Appendix A provides definitions of the CMAQ-RADM2 gas and aerosol specie categories. The speciation profiles were source specific, such that different emission sources had different speciation schemes. The profiles were compiled from information in the SPECIATE program (U.S. EPA, 1999b). For the on-road mobile sources, SMOKE used the MOBILE5b emissions factor model (U.S. EPA, 2000) to generate hourly temperature dependent emission factors for the modeling episode. Temperature adjustments on mobile emissions were important since there are more evaporative emissions at higher ambient temperature. For point sources, the SMOKE processor calculated the active plume rise for each stack source based on stack parameters, wind speed and temperature. The total stack emissions were partitioned to different vertical layers to represent the spatial location of primary pollutants.

Figure 3: Schematic of the modeling system used in this sensitivity study.

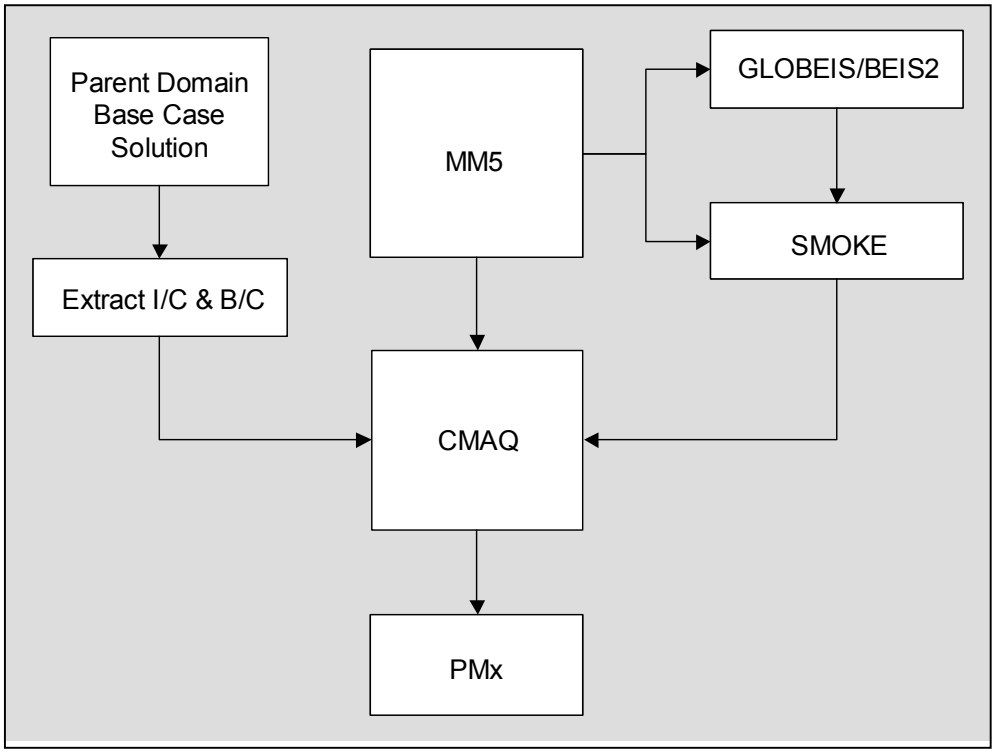

Table 1: Anthropogenic emission sources and pollutants included in the Northwest Regional Modeling Center (NWRMC) 1996 emission inventory (Washington State Department of Ecology et al., 2002).

Category	Pollutants
AREA SOURCES	
Architectural Surface Coating	VOC
Industrial Surface Coating	VOC
Solvent Cleaning	VOC
Commercial/Consumer Solvents	VOC
Livestock	NH_3
Soil	NH_3
Vegetation (Biogenics)	VOC, NO_x
NONROAD MOBILE SOURCES	
Agricultural Equipment	CO, NH_3, NO_x, PM_{10}, $PM_{2.5}$, SO_2, SO_4, VOC
Airport Ground Support Equipment	CO, NH_3, NO_x, PM_{10}, $PM_{2.5}$, SO_2, SO_4, VOC
Commercial Equipment	CO, NH_3, NO_x, PM_{10}, $PM_{2.5}$, SO_2, SO_4, VOC
Construction and Mining Equipment	CO, NH_3, NO_x, PM_{10}, $PM_{2.5}$, SO_2, SO_4, VOC
Industrial Equipment	CO, NH_3, NO_x, PM_{10}, $PM_{2.5}$, SO_2, SO_4, VOC
Lawn and Garden Equipment	CO, NH_3, NO_x, PM_{10}, $PM_{2.5}$, SO_2, SO_4, VOC
Logging Equipment	CO, NH_3, NO_x, PM_{10}, $PM_{2.5}$, SO_2, SO_4, VOC
Oil Field Equipment	CO, NH_3, NO_x, PM_{10}, $PM_{2.5}$, SO_2, SO_4, VOC
Pleasure Craft	CO, NH_3, NO_x, PM_{10}, $PM_{2.5}$, SO_2, SO_4, VOC
Railroad Equipment	CO, NH_3, NO_x, PM_{10}, $PM_{2.5}$, SO_2, SO_4, VOC
Recreational Equipment	CO, NH_3, NO_x, PM_{10}, $PM_{2.5}$, SO_2, SO_4, VOC
Underground Mining Equipment	CO, NH_3, NO_x, PM_{10}, $PM_{2.5}$, SO_2, SO_4, VOC
Aircraft	CO, NH_3, NO_x, PM_{10}, $PM_{2.5}$, SO_2, SO_4, VOC
Locomotives	CO, NOx, PM_{10}, PM2.5, SO2, VOC
ONROAD MOBILE SOURCES	
Onroad Mobile Sources	CO, NH_3, NO_x, PM_{10}, $PM_{2.5}$, SO_2, SO_4, VOC
POINT SOURCES	
Major Sources	CO, NH_3, NO_x, PM_{10}, $PM_{2.5}$, SO_2, VOC

2.2.2.2 Biogenic Emissions

Biogenic emissions are natural emissions from soil, plants and other biological activities. The 1996 NWRMC biogenic emissions inventory was generated using the Global Biosphere Emissions and Interactions System (GLOBEIS) emissions model (Guenther et al., 2000). This model uses the latest Biogenic Emissions Landuse Dataset Version 3 (BELD3) (U.S. EPA, 2001) and predicted hourly solar radiation and temperature to calculate biogenic hydrocarbon emissions for the simulation period across the domain. The outputs from GLOBEIS were hourly emissions of 18 terpene species, methyl-butanol (MBO), isoprene and other non-methane VOCs. Since GLOBEIS does not estimate natural NOx emissions, the Biogenic Emissions Inventory System2 (BEIS2) biogenic emissions model was used to provide NOx emissions from plants and soils (U.S. EPA, 1998).

Table 2 shows the average daily emissions over the sensitivity domain processed by the SMOKE, GLOBEIS and BEIS2 models. Between biogenic and anthropogenic emissions, biogenics made up 93% of total daily VOC emissions and anthropogenics made up 80% of total daily NO emissions across the domain. In terms of primary aerosol emissions, the inventory contained only anthropogenic sources. Primary biogenic aerosols, mostly from biomass burning, were not accounted for the 1996 NWRMC inventory. Figures 4a and 4b show the spatial distribution of VOC and NOx emissions within the first layer of the domain. The spatial patterns clearly showed emission hotspots around the high population and high traffic locations.

Table 2: Average daily biogenic and anthropogenic emissions (metric tons per day) across the sensitivity domain.

Model Species*	Area and Non-Road Mobile Sources	On-Road Mobile Sources	Point Sources	Total Anthropogenic Sources	Biogenic Emissions	Total Emissions	Percent Anthropogenic
ALD	13	6	0	19	849	868	2%
CSL	0		0	1		1	100%
ETH	53	16	3	73	184	256	28%
HC3	245	40	12	297	6199	6496	5%
HC5	357	87	10	453		453	100%
HC8	387	101	15	503		503	100%
HCHO	29	2	3	35	1634	1669	2%
ISO	0				2099	2099	0%
KET	11		4	14	1433	1447	1%
OL2	78	41	4	123	763	886	14%
OLI	103	21	4	128	2860	2988	4%
OLT	46	35	3	84	7904	7988	1%
ORA2	0		0	0	368	368	0%
TERPB	0				8545	8545	0%
TOL	184	115	12	311		311	100%
XYL	251	90	6	347		347	100%
Total VOC	1758	554	77	2388	32838	35226	7%
CH4	427	108	13	548		548	100%
CO	13071	6129	820	20020	5072	25092	80%
NH3	65		15	80		80	100%
NO	674	484	157	1314	329	1644	80%
NO2	70	39	27	136		136	100%
SO2	264		487	751		751	100%
SULF	21		6	27		27	100%
PEC	74		6	79		79	100%
PMC	36		44	80		80	100%
PMFINE	30		60	90		90	100%
PNO3	1		0	1		1	100%
POA	82		14	96		96	100%
PSO4	4		13	16		16	100%

* Model species used in the CMAQ model are defined in Appendix A.

Figure 4: Spatial distribution of biogenic and anthropogenic VOC and NOx primary emissions (moles compound s^{-1} $grid^{-1}$) within the first layer of the domain.

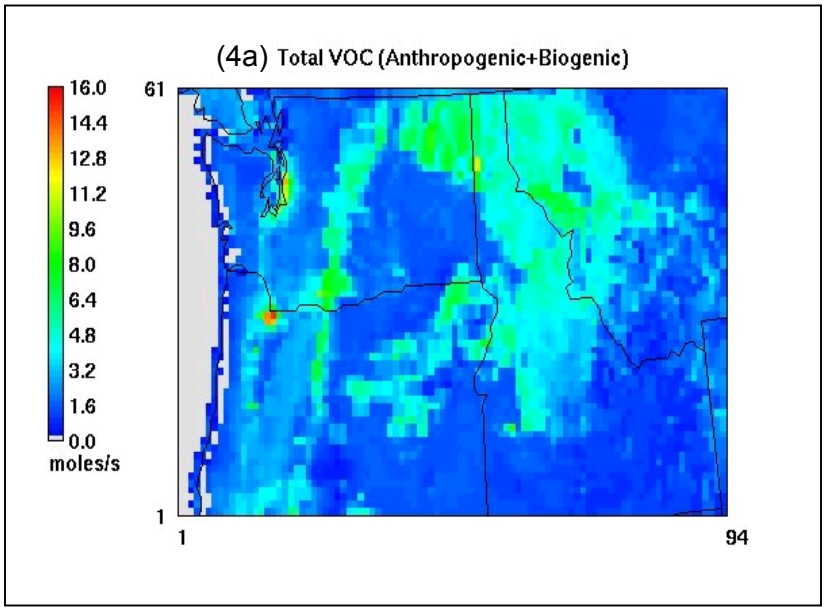

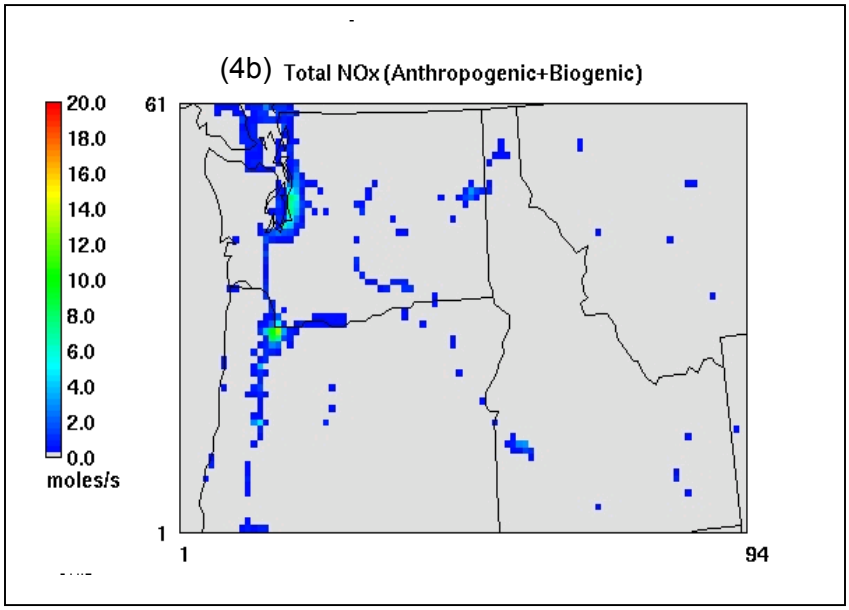

2.2.2.3 Meteorology

Accurate and complete meteorological information is also critical for accurate air quality modeling. Wind speed and wind direction determine the transport of pollutants. Temperature, relative humidity and short and long-wave radiation determine the chemical reaction dynamics. The MM5 (version-3) model was applied to simulate hourly meteorological conditions for CMAQ. MM5 is the Fifth-Generation PSU/NCAR Mesoscale Meteorological model. The model was applied using the one-way nesting method from 36km down to 12km grid resolution. Figure 5 shows the MM5 simulations domain. Four-dimensional data assimilation (FDDA) analysis nudging was applied to both domains to adjust for the predicted wind speed, temperature and atmospheric moisture. The primary function of the FDDA nudging was to improve the MM5 solution towards achieved meteorological analysis fields. In this application, the analysis fields were from the National Center for Environmental Prediction (NCEP) Global Data Assimilation System (GDAS) database. The MM5 solution for wind speed, wind direction and temperature were compared against several surface and upper air monitoring stations in the domain. Table 3 summarizes the model performance statistics in terms of absolute error, normalized gross error and index of agreement. For detailed MM5 performance statistics please refer to the paper by O'Neill and colleagues (2002).

2.2.2.4 The Community Multi-Scale Air Quality Model (CMAQ)

CMAQ was the core chemical transport model in the framework. It is a three-dimensional Eulerian grid model developed by the EPA (U.S. EPA, 1999a). The model solves the specie conservation equation for each grid cell, and contains modules that offer a choice of gas-phase chemical mechanisms (RADM2 and CB-IV). It is also one of the first models to include cloud processes, aerosol dynamics and plume-in-grid modeling techniques to simulate chemical dynamics in the atmosphere (Byun and Ching, 1999). In this application of CMAQ, the RADM2 gas-phase chemical mechanism was applied with aerosol dynamics and cloud processes.

Figure 5: MM5 simulation domain. Grid resolution for parent domain (D02) was at 36 km and nested domain (D03) was at 12 km.

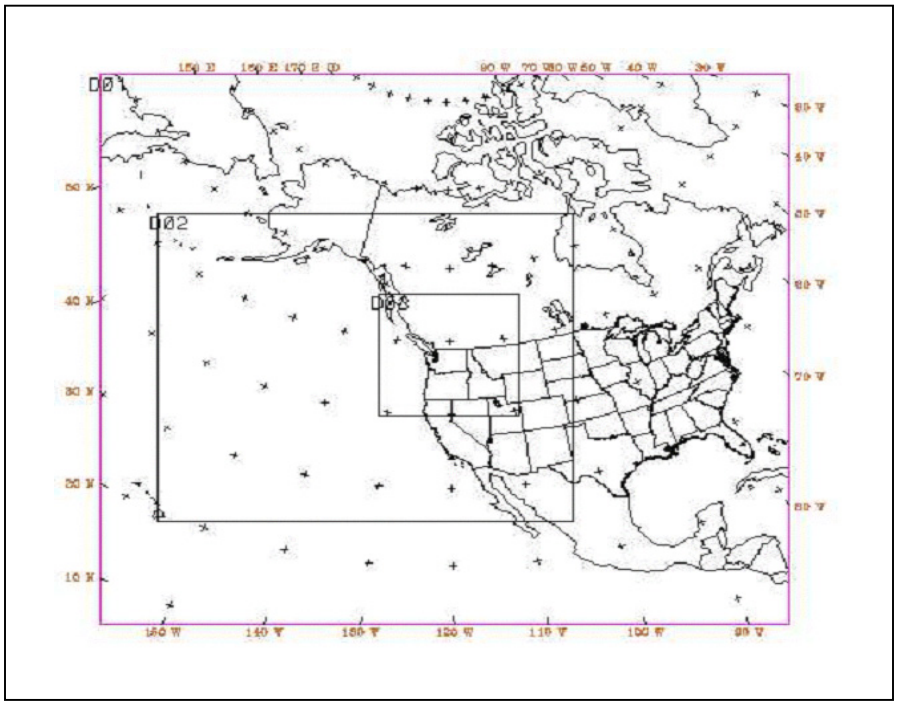

Table 3: MM5 model performance statistics for wind speed, wind direction and temperature compared with 46 surface observational stations (O'Neill et al., 2002).

	Wind Speed (m/s)	Wind Direction (degree)	Temperature (^{o}C)
Mean Error	-1.1	6.4	0.09
Absolute Mean Error	2.0	51	3.4
Index of Agreement*	0.70	0.88	0.80

*Index of one indicates perfect agreement between modeled and observed values.

There are three modules in CMAQ to perform ozone chemistry and aerosol dynamics calculations. The RADM2 gas-phase chemical mechanism carried out the gas-phase and photolytic reactions, while the inorganic and organic aerosol modules performed aerosol phase partitioning calculations to determine the formation of secondary aerosol in the air.

The RADM2 chemical mechanism contains 137 gas-phase reactions and 21 photolytic reactions involving 57 modeled chemical species (Appendix A). The species can be divided into organic and inorganic categories. Inorganic chemistry is better understood than organic chemistry. There are ten modeled inorganic species in the RADM2 mechanism. All of them are explicitly defined in terms of their reaction and kinetics. Organic chemistry, on the other hand, is much more complex and involves more species. Since there are more organic compounds in the atmosphere, VOCs are 'lumped' into modeled groups to reduce computational costs. Molecules with similar oxidation potential and/or similar molecular weight and structure are lumped together as one modeled specie. The RADM2 in CMAQ contains twelve lumped species and five explicitly defined organic species. The five explicit species are: methane, ethane, ethene, isoprene and formaldehyde.

In addition to the formation of ozone and other gas phase products, the RADM2 mechanism also calculates the formation of aerosol precursors such as H_2SO_4, HNO_3, NH_4^+ and condensable organics. These species are precursors to secondary aerosols in the air. They are formed from the oxidized products of SO_2, NOx, NH_3 and VOC gases. Once these condensable species are formed, they are passed to the inorganic and organic aerosol modules for partitioning between gas/aerosol phases to determine the final formation of secondary aerosols in the air.

CMAQ adopts the Model for an Aerosol Reacting System (MARS) inorganic aerosol module to predict inorganic secondary aerosols of sulfate (ASO4), nitrate (ANO3), ammonium (ANH4) and aerosol water (AH2O) (Saxena et al., 1986). The module assumes thermodynamic equilibrium, such that equilibrium exists instantly between the gas and the particulate phase of

all particle sizes. The chemical compositions of the inorganic aerosols depend on the temperature, relative humidity and molar ratio of total ammonia (TNH4 = $[NH_4^+]$ + $[NH_3]$) to total sulfate (TSO4 = $[SO_4^{2-}]$): TNH4/TSO4. Temperature and relative humidity determine the equilibrium constants and aerosol water content. The TNH4/TSO4 molar ratio determines the dominant aerosol composition in the system. If the TNH4/TSO4 ratio is greater than 2, then the abundant ammonium cation neutralizes all sulfate ions and some of nitrate to form ammonium sulfate ($(NH_4)_2SO_4$) and ammonium nitrate (NH_4NO_3) salts. If the ratio is between 0 and 2, then the sulfate is neutralized at different levels by ammonium to form sulfuric acid (H_2SO_4), ammonium bisulfate (NH_4HSO_4) and/or letovicite ($(NH_4)_3H(SO_4)_2$). In both cases, the concentrations of the sulfate, nitrate, and ammonium ions are determined by iterative equilibrium calculations with the relevant equilibrium constants.

CMAQ does not explicitly treat sea salt chemistry and crustal species (Ca^+, Mg^+, K^+ and CO_3^{-2}). In comprehensive reviews by Zhang et al. (2000) and Saxena et al. (1986) they showed that even though MARS has simplified inorganic aerosol chemistry, results are comparable to those predicted by other more complicated methods. However, since it does not have sea salt and crustal species chemistry, it must be used with caution in areas where sea-salt contribution or wind-blown dusts are important. With introduction of crustal species and sea salt chemistry, the formation of secondary aerosol can change. For example, with introduction of sea salt, the additional sodium and chloride ions increases secondary aerosol formation to include species such as: ammonium chloride (NH_4Cl), sodium nitrate ($NaNO_3$), sodium sulfate (Na_2SO_4) and sodium bisulfate ($NaHSO_4$).

Secondary organic aerosol (SOA) formation in CMAQ is based on the vapor saturation principle of (Pandis et al., 1992). Several air quality models adopt this approach to estimate SOA formation in the atmosphere (Jacobson, 1997; Lurmann et al., 1997; Middleton, 1997). In this approach, SOA is estimated from the amount of condensable organics from the gas-phase mechanism. Condensable organics are long-chain hydrocarbons that are oxidized by

atmospheric oxidants such as ozone (O_3), nitrate radical ($NO_3^{\cdot}$) and hydroxyl radical ($OH^{\cdot}$). These condensable organics have low volatility and can partition into the aerosol phase readily. CMAQ uses tabulated aerosol yield factors to estimate the fraction of SOA formed from total condensable organic concentrations. Six such species are modeled in CMAQ. Their aerosol yield factors are listed in Table 4. SOA formed from these species are divided into either anthropogenic or biogenic origin. VOC species: HC8, OLI, TOL, XYL and CSL are anthropogenic. Their aerosol products are lumped into the AORGA group as anthropogenic aerosol. Terpenes (TERP) are biogenic emissions and their aerosol products are grouped into the AORGB category as biogenic aerosol.

CMAQ's approach in estimating the SOA formation is simplified. This is because of the complexity of atmospheric organic chemistry and the limited knowledge on SOA formation mechanisms in the ambient environment (Turpin et al., 2000). One major disadvantage of using this method is that the aerosol yields are empirically determined in smog chambers. They are very chemical-specific, and the yields do not take into account the actual kinetics during the formation of the secondary and tertiary oxidized species. The method also does not treat organic aerosol dynamics such as absorption, adsorption, or dissolution once SOAs are formed. Seigneur et al. (1999) suggest that this fixed yield approach is applicable for compounds that have a low vapor pressure, but it is likely to be inaccurate for compounds with high vapor pressures.

Table 4: Fixed aerosol yield factors for modeled condensable organic gases in CMAQ.

Category	CMAQ Condensable Organic Gas Precursor	Aerosol Yield ((μg m^{-3}) ppm^{-3})
AORGA (Anthropogenic)	CSL	221
	HC8	380
	OLI	247
	TOL	424
	XYL	342
AORGB (Biogenic)	TERP	740

In terms of particle size distribution and aerosol dynamics, CMAQ uses the approaches of the Regional Particulate Matter (RPM) module (Binkowski and Shankar, 1995). In this module, the particle size distribution is based on the modal approach where particles are approximated by three lognormal distributions, or modes, that over-lap each other. The three modes distinguish the size of total modeled particles in CMAQ. The Aitkin (I) mode represents newly nucleated fine particles with geometric mean diameter of 3.5nm, the Accumulation (J) mode represents larger particles that formed from coagulation of the I mode particles, and the Coarse mode represents even larger particles such as sea salt and wind-blown dust. The Coarse mode particles have geometric mean diameter >6μm. Both the I and the J mode aerosols are considered fine particles that attribute to visibility degradation. The Coarse mode particles are mostly primary pollutants that are emitted from emission sources. There are no secondary contributions of Coarse mode particles in the atmosphere. The aerosol dynamic processes that are accounted in CMAQ are coagulation, condensation growth, nucleation, dry deposition and particle mass transfer.

2.2.2.5 Post Processing

CMAQ outputs aerosol species mass concentrations in three modes. Appendix B lists the CMAQ aerosol specie labels and their corresponding descriptions. Nine species are accounted for in both the Aitkin and Accumulation modes: ASO4, ANO4, ANH4, AH2O, AORGA, AORGB, AORGPA, AEC and A25. Only three species are counted as Coarse mode particles: SEAS, ACORS and ASOIL. The PMx program (Jiang and Yin, 2002) was used to post-process CMAQ aerosol output from lognormal modal concentrations into aerodynamic size resolution concentrations. This program accounts for the modal standard deviations and geometric mean diameters to locate the appropriate cut off points for the PM size range in the three lognormal distributions. Although PM2.5 in CMAQ can be approximated by adding the I and J mode modal concentrations together, the results from the PMx are more explicit. This is because

adding the I and J mode particles can over-estimate the actual PM2.5 concentrations, as the tail of the J mode distribution can have aerodynamic diameters greater than 2.5μm.

2.2.3 Configuration of Sensitivity Runs

Sensitivity simulations were performed using the direct emission change method to examine the final changes in both aerosol and ozone formation. All simulations shared the same configuration as the base-case run, except for stepwise, domain-wide changes in VOC, NOx, SO2 or NH3 emissions by ±25%, ±50% or ±100% from the base-case emissions. For combined emissions sensitivity, NOx together with VOC (NOx&VOC) and NOx together with NH3 (NH3&NOx) were also performed.

In the base-case simulation, the emissions inventory contained both anthropogenic and biogenic sources with 0% change. For other sensitivity simulations, biogenic emissions were included and unchanged. The only change to biogenic emissions was during biogenic VOC sensitivity simulations, where biogenic VOCs (bVOC) were adjusted. In the biogenic VOC sensitivity runs, a full set of anthropogenic emissions was included. Changes in ozone and PM2.5 mass concentration from the sensitivity simulations were compared against the base-case results. Any changes in the sensitivity simulations were directly due to the changes in precursor emissions. The results for ozone and PM2.5 were analyzed for different areas in the domain.

One disadvantage to this sensitivity analysis method was that the absolute amounts of precursor emissions changes were not uniform across the domain. This is because fixed percentage changes on precursor emissions produced a higher magnitude of change for areas with high base-case emissions but a relatively low magnitude of change for areas with low base-case emissions. This uneven change in absolute emissions across the domain might result in low emission areas being insensitive to changes in precursor emissions.

2.3 Ozone and Aerosol Formation Chemistry in the Atmosphere

Prior to evaluating the ozone and aerosol sensitivity with the air quality model, it is helpful to review the underlying atmospheric chemistry related to the formation of these pollutants. More detailed reviews of the chemistry of secondary aerosol and ozone formation have been covered in many other studies (Atkinson, 2000; Blanchard, 2000; Lurmann et al., 1997; Meng et al., 1997; Meng et al., 1998; Saxena et al., 1986; Seinfeld and Pandis, 1998; Turpin et al., 2000).

2.3.1 Aerosol Formation Chemistry

Secondary aerosol formation involves complex physical and chemical processes in conjunction with each other. In physical processes, nucleation, condensation and coagulation contribute to aerosol formation and particle growth. In chemical processes, aerosols are reaction products that have low saturation vapor pressures and exist as solid phase salts or aqueous phase ions. Both organic and inorganic gas reactions can contribute to the formation of aerosols. Inorganic aerosol chemistry is better understood than organic aerosol chemistry due to the complex distribution of organic compounds, and the difficulties in measuring the primary and secondary contribution of organic aerosol in the air (Seigneur, 2001; Turpin et al., 2000). This section focuses on the chemical formation of secondary inorganic aerosols.

Numerous chemical species have been identified in the composition of inorganic fine aerosols. The most prevalent inorganic aerosols in urban areas are sulfate, nitrate, ammonium and water (Seinfeld and Pandis, 1998). Chemical systems involving their gaseous precursors – SO_2, H_2SO_4, HNO_3, NH_3 and H_2O – have been subject to much theoretical and experimental investigation. Sulfate in the atmosphere comes from the oxidation of sulfur dioxide, which is ubiquitous in anthropogenic emissions. In acidic environments, sulfate exists as sulfuric acid (reactions R1-R3).

$$SO_2 + OH^{\cdot} \rightarrow\rightarrow H_2SO_4 \qquad \text{(R1)}$$

$$SO_2 + H_2O_2 \rightarrow H_2SO_4 \qquad \text{(R2)}$$

$$SO_2 + O_3 \rightarrow\rightarrow H_2SO_4 \qquad \text{(R3)}$$

Ammonia is the most abundant basic gas and the dominant inorganic cation in the atmosphere. It is emitted from livestock operations and fertilizers. Once emitted, it can partition into gas or aqueous phases, depending on the chemical system (reaction R4).

$$NH_3 + H_2O \Leftrightarrow NH_4^+ + OH^- \qquad \text{(R4)}$$

Nitrate in the form of nitric acid comes from the oxidation of NOx, which is also abundant in urban air masses (reactions R5-R6).

$$NO_2 + OH^{\cdot} \rightarrow HNO_3 \qquad \text{(R5)}$$

$$N_2O_5 + H_2O \rightarrow 2HNO_3 \qquad \text{(R6)}$$

Among sulfate, nitrate and ammonia, various secondary aerosols can form depending on the concentration of each individual species, temperature and relative humidity. In the solid phase, ammonium bisulfate (NH_4HSO_4), letovicite ($(NH_4)_3H(SO_4)_2$), ammonium sulfate ($(NH_4)_2SO_4$) and ammonium nitrate (NH_4NO_3) salts can be present when the relative humidity (RH) is lower than the delinquence relative humidity (DRH) of these salts. Appendix C lists the DRH of these salts. When RH is higher than the DRH, the salts dissolve in water and aerosols are present as $NH4^+$, HSO_4^-, SO_4^{-2} and NO_3^- ions.

To identify the formation of aerosol compositions in this three-compound chemical system, one usually refers to the system's total ammonia to total sulfate molar ratio: TNH4/TSO4. The science behind the ratio is as follows. Sulfate ions have very low volatility and are highly hygroscopic. They exist almost completely in the aerosol phase when formed. Nitrate and ammonia, on the other hand are more volatile. They can partition between both gas and aerosol phase. The amount partitioned depends on equilibrium constants and the concentrations of all three species in the system. When ammonia and nitric acid are present in the gas-phase with no sulfate, nitrate as nitric acid can react directly with ammonia to form secondary PM as ammonium nitrate aerosols (reaction R7):

$$NH_{3(g)} + HNO_{3(g)} \Leftrightarrow NH_4NO_{3(s)} \qquad (R7)$$

At high relative humidity (RH>DRH (NH_4NO_3)), the ammonium nitrate salt dissolves and partitions into the aqueous phase as nitrate and ammonium ions.

However the formation of ammonium nitrate also depends on sulfate concentration. When all three compounds are present in the system, sulfate ions are thermodynamically favored to react with ammonium ions and exist as neutralized ammonium bisulfate, letovicite or ammonium sulfate, depending on the ammonia concentration (Saxena et al., 1986; Seinfeld and Pandis, 1998). When this happens, the ammonia concentration is reduced, and less ammonia is available to form ammonium nitrate with nitric acid (reaction R7). The formation of nitrate aerosol becomes important only when ammonia concentration is increased and most of the sulfate in the system is neutralized to ammonium sulfate.

Using the ammonia to sulfate molar ratio makes it easier to estimate the aerosol composition in this three-compound chemical system (table 5). At ratios 0.5-1.25, ammonium bisulfate is the dominant component of the system, as ammonium concentration is low. When ratios reach unity, letovicite is formed and it gradually replaces ammonia bisulfate to be the dominant specie, until ratios reach about 1.5. At ratios above 1.5, ammonium sulfate starts to form and it becomes the only sulfate component as ratios exceed 2. At the same time, nitrate aerosol concentration increases from the formation of ammonium nitrate.

The transition of neutralized sulfate at different TNH4/TSO4 ratios divides the chemical system into two regions: ammonia-poor and ammonia-rich regimes. Ammonia-rich is defined when the molar ratio of total ammonia to sulfate is greater than 2, and ammonia-poor is when the ratio is less than 2.

In the ammonia poor case, there is insufficient NH_3 to neutralize the available sulfate, and the system is acidic from the presence of both H_2SO_4 and HNO_3 acids. Sulfate in this condition exists as bisulfate and/or letovicite depending on the ammonia availability. The gas phase NH_3 is low and the formation of ammonia nitrate salt is also very low.

Table 5: Dominant aerosol composition as a function of the TNH4/TSO4 ratio in a two-component chemical system.

TNH4/TSO4 Ratio							Dominant Chemical Specie
< 0.5	0.75	1	1.25	1.5	1.75	> 2	
←							H_2SO_4
●	———	●					NH_4HSO_4
		●	———	●			$(NH_4)_3H(SO_4)_2$
					———	→	$(NH_4)_2SO_4$

In the ammonia rich case however, the formation of ammonium nitrate is higher. This is because when the ammonia molar concentration is more than twice that of the sulfate molar concentration, the system is dominant with neutralized $(NH_4)_2SO_4$ aerosol (solid or aqueous phase depending on RH), and there is available ammonia to react with nitric acid to produce ammonium nitrate aerosol.

CMAQ's inorganic aerosol module is base on the same principle of identifying the ammonia rich and ammonia poor regimes. In the following discussion we relate the PM2.5 responses in different areas to the ammonia-rich and ammonia-poor regions. This measurable ratio is a good indicator of how PM2.5 responds to changes in the SO_2, NOx and NH_3 precursor emissions.

2.3.2 Ozone Formation Chemistry

Ozone formation chemistry is better understood than aerosol formation chemistry. In the troposphere, ozone is formed from photochemical reactions involving NOx, VOC. Reactions R8 and R9 show the ozone formation pathway from the reaction of atomic oxygen with molecular oxygen. In the troposphere, the main source of atomic oxygen is the photolysis of NO_2 at wavelengths <424nm (Seinfeld and Pandis, 1998).

In an unpolluted atmosphere, the ozone concentration is maintained by reaction R10, which continuously removes ozone through reactions with NO, which regenerates NO_2 and O_2. This cycle of ozone production and destruction establishes the background steady state concentration of ozone around 30 to 40ppbv.

$$NO_2 + h\nu \rightarrow NO + O \qquad \text{(R8)}$$

$$O + O_2 \rightarrow O_3 \qquad \text{(R9)}$$

$$O_3 + NO \rightarrow NO_2 + O_2 \qquad \text{(R10)}$$

In the polluted atmosphere however, the chemical production of ozone can increase from the introduction of higher VOC and NOx emissions. Anthropogenic NOx are mainly emitted from automobiles and power plants while VOCs are released from a wider range of sources, including automobiles, various industrial processes, solvent use, and vegetation. NOx emissions from automobiles consist of approximately 90% NO and 10% NO_2. Initially at very high NO levels, ozone is reduced through reaction R10, however once the plume starts to dilute and mix with VOCs, there is a net ozone production from the catalytic conversion of NO to NO_2 as follows:

$$OH^{\cdot} + R\text{-}H + 2O_2 \rightarrow\rightarrow RO_2^{\cdot} + HO_2^{\cdot} + H_2O + R'CHO \qquad (R11)$$

$$RO_2^{\cdot} + NO \rightarrow NO_2 + RO^{\cdot} \qquad (R12)$$

$$HO_2^{\cdot} + NO \rightarrow NO_2 + OH^{\cdot} \qquad (R13)$$

These three general reactions show NO being converted to NO_2 in the presence of VOCs which act as catalysts. R-H in reaction R11 denotes the carbon-hydrogen bonds from VOCs. In the daytime when hydroxyl radical ($OH^{\cdot}$) concentrations are high, R-H is oxidized to form peroxy radicals ($RO_2^{\cdot}$) and hydroperoxy radicals ($HO_2^{\cdot}$). These two highly reactive radicals can readily convert NO to NO_2 (reactions R12, R13) without deteriorating ozone as in reaction R10. From the above reactions, one molecule of VOC can catalyze the formation of at least 2 molecules of NO_2. The NO_2 molecules can, in turn, form 2 molecules of ozone through R8 and R9. These reactions provide a continuous of ozone production mechanism and results in accumulated ozone concentrations. VOCs in this description are generic reactive hydrocarbons. Since VOCs of different molecular structures have different reactivities, several modeled VOC species are required in the RADM2 mechanism to better represent the reaction kinetics in the atmosphere.

In terms of ozone sensitivity to changes in NOx and VOC emissions, it is known that under some conditions, ozone formation is controlled by NOx concentrations and is insensitive

to VOC concentrations. In other cases, ozone is more sensitive to NOx emissions, but the change is non-linear, where increases in NOx can decrease ozone. These two cases of ozone response are often referred to as NOx-sensitive and VOC-sensitive, respectively.

In the traditional ozone sensitivity study, trajectory or box models were used (Ansari and Pandis, 1999; Jacobson, 1997) and the two sensitivity regions were determined by the VOC to NOx concentration ratio: [VOC]/[NOx] (Jiang et al., 1997; Sillman, 1999). However, it is difficult to use this ratio as the determining factor when three-dimensional grid models, like CMAQ, are applied. This is because grid models calculate the NOx and VOC concentrations at each grid cell for each specific time step. There are no histories of initial emission concentrations from upwind sources, and no information on the paths of the pollutant plume. A more adequate method of judging the VOC/NOx sensitivity is by looking at the secondary chemical species such as the HNO_3 to H_2O_2 ratio: $[HNO_3]/[H_2O_2]$. This ratio has been used by other studies to measure the ozone response to changes in NOx and VOC emissions in other regions (Andreani-Aksoyoglu et al., 2001; Chock et al., 1999; Nenes et al., 1998; Saxena et al., 1986; Sillman, 1995).

The science behind this secondary product ratio ($[HNO_3]/[H_2O_2]$) is that, at high VOC concentrations (NOx sensitive), the oxidized VOCs undergo radical + radical reactions (R14) to form hydrogen peroxide (H_2O_2), and this causes the ratio to go down. On the other hand, at high NOx concentrations (VOC sensitive), NOx reacts with $OH^{\cdot}$ to form HNO_3 (R15) and this causes the ratio to increase.

$$OH^{\cdot} + NO_2 \rightarrow HNO_3 \qquad \text{(R14)}$$

$$HO_2^{\cdot} + HO_2^{\cdot} \rightarrow H_2O_2 + O_2 \qquad \text{(R15)}$$

Therefore, regions with high HNO_3/H_2O_2 ratio are usually NOx abundant and VOC-sensitive, and regions with low ratios are NOx limited and NOx-sensitive. This approach is adopted in the following section to observe the areas of different ozone sensitivity and compare them against the sensitivity simulation results.

2.4 Results and Discussion

This section presents the results and discussion of the CMAQ base-case and sensitivity simulations. The discussion is divided into three parts. The first part briefly discusses the base-case simulation results. The second part covers the PM2.5 sensitivity for four different sites in the domain and the third part focuses on ozone sensitivity in relation to the NOx and VOC emissions at six different locations.

In analyzing the CMAQ simulation results, time series comparisons were made at various points in the domain. Different locations reached peak ozone and aerosol concentrations at different times throughout the simulation period. The analyses focus on the hour when base-case predicted PM2.5 and ozone reached maximum concentrations for individual locations. At these locations, maximum predicted ozone levels usually occurred in the afternoon when solar radiation was high to enhance ozone chemical production. However, the maximum predicted PM2.5 was not as consistent. Maximum PM2.5 concentrations in a location can occur at different times of the day. This is because the final PM2.5 concentration depends on more variables, such as, emission of primary aerosols, concentrations of gaseous precursors, concentrations of atmospheric oxidants, the evolution of planetary boundary layer (PBL) and the physical processes of the aerosol dynamics.

2.4.1 Base-Case Results

The base-case results are similar to the results reported by O'Neill [2002] using the NWRMC emissions inventory. For additional base-case model analyses including model performance statistics, please refer to their work; only a brief description is provided here.

The predicted 1-hour PM2.5 contour plot is shown in Figure 6 for July 14, 1996 at 6 am PST, when maximum domain-average PM2.5 concentrations occurred. The high concentration early in the morning is related to the lack of vertical mixing associated with stable atmospheric conditions and a low mixing height. PM2.5 concentrations between 35μg/m^3 to 40μg/m^3 were

predicted for areas around the Columbia River Gorge, Central Idaho and the north slopes of the Olympic Mountains in the Puget Sound region.

Organic aerosols contributed a larger proportion to the total PM2.5 composition compared to inorganic aerosols throughout the domain. In CMAQ, inorganic PM2.5 is made up of sulfate (ASO4), ammonium (ANH3) and nitrate (ANO3) aerosols. Aerosol water (AH2O) is not included in the inorganic aerosol. The organic PM2.5 consists of secondary anthropogenic (AORGA), primary organic (AORGPA) and secondary biogenic (AORGB) aerosols. Figures 7 and 8 show the percentage organic and inorganic aerosol contribution to the total PM2.5, respectively. Organic aerosols contributed 60% to 80% in central Idaho, western Montana and the Olympic Mountains in Washington. These regions had high biogenic terpene emissions, which led to formation of high secondary organic aerosol. Inorganic aerosols contributed much less to the total PM2.5 in the Pacific Northwest region. Inorganic aerosols represented 12% to 24% in the western regions, and 24% to 30% in the southern and eastern parts of the domain. The higher inorganic composition in the southern and eastern region was due to the lower total PM2.5 concentration in the region and the higher inorganic sulfate levels in the area.

The predicted PM2.5 components were compared with observational data from six Interagency Monitoring of PROtected Visual Environments (IMPROVE) observational sites. Since measurements from the IMPROVE database were 24-hour averages for July 13, 1996, the predicted PM2.5 concentrations were averaged over the first simulation day for comparison. Figure 9 shows the location of these six sites in the domain. The comparisons were made for fine PM2.5 component fractions for sulfate aerosol (SO4), nitrate aerosol (NO3), organic carbon (OC), elemental carbon (EC) and soil fraction (A25I). Figures 10a and 10b show the aerosol contributions by component for the six sites and the extracted CMAQ predicted results. The numbers by the chart indicate the aerosol mass concentration in μg m^{-3} for each fine PM component. The charts showed that CMAQ was able capture the major component

contributions from OC, A25I and SO4 relatively well for the six sites, however, the model underestimated the contribution from NO3.

In terms of ozone predictions, Figure 11 shows the 1-hour predicted ozone contour for July 14, 4pm PST when maximum concentrations occurred. The highest ozone levels of 184 ppbv occurred in areas east of Portland, Oregon, followed by 151 ppbv and 144 ppbv southeast of Seattle, and immediately west of Seattle at the foot of the Olympic Mountains, respectively. Elevated ozone concentrations were also obvious for regions along the Interstate-5 (I-5) Freeway, where ozone was sustained at levels between 70 ppbv to 130 ppbv. In addition, in areas surrounding other smaller cities such as Boise, ID, Spokane, WA and near the Tri-cities region (Kennewick, Pasco and Richland, WA), the predicted ozone concentrations ranged between 70 ppbv to 93 ppbv.

Figure 12 shows the highest predicted 8-hour averaged ozone concentration (July 14, 11am to 6pm). The color scale was set to distinguish areas that were likely to violate the 8-hour, 80 ppbv standard. More areas were at risk of non-attainment with this stricter standard. Smaller cities such as Spokane WA, Tri-cities, WA and Boise, ID had predicted levels of 74 ppb, 98 ppb, and 83 ppbv respectively.

Figure 6: Base-case 1-hour PM2.5 concentrations (μg m^{-3}) for July 14, 1996 at 6am PST.

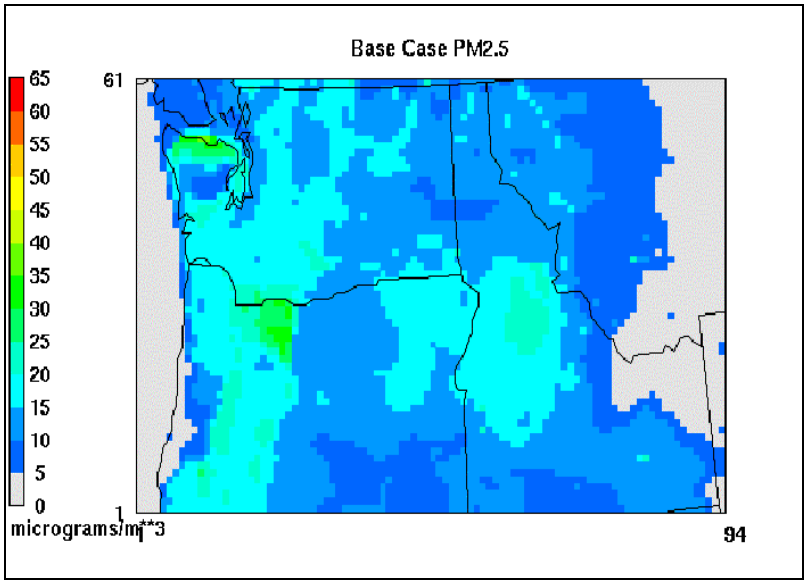

Figure 7: Percentage organic aerosol contribution to the total PM2.5 concentration in the base-case simulation.

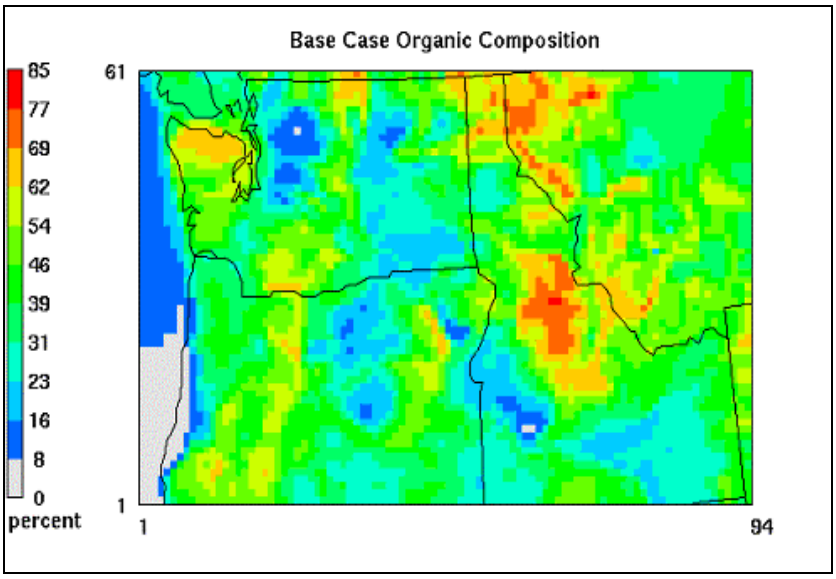

Figure 8: Percentage inorganic aerosol contribution to the total PM2.5 concentration in the base-case simulation.

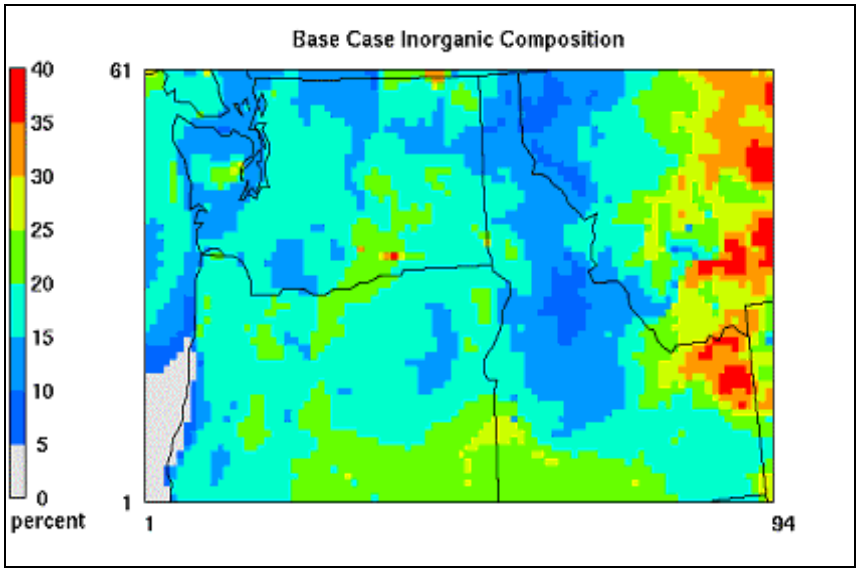

Figure 9: Locations of IMPROVE PM monitoring sites for model comparisons.

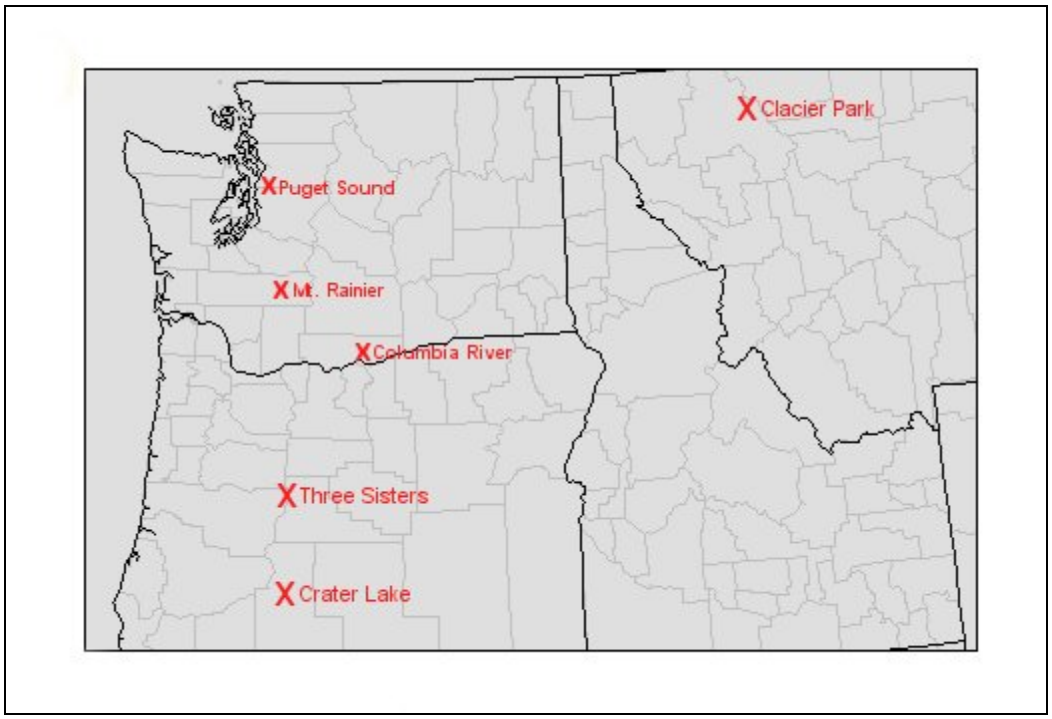

Figure 10a: 24-hour averaged fine PM component concentrations for IMPROVE observation data and CMAQ predicted output for July 13, 1996.

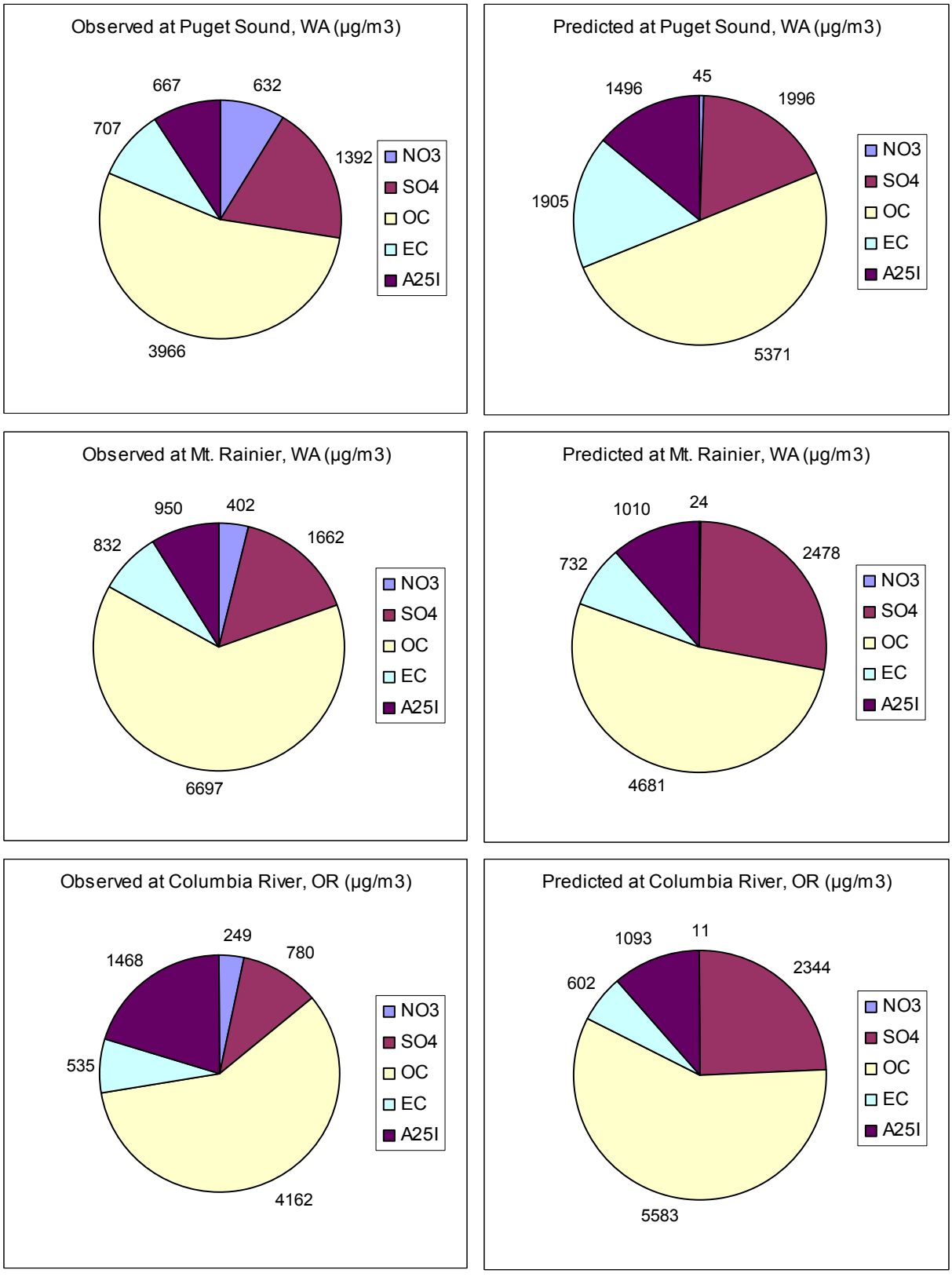

Figure 10b: 24-hour averaged fine PM component concentrations charts for IMPROVE observation data and CMAQ predicted output for July 13, 1996.

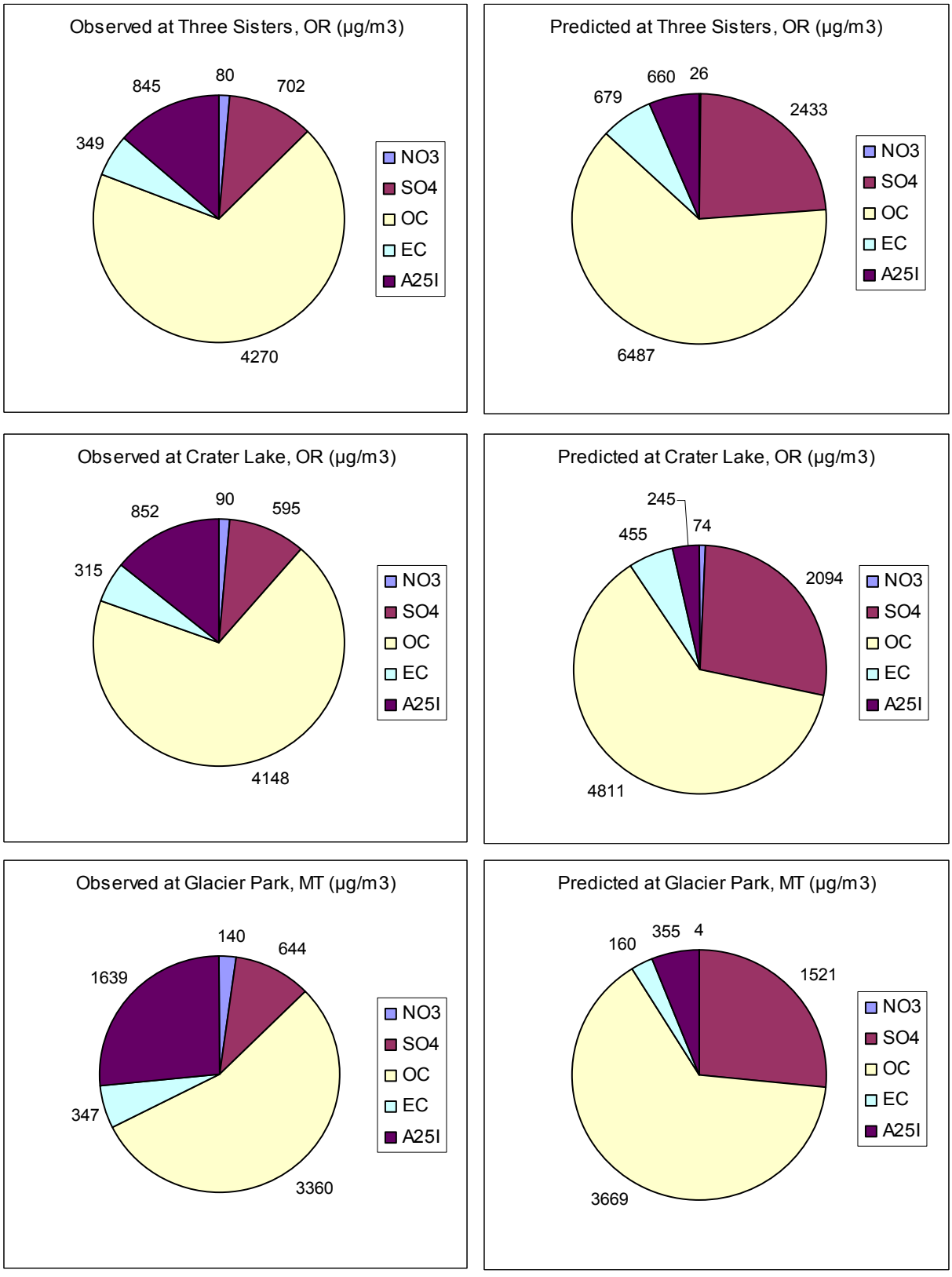

Figure 11: Base-case 1-hour ozone concentrations (ppbv) for July 14, 4pm PST.

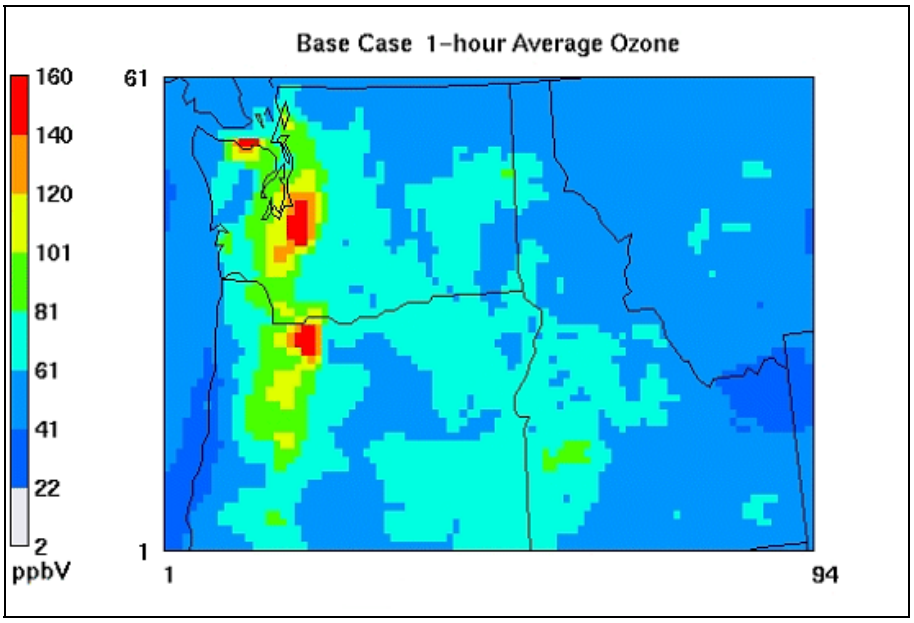

Figure 12: Base-case 8-hour ozone average concentrations (ppbv) for July 14 (11am to 6pm PST).

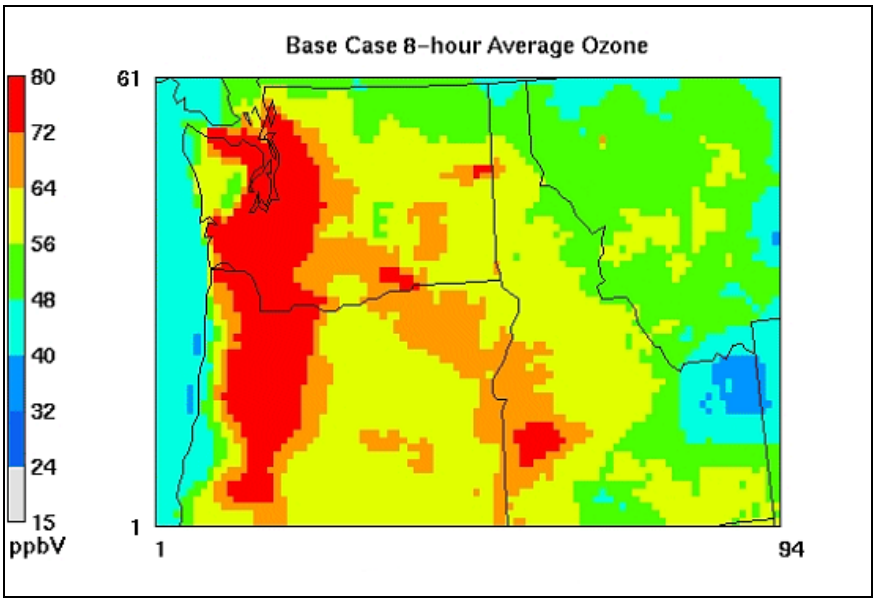

2.4.2 Sensitivity of PM2.5 Concentrations to Precursor Emission Changes

Aerosol sensitivity at a specific location is determined by the amount of aerosols and precursor gases transported to the location. PM2.5 in different areas responds differently to changes in emissions. Four different locations in the domain were selected to represent different systems of response to precursor emission changes. The four locations were Enumclaw, downwind of Seattle, WA; Carus, downwind of Portland, OR; the Columbia River Gorge National Scenic area (CORI) between Oregon and Washington; and the Craters of the Moon National Monument (MC) in Idaho. Figure 13 shows the locations of these sites in the domain. Both Enumclaw and Carus are heavily populated and are affected by large anthropogenic emissions from the nearby urban centers. Both areas had high base-case PM2.5 concentrations compared to the rest of the domain. Enumclaw had peak PM2.5 of 28 $\mu g/m^3$ on July 15, 4am PST, and Carus had peak PM2.5 concentrations of 28 $\mu g/m^3$ on July 14, 1pm PST. The Columbia River (CORI) site is located in the center of the Columbia River Gorge, between the Washington and Oregon State border. The region was designated as a Class I National Scenic area and is protected from visibility degradation. The highest base-case PM2.5 at CORI was 24 $\mu g/m^3$, which occurred on July 14, 9pm PST. The Craters of the Moon (MC) in southeastern Idaho is at 2,000m above sea level and 230km east of Boise. The site is a rural area with little influence from anthropogenic emissions. The maximum predicted base-case PM2.5 concentration was 11 $\mu g/m^3$. The peak concentration occurred on July 14, 5pm PST.

Figure 13: Selected PM2.5 sensitivity locations: Enumclaw in Washington, Carus in Oregon, Columbia River (CORI) in Washington and Craters of the Moon (MC) in Idaho.

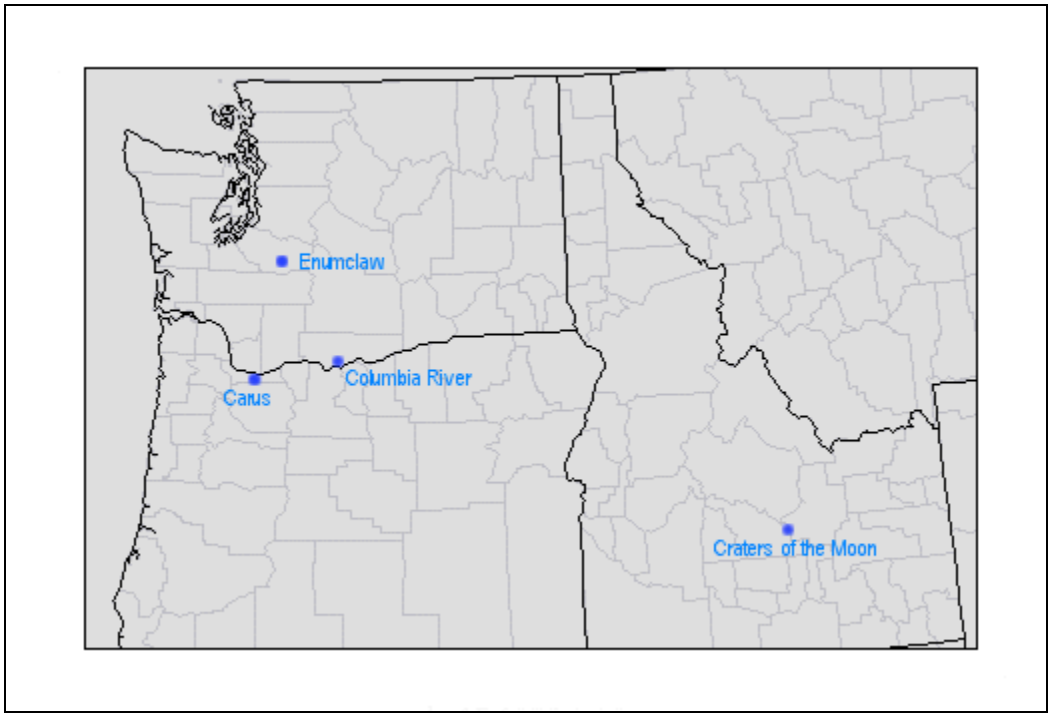

Figures 14a thorough 14d show the results of PM2.5 concentration changes due to changes in the anthropogenic NH3, NOx, SO2 and combined NH3&NOx emissions for Enumclaw, Carus, CORI and MC, respectively. The y-axis indicates the resultant PM2.5 concentration after different precursor emission changes, and the x-axis indicates the percent emission change from the base-case. The base-case result is indicated by 0% emission change, while 100% represents twice the domain wide emission from the base-case and -100% represents zero domain wide emission for the specific specie. Different lines on the figure represent PM2.5 sensitivity for different precursor emissions. Each line is made up of seven points from six sensitivity simulations and one base-case simulation. Appendix D1 through D4 shows the numerical results and the calculated percentage PM2.5 changes from the base-case concentration.

All four sites had a different response to changes in precursor emissions. Enumclaw with the high base-case PM2.5 concentration was sensitive to NOx and NH3 emission changes. Carus and CORI behaved more similarly to each other, but different from Enumclaw. They were insensitive to NH3 changes, but rather sensitive to SO2 changes. In contrast, MC had the lowest base-case PM2.5 concentration, and it was insensitive to almost all the precursor emission changes. Appendix E1 to E4 contains the full set of simulation results for each site during the maximum predicted PM2.5 hour.

Figure 14a: PM2.5 concentrations due to percent changes in domain wide inorganic anthropogenic emissions for Enumclaw, WA.

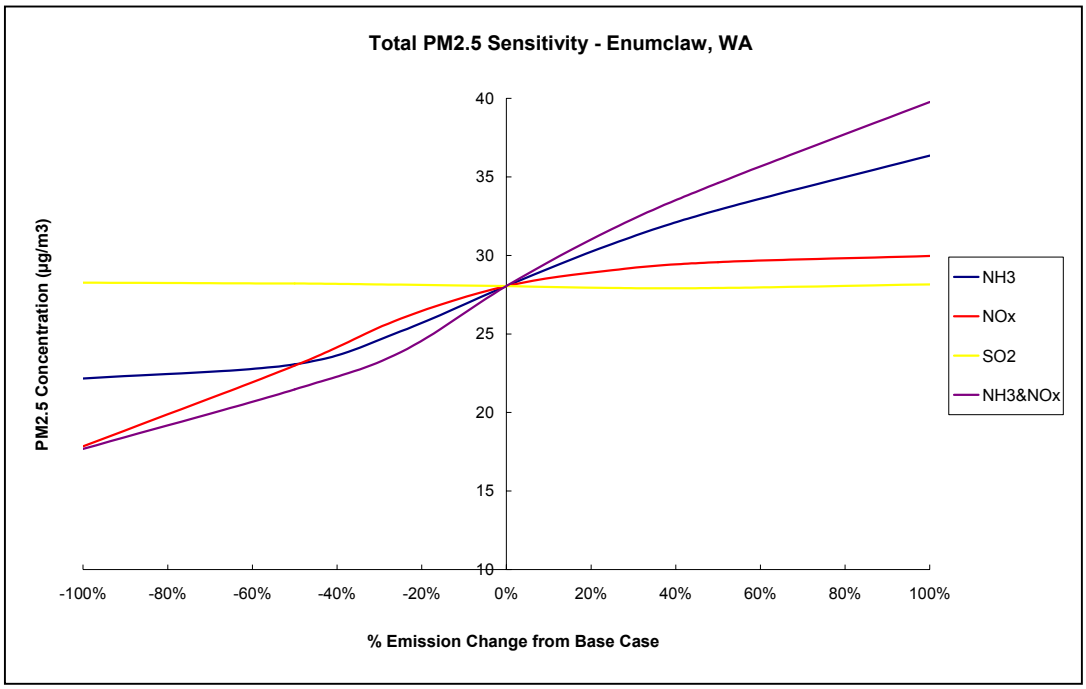

Figure 14b: PM2.5 concentrations due to percent changes in domain wide inorganic anthropogenic emissions for Carus, OR.

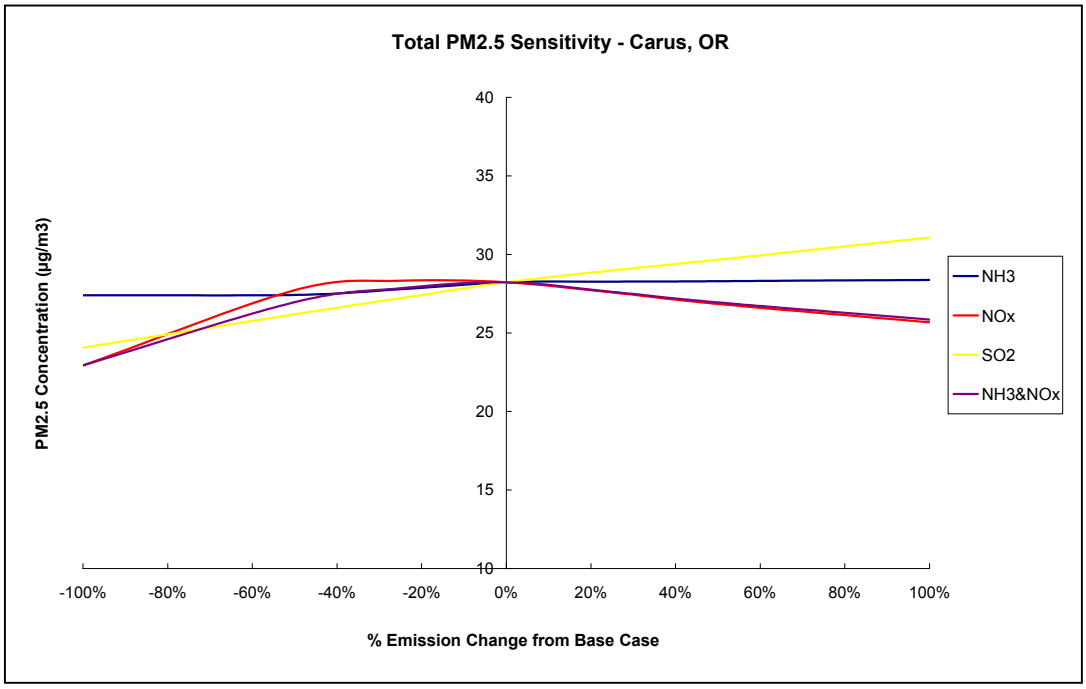

Figure 14c: PM2.5 concentration due to percent changes in domain wide inorganic anthropogenic emissions for Columbia River (CORI), WA.

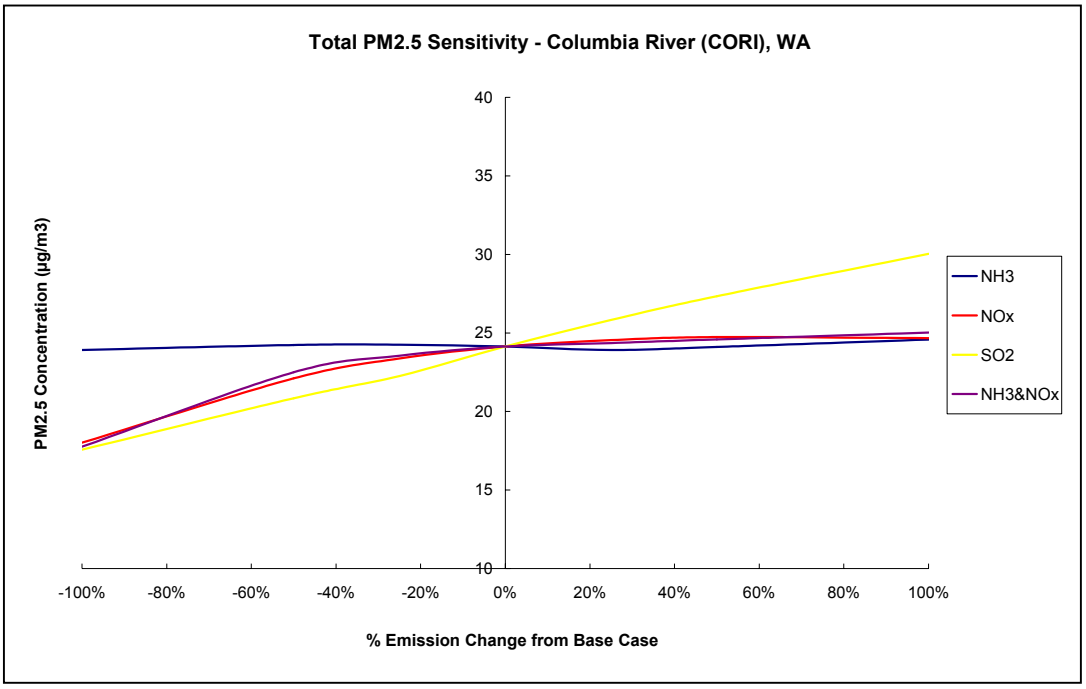

Figure 14d: PM2.5 concentration due to percent changes in domain wide inorganic anthropogenic emissions for Craters of the Moon, ID.

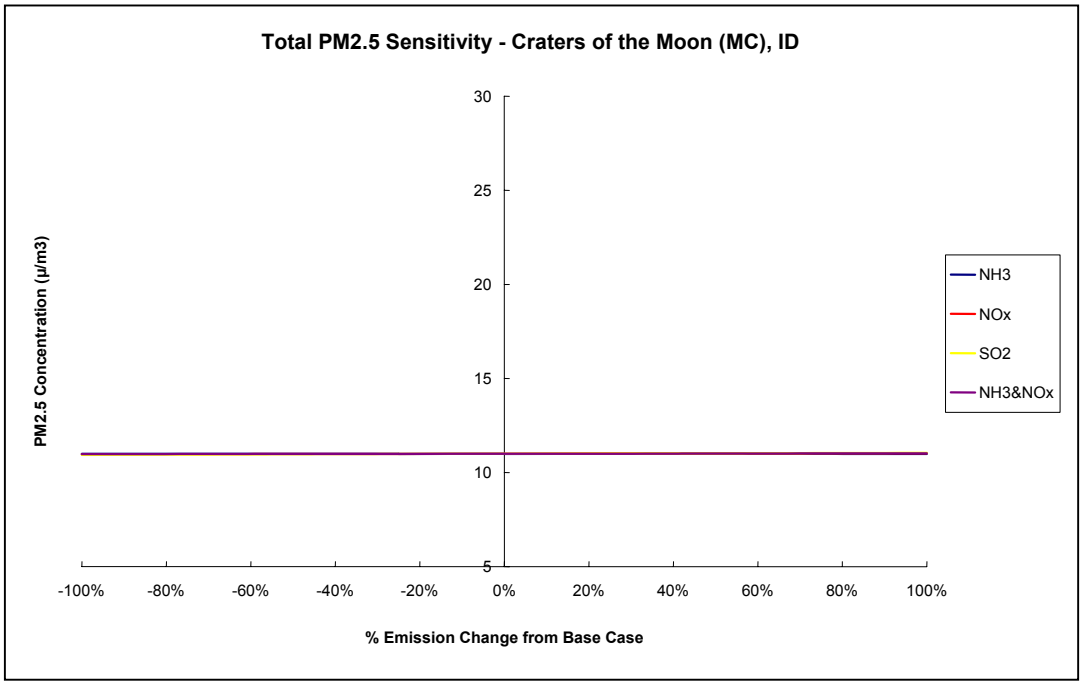

2.4.2.1 PM2.5 Sensitivity to Inorganics in Enumclaw

In Enumclaw, PM2.5 was most sensitive to NH3&NOx combined changes and insensitive to SO2 changes. A 100% increase in NH3&NOx combined emissions resulted in a 42% increase in PM2.5, while a -100% decrease in NH3&NOx combined emissions lowered the PM2.5 by -37%. This strong sensitivity could be attributed to the sensitivities of individual NOx and NH3 changes. The combined response of NH3&NOx was roughly equal to the additive sensitivity of NH3 and NOx changes independently. However, PM2.5 was more sensitive to increases in NH3, less sensitive to increases in NOx, and more sensitive to NOx reduction than NH3 reduction. SO2 emission changes had the least influence on total PM2.5 in Enumclaw. Domain wide increases and decreases of SO2 produced no change in the final PM2.5 formation.

Two reasons caused Enumclaw to have this sensitivity behavior. The first is the high ammonia molar concentration compare to the sulfate molar concentration. The second is the high HNO3 concentration from the influence of the Seattle metropolitan area.

In the base-case simulation, Enumclaw had a TNH4/TSO4 ratio of 5.2. This represented an ammonia-rich environment where the high ammonia concentration neutralizes all the sulfate ions. The ratio also indicated that there was available ammonia to support the formation of ammonium nitrate. The excess ammonia in the system led to high NOx sensitivity to total PM2.5 formation. This is because any change in NOx, which led to changes in HNO3, directly increases or decreases ammonium nitrate formation. Increased HNO3 will also increase ammonium nitrate, as free ammonia is available in the ammonia-rich environment. Decreases in HNO3 lowers PM2.5 as less ammonium nitrate is formed in the air. Since the ammonia availability caused the NOx sensitivity, the degree of sensitivity depends on the concentration of available ammonia. When all the ammonia was used up by the increased HNO3, further increases in HNO3 would not increase PM2.5. This was observed in the plateau of PM2.5 concentrations when NOx was increased beyond 25%.

In addition to NOx sensitivity, Enumclaw was also sensitive to NH3 changes. The high sensitivity to NH3 was due to the high HNO3 concentrations in this area. High NOx from automobiles led to high HNO3, as HNO3 is one of the principle secondary products of NOx oxidation (reaction R5). At high HNO3 levels, any increase in NH3 directly increased the formation of ammonium nitrate in the air. This is because all sulfates in the system were neutralized and the additional NH3 was available for nitric acid to form ammonium nitrate. Thus, increase NH3 increased total PM2.5. There was little or no change in sulfate aerosol concentrations since all sulfates already existed as ammonium sulfate in the ammonia-rich environment. However, when NH3 was decreased, it affected both nitrate and sulfate aerosol formation. When NH3 was initially lowered, ammonia nitrate decreased first, as less HNO3 could partition into the aerosol phase. This decreased the total PM2.5. When NH3 was further decreased and the TNH4/TSO4 ratio fell below 2, there was little or no ammonia nitrate left in the system and ammonium sulfate started to loose ammonium ions to become ammonium bisulfate or letovicite. When all NH3 was eliminated from the system, the sulfate aerosol eventually presented as H2SO4 aerosol and the system became highly acidic. With the gradual decreases in NH3 emissions, the rate of PM2.5 reduction was also slowed, as observed in the flatter tail end of the NH3 sensitivity curve (figure 14a). This is because less-neutralized sulfate salts have lower deliquescence relative humidity, and the sulfate (as H2SO4) is more hygroscopic than all the sulfate salts. Thus, as sulfate changed from ammonium sulfate to bisulfate, or letovicite to H2SO4, water aerosol content increased gradually. The increases in water aerosol increased the total aerosol mass concentrations and slowed the decrease of PM2.5 concentrations.

The combination of high HNO3 and ammonia-rich conditions was the reason for the insensitivity of PM2.5 to SO2 changes at Enumclaw. Under this condition, when SO2 emissions were reduced, which lowered the sulfate aerosol in the system, more NH3 was released and made available to HNO3 to form nitrate aerosols. This increase in nitrate aerosols balanced the

decrease in sulfate aerosols and prevented the PM2.5 in the system from decreasing. PM2.5 was thus insensitive to SO2 reductions. The reverse is also true when SO2 emissions increased. As SO2 increased, more sulfate ions took up the available NH3 in the air and reduced the formation of ammonium nitrate. The increase in sulfate aerosol was compensated by the decrease in nitrate aerosol. Therefore, PM2.5 was also insensitive to changes in SO2 precursor emission in this system.

NH3&NOx combined emission changes had the greatest affect on the total PM2.5 concentrations. When both NH3 and NOx were increased together, ammonium nitrate aerosols were directly increased. This was because there was no more restraining on the available NH3, as when NOx was increased by itself. Even though HNO3 concentration was high in the base-case environment, the increase of NH3&NOx together produced even higher PM2.5 than the NH3 alone. This showed that PM2.5 production efficiency increased when additional NOx were introduced. For the reduction in NH3&NOx combined emissions, the system behavior was more similar to decrease in NOx than that of NH3. This was because when all NOx in the system were reduced or set to zero, the formation of major atmospheric oxidants were also lowered. NOx are the precursors to ozone (reaction R8) and ozone affects the hydroxyl radical ($OH^{\cdot}$) and nitrate radical ($NO3^{\cdot}$) concentrations in the air (reactions R16 and R17).

$$O_3 + H_2O \rightarrow\rightarrow 2OH^{\cdot} \qquad \text{(R16)}$$

$$O_3 + NO_2 \rightarrow NO_3^{\cdot} + O_2 \qquad \text{(R17)}$$

When NOx was removed from the system, all major atmospheric oxidants were also reduced. Thus, both inorganic and organic aerosols decreased. Since NOx indirectly influences both organic and inorganic aerosol formation and NH3 did not significantly change organic aerosol chemistry, the combined NOx&NH3 reduction was similar to the NOx reduction alone.

2.4.2.2 PM2.5 Sensitivity to Inorganics in Columbia River and Carus

PM2.5 sensitivity in Carus and Columbia River (CORI) was very different from that of Enumclaw, but somewhat similar to each other. The fact that Carus and CORI are only 125km apart may explain the similarities between the two areas.

In both systems, PM2.5 was highly sensitive to changes in SO2 emissions but rather insensitive to changes in NH3. CORI was slightly more sensitive to SO2 changes than Carus. With 100% increase in SO2, PM2.5 in CORI increased by 24% but only 10% in Carus, and when SO2 was removed completely, PM2.5 in CORI was reduced by -27% but only -15% in Carus. This difference in SO2 sensitivity could be attributed to the dissimilar ammonia loading at the two sites. In the base-case simulation CORI had a TNH4/TSO4 ratio near 1 and Carus had a ratio of 1.5. Both sites were considered to be ammonia-poor but CORI had considerably lower ammonia concentrations with respect to sulfate than Carus. Since sulfate aerosols have very low volatility and exist completely in aerosol phase, when SO2 concentrations increased and were oxidized to form sulfate, they partitioned into the aerosol phase immediately. This caused the ammonia-poor region to be more sensitive to SO2 emissions. The increase was sharper for the “ammonia-poorer” region, such as CORI. Since all the ammonia in the area was bound to the sulfate aerosol, the additional sulfate would have to exist in a more hygroscopic form as H2SO4. The higher hygroscopicity of H2SO4 attracted more water and increased aerosol water content in each new sulfate aerosol formed. Therefore increased SO2 in ammonia-poor region increased total PM2.5, and this increase is sharper when ammonia concentrations are lower. The reverse also holds when SO2 emissions were reduced. As SO2 was lowered, the rate of PM2.5 decrease was slower in the higher ammonia region because more available ammonia could neutralize the additional sulfates. As more sulfate was neutralized, sulfate in the system existed as sulfate salts, which had lower hygroscopicity than the un-neutralized sulfate. The formation of sulfate salts slowed down the increase of aerosol

water and slowed the decreasing rate of total PM2.5. Between Carus and CORI, Carus had higher levels of ammonia, thus it had a sharper sensitivity to SO2 emission changes than CORI.

PM2.5 concentrations in Carus and CORI were insensitive to changes in NH3 precursor emissions. This was again due to the low ammonia molar concentration relative to sulfate molar concentration in these two regions. Both regions were ammonia-poor with sulfate to ammonia ratio less than two. Under these conditions sulfate aerosol exists partly as neutralized sulfate salt and partly as un-neutralized H2SO4. When this happens, the sulfates in both forms act as buffers to changes in ammonia concentrations. As ammonia increases, the un-neutralized sulfate takes up the additional ammonium and exists as sulfate salts. This reduces the build up of ammonia in the air and resists the formation of ammonia nitrate. As ammonia decreases, the neutralized sulfate gives up their ammonium ion and exists as un-neutralized sulfate. The un-neutralized sulfate is more hygroscopic and increases the aerosol water content in the air, which balances the reduction in ammonium aerosol. This shifting of sulfate composition in ammonia-poor regions causes the PM2.5 to be relatively insensitive to changes in NH3 emissions. From the PM2.5 response to NH3 emission in CORI and Carus we can also deduce that the 100% increase in NH3 emission did not change their regime from ammonia-poor to ammonia-rich. This is because, if the increase in NH3 caused their TNH4/TSO4 to be greater than 2, then all the sulfate aerosols in the systems would be completely neutralized. The additional ammonia could then react with nitric acid to form secondary nitrate aerosols, and increase the total PM2.5 level in the system.

One interesting and unexpected result between CORI and Carus that set them apart is their sensitivity towards NOx emission changes. When NOx emissions were lowered, both CORI and Carus had lower total PM2.5. However when NOx emissions were increased, the two had different behavior. In CORI, the increases in NOx did not change the total PM2.5 concentration, but in Carus, the increases in NOx actually lowered the PM2.5 formation.

In both locations, the decrease in PM2.5 with lower NOx was because of the reduction in atmospheric oxidants. This phenomenon was similar to that in Enumclaw. When NOx was decreased, less ozone was formed and fewer hydroxyl radicals and nitrate radicals were present. With lower atmospheric oxidants available, less SO2 and VOCs were oxidized for sulfate aerosol and SOA formation. Therefore, as NOx is reduced, more aerosol precursors remain in gas-phase thus reducing the formation of secondary PM2.5.

The difference between CORI and Carus occurred when NOx emissions were increased. In CORI, PM2.5 remained unchanged when NOx was increased. This was because ammonia ions were not available to react with the increased nitric acid from the increased NOx emissions. The partition of nitric acid to the aerosol phase at low ammonia levels was low, and driven only by phase equilibrium. Without enough ammonia in the air, the formation of ammonia nitrate was lowered. However, this PM2.5 sensitivity was different in Carus. When NOx emissions were increased, negative PM2.5 sensitivity was observed in the simulation results. The reason was because of the low ozone formation in Carus when NOx emissions were increased. Maximum base-case PM2.5 in Carus occurred at midday (1pm, PST) when solar radiation was high and ozone production was also high. When NOx was suddenly increased under this condition, the high NOx could not increase ozone production. Instead, the additional NO removed the ozone that was already in the air via reaction R10. This lowered the ozone concentration in the air and reduced the atmospheric oxidant level. Lower oxidants reduce secondary PM2.5 production in both inorganic and organic aerosols similar to the response when NOx is reduced. This negative sensitivity demonstrates the non-linear ozone production influencing the formation of secondary PM2.5 by altering the atmospheric oxidant concentration. The negative NOx sensitivity was not observed in CORI or Enumclaw because both regions had low NOx emissions during their peak base-case PM2.5 period. CORI is further away from the Portland metropolitan area. The NOx concentration in CORI was not high enough to remove the ozone in the area. In Enumclaw, the peak base-case PM2.5 occurred in the early morning (4am PST)

when ozone production was low. The difference in ozone between the base-case and the sensitivity case at Enumclaw was not significant enough to produce changes in ozone production as in Carus.

In terms of NH3&NOx combined emissions change, both Carus and CORI were sensitive to the changes. However, when observed closely, this combined emission sensitivity mirrors that of NOx sensitivity alone and is less influenced by NH3 emissions. This was not surprising as both Carus and CORI were ammonia-poor regions. They were both insensitive to changes in NH3 emissions.

2.4.2.3 PM2.5 Sensitivity to Inorganics at Craters of the Moon

PM2.5 at the Craters of the Moon was insensitive to all the inorganic PM2.5 precursor emission changes. The predicted base-case PM2.5 was also among the lowest across the domain. The TNH4/TSO4 ratio in MC was less than two (TNH4/TSO4 = 0.73). Inorganic aerosols under this condition existed as partly neutralized sulfates.

PM2.5 insensitivity to emission changes at this site may be attributed to the low base-case precursor emissions in rural areas. When the base-case precursor emissions were low, the percentage changes in these emissions resulted in only minor changes in absolute terms. With little changes in precursor emissions, there was little or no change in atmospheric oxidant concentration. Therefore, the resultant PM2.5 change was insignificant.

2.4.2.4 PM2.5 Sensitivity to Organics

Organic aerosol sensitivities at the four locations were very similar to each other but the degrees of sensitivity were different. Figures 15a to 15d show the total PM2.5 sensitivities for emission changes in anthropogenic VOCs (aVOC), biogenic VOCs (bVOC), anthropogenic NOx (NOx) and anthropogenic NOx combined with anthropogenic VOCs (NOx&VOC) for Enumclaw, Carus, CORI, and MC respectively. Numerical results and the percentage PM2.5 change for the four sites are listed in Appendix F1 to F4. PM2.5 changed linearly with VOCs at all sites, but different regions had different degrees of aerosol sensitivity. The degree of organic aerosol

sensitivity can be measured by the slopes of each sensitivity line on the graph. Table 6 shows the slopes of aVOC and bVOC. The slopes indicate changes in PM2.5 for a unit percentage change in precursor VOC emissions.

Biogenic VOCs generally produce a bigger change in PM2.5 concentrations than anthropogenic VOCs, except for Carus where anthropogenic VOCs produced greater changes. The higher sensitivity to biogenic VOCs in Enumclaw, CORI and MC was because biogenic VOCs are present at much higher levels (over 93%) than anthropogenic VOCs in the domain during the peak PM2.5 period. Furthermore, among all the condensable organics treated by CMAQ, biogenic terpene emissions have the highest aerosol yield. As aerosol yield increases, the formation of SOA per mole of oxidized VOC is also higher.

In Carus however, PM2.5 was more sensitive to anthropogenic VOC than biogenic VOC. This was because the base-case peak PM2.5 in Carus happened during mid-afternoon when anthropogenic VOC emissions outweigh biogenic VOC emissions in urban areas. Although biogenic VOC were more abundant than anthropogenic VOCs, their spatial distribution was concentrated in rural areas. In urban areas, during the daytime, the biogenic VOCs were relatively low compared to anthropogenic emissions. High levels of anthropogenic VOCs from Portland could contribute to Carus. If this happened, the increases in anthropogenic VOCs would cause Carus to have higher anthropogenic VOCs than biogenic VOCs.

Figure 15a: PM2.5 concentrations due to percent changes in domain wide anthropogenic VOC (aVOC), biogenic VOC (bVOC), anthropogenic NOx (NOx) and combined anthropogenic VOC and NOx (NOx&VOC) for Enumclaw, WA.

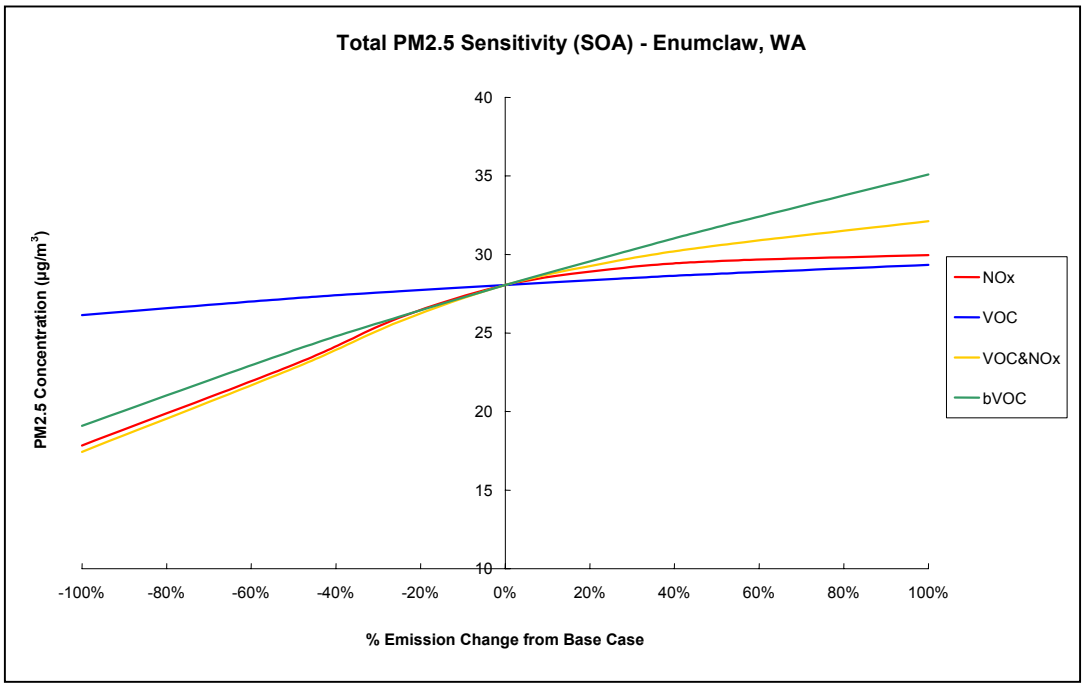

Figure 15b: PM2.5 concentrations due to percent changes in domain wide anthropogenic VOC (aVOC), biogenic VOC (bVOC), anthropogenic NOx (NOx) and combined anthropogenic VOC and NOx (NOx&VOC) for Carus, OR.

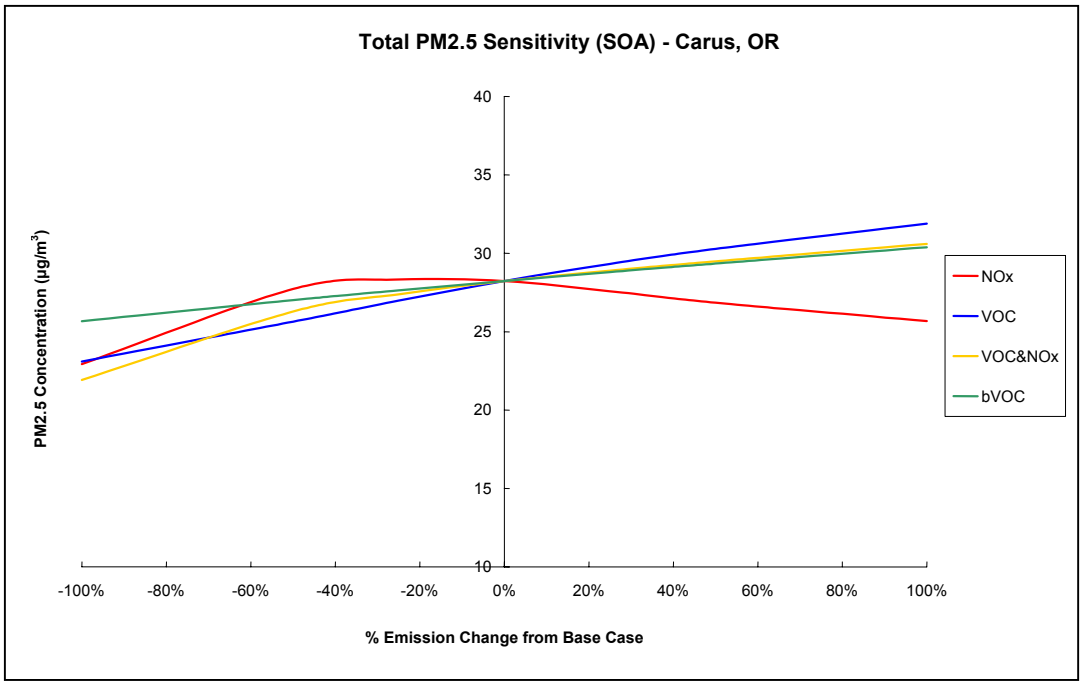

Figure 15c: PM2.5 concentration due to percent changes in domain wide anthropogenic VOC (aVOC), biogenic VOC (bVOC), anthropogenic NOx (NOx) and combined anthropogenic VOC and NOx (NOx&VOC) for Columbia River (CORI), WA.

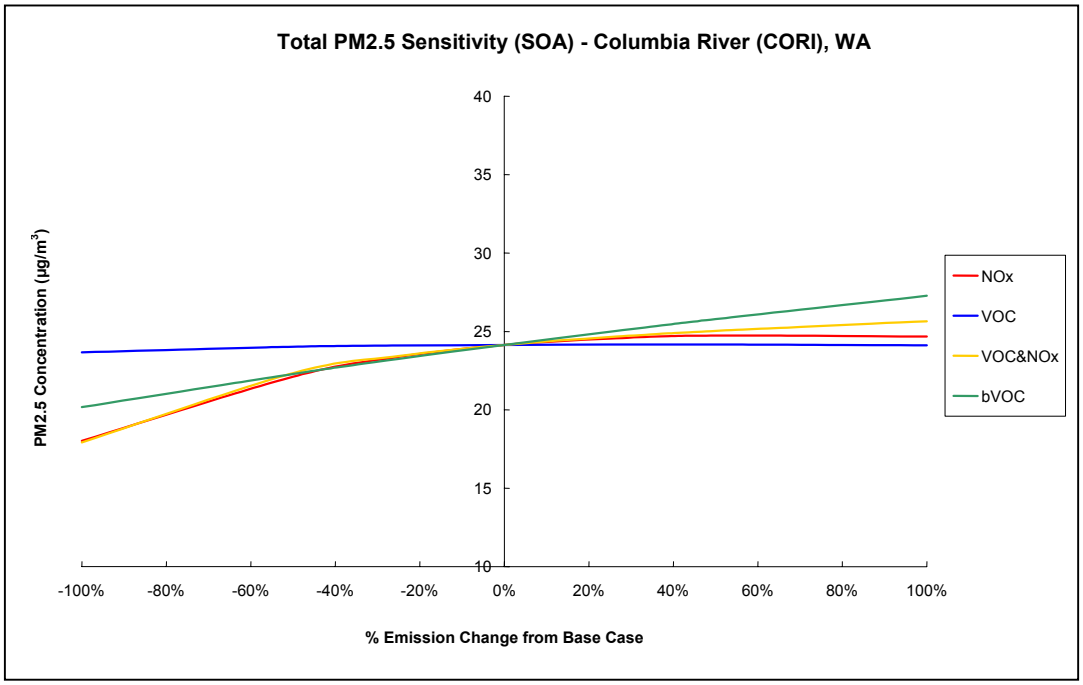

Figure 15d: PM2.5 concentration due to percent changes in domain wide anthropogenic VOC (aVOC), biogenic VOC (bVOC), anthropogenic NOx (NOx) and combined anthropogenic VOC and NOx (NOx&VOC) for Craters of the Moon, ID.

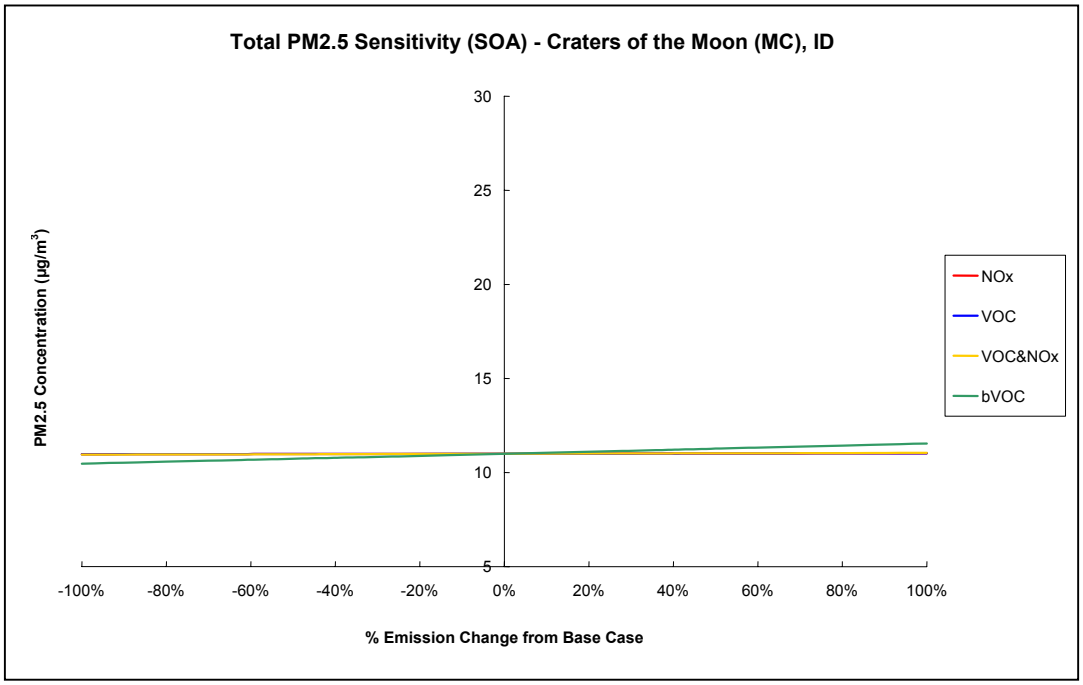

Table 6: Degrees of PM2.5 sensitivity towards percentage anthropogenic VOC (aVOC) and biogenic VOC (bVOC) precursor emissions change ($\mu g/m^{-3}$ PM2.5 over % VOC emission change).

	Anthropogenic VOC Sensitivity (ΔPM2.5/ΔaVOC)	Biogenic VOC Sensitivity (ΔPM2.5/ΔbVOC)
Enumclaw, WA	1.6	8.0
Carus, OR	4.4	5.5
Columbia River, WA	0.2	3.7
Craters of the Moon, ID	0.02	0.6

PM2.5 was slightly more sensitive to NOx&VOC combined emissions than the additive responses of anthropogenic VOCs and NOx independently. This was because when NOx and VOC were increased together, the ozone chemical production rate increased at the same time. When ozone levels are higher, there are more atmospheric oxidants to produce organic and inorganic secondary aerosols. Enumclaw with high base-case PM was the most sensitive while MC with low base-case PM was the least sensitive to the combined emission change. The negative PM2.5 sensitivity in Carus when NOx was increased is not evident if anthropogenic VOCs were increased together. This is because the additional VOCs provided more pathways for ozone formation. As more ozone was formed, more oxidants were available to generate higher secondary aerosol concentrations.

The CMAQ organic aerosol sensitivity cases presented here are simpler than the inorganic aerosol cases. This is largely due to the simplified organic aerosol algorithm in CMAQ. SOA formation in the model is based on the vapor saturation principle, where a fixed fraction of condensable organics is transferred to the aerosol phase regardless of changes in chemical composition and environmental conditions. This method produces secondary organic aerosol proportional to the concentration of VOCs and oxidants in the air. This simple fixed aerosol yield routine may not be sufficient to capture the complex SOA dynamics. Recent experiments showed that the fraction of aerosols formed from different condensable organics are not fixed. The yields varied for different VOC species, and are functions of temperature and total organic aerosol mass concentrations (Griffin et al., 1999; Odum et al., 1996). Furthermore, the aerosol phase partitioning involves more complex processes in addition to the vapor saturation principle. Additional processes such as absorption, dissolution and adsorption of low-volatile organic gases can all be important in the formation of organic aerosols.

2.4.3 Ozone Sensitivity

Ozone formation in the troposphere changes non-linearly with VOC and NOx concentrations. The levels of precursor emissions determine the concentration of ozone

produced at a location. In this study, six sites were selected to evaluate the ozone sensitivity to emission changes. Figure 16 shows the locations of these selected sites. Five of the sites were chosen downwind of urban areas and one was chosen to represent rural areas. The urban sites were: Carus, OR, Enumclaw, WA, Spokane, WA, Tri-cities, WA and Boise, ID; the rural site was the Craters of the Moon in Idaho. Of the six locations, Carus and Enumclaw had the highest base-case predicted ozone of 184 ppbv and 149 ppbv, occurring on July 14 5pm PST and July 14 3pm PST respectively. Both sites are downwind of major cities and they suffer from very high anthropogenic pollutants. The other three urban areas, Tri-cities, Boise and Spokane had slightly lower anthropogenic emissions. Their predicted base-case ozone levels were 115 ppbv, 93 ppbv and 86 ppbv, occurring on July 15 10am PST, July 14 4pm PST and July 14 4pm PST respectively. Craters of the Moon had the lowest predicted peak ozone of 70 ppbv, occurring on July 15 1pm PST. This was because of the low anthropogenic emission influence in the rural area.

Figures 17a through 17d show the ozone sensitivity to changes in precursor emissions for the six locations. Each line on the graph represents the predicted ozone level as a result of the indicated emission changes at the specific site. The y-axis indicates the ozone concentration in ppbv from seven CMAQ simulations. The x-axis indicates the percentage emissions change to precursor emissions for all six sites. The base-case ozone for each site is represented with 0% change in emissions on the x-axis. The numerical results and calculated percentage ozone changes from the base-case are shown in Appendix G1 to G4.

Figure 16: Selected ozone sensitivity locations: Enumclaw, Spokane, Tri-cities in Washington; Carus in Oregon; Boise and Craters of the Moon in Idaho.

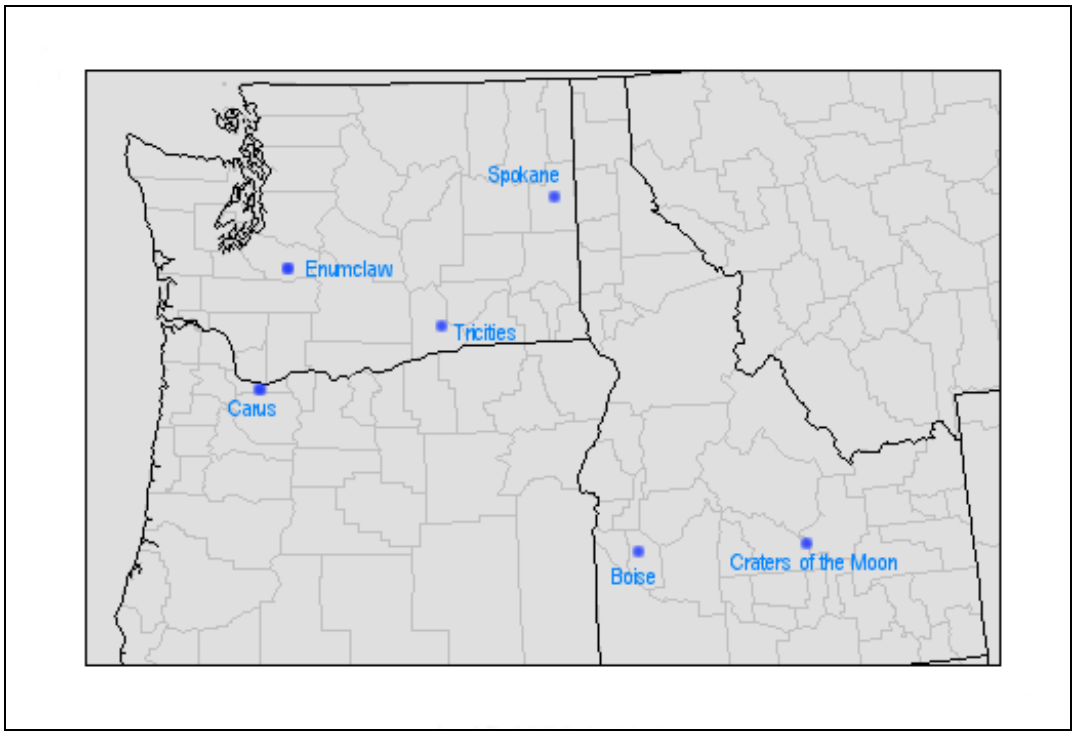

Figure 17a: Ozone concentrations due to percent domain wide anthropogenic VOC emission change for the six locations.

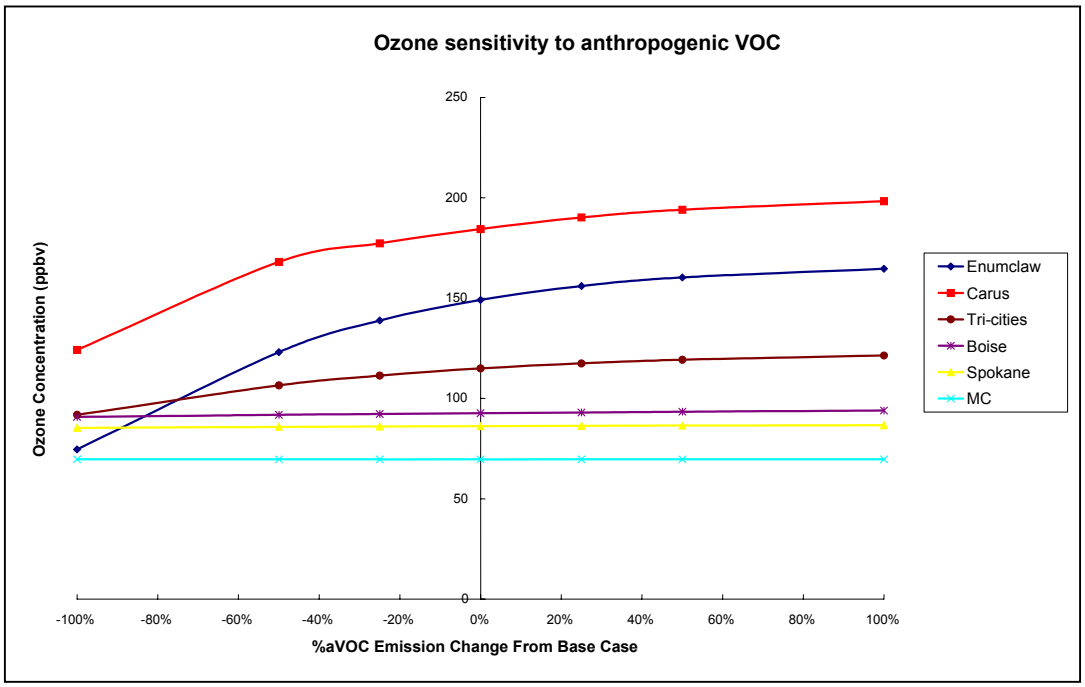

Figure 17b: Ozone concentration due to percent domain wide anthropogenic NOx emission changes for the six locations.

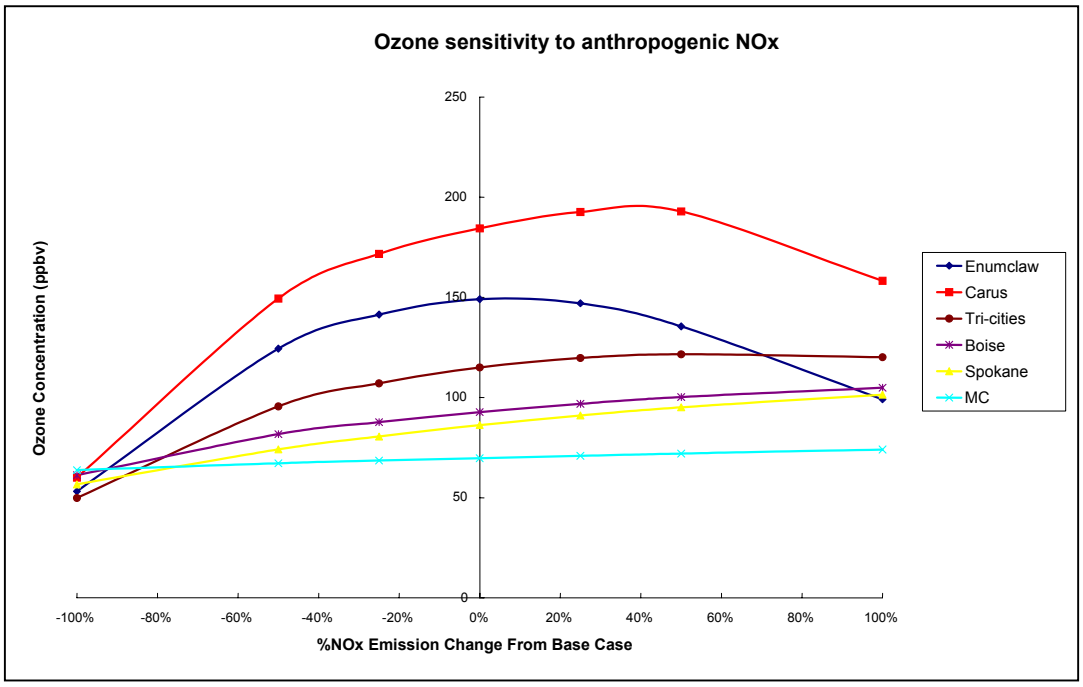

Figure 17c: Ozone concentration to percent domain wide anthropogenic VOC and NOx emission changes for the six locations.

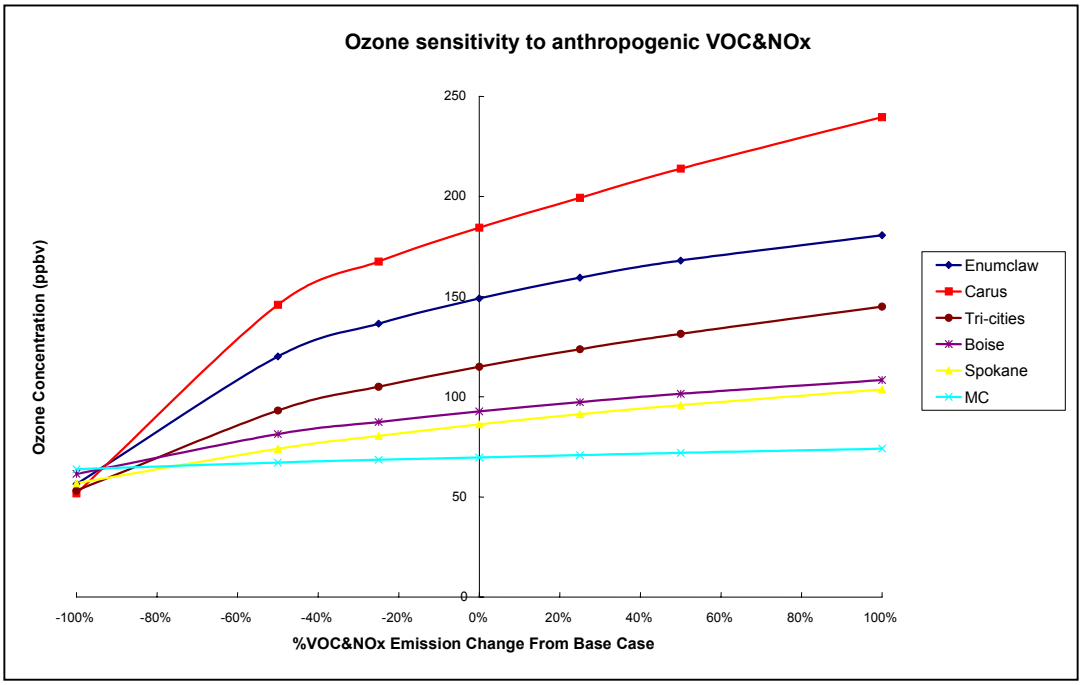

Figure 17d: Ozone concentration to percent domain wide anthropogenic NOx emission changes for the six locations.

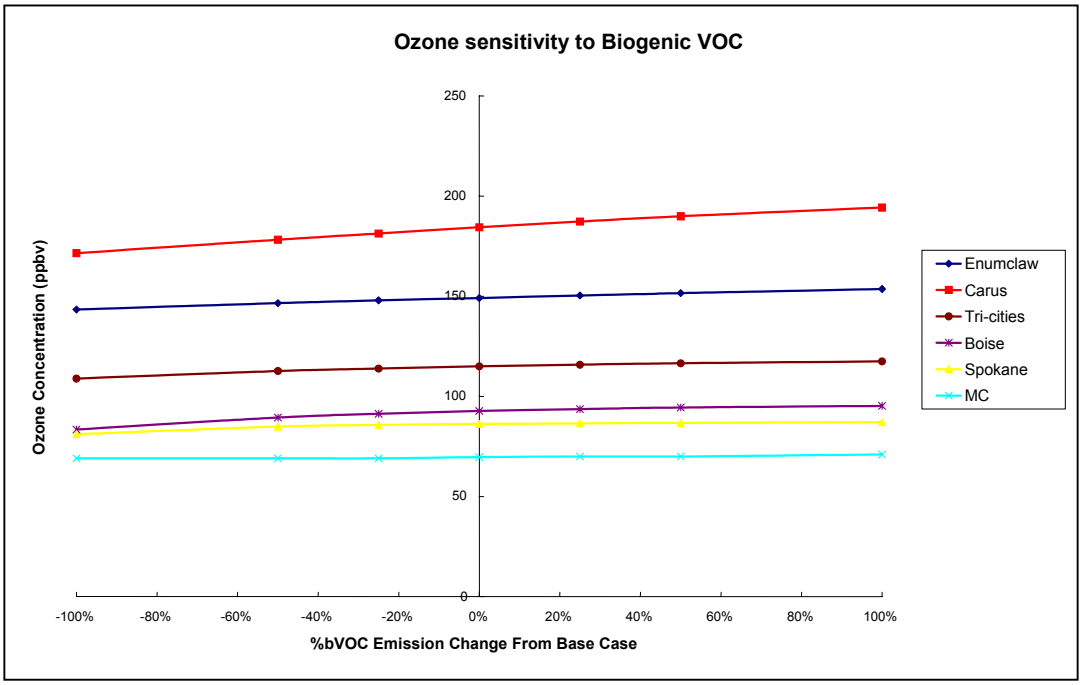

2.4.3.1 Ozone Sensitivity to VOC Emissions

The results illustrate that ozone correlated positively with combined VOC&NOx emissions, anthropogenic VOCs and biogenic VOCs. The correlation was strongest for VOC&NOx combined emissions, and weakest for biogenic VOC changes.

The strong ozone sensitivity with combined VOC&NOx emissions was expected, as both VOC and NOx are primary precursors to ozone formation in the troposphere. When both emissions were increased or decreased together, they influenced the reaction rates for reactions R8, R9, R11, R12 and R13, which increased or decreased the ozone concentration respectively. Therefore high VOC&NOx emissions led to high ozone formation and low VOC&NOx emissions decreased ozone at all sites. The degrees of ozone sensitivity between the six locations were different. Carus, with the highest base-case ozone level was most sensitive, and Craters of the Moon with the lowest base-case ozone level was the least sensitive to the combined VOC&NOx emission changes.

When anthropogenic VOC was changed with constant NOx levels, ozone changed more distinctly in urban areas over rural areas. Large urban cities such as Enumclaw, Carus and Tri-cities had the greatest ozone change, follow by smaller changes in Boise and Spokane. Craters of the Moon as the only rural site, was insensitive to anthropogenic VOC changes. The differences were primarily due to the different base-case NOx concentrations at the six locations. NOx, emitted mostly from automobiles, was present at high levels in the urban areas. High NOx in the regions outweighed the VOC concentration, which caused VOC to become the limited reactant for ozone. Therefore, when VOC emissions were increased, more catalysts ($RO_2^{\cdot}$ and $HO_2^{\cdot}$) were formed, which converted the plentiful NO to NO_2, and produced more ozone. For rural areas, ozone was insensitive to changes in VOC emissions. This was because rural areas usually had lower NOx but relatively higher levels of VOCs from the biogenic sources. The limiting reagents for ozone in this case were NOx emissions. Therefore when NOx availability was low, any changes in VOC catalysts did not alter the formation of ozone.

Biogenic VOCs had a smaller influence on total ozone formation compared to anthropogenic emissions. Similar levels of ozone change had been reported in the literature for the Pacific Northwest Region (Jiang, et al., 2001). Although biogenic VOCs were highly reactive and more abundant than anthropogenic VOCs, biogenic VOC distributions were mainly in rural regions where NOx concentrations were low. In urban areas where VOCs were the limiting reagents, changing biogenic VOCs had a relatively small impact on the ozone formation. The uneven distribution of biogenic emissions also caused higher biogenic VOC sensitivity than anthropogenic VOC sensitivity for smaller cities and rural sites. Boise, Spokane and Craters of the Moon with low NOx emissions had little or no change to ozone when anthropogenic VOCs were changed. But when biogenic VOCs were adjusted, ozone in all three regions experienced higher changes than similar adjustments to anthropogenic VOCs. This suggests that biogenic VOCs in the small urban and rural areas had a higher impact on ozone formation and were the main source of ozone catalyst compared to urban regions.

2.4.3.2 Ozone Sensitivity to NOx Emissions

Changing anthropogenic NOx emissions produced the most discrete ozone results between the urban and rural areas. Carus and Enumclaw with the highest base-case ozone exhibited negative sensitivity, where ozone decreases with increased NOx. The other four sites all showed linear ozone changes with NOx emissions. The non-linear ozone behavior with NOx is common in large urban areas and had been illustrated in many other studies (Barna et al., 2001; Jiang, 2001; Sillman, 1999). The inverse ozone and NOx relationship was because of high NOx concentrations with respect to VOCs in these areas. Under high NOx conditions, further increases in NOx with fixed VOC levels decreased ozone levels via two combined methods. First, the newly introduced NO emissions directly removed the ambient ozone via reaction R10. This reaction referred to as NO titration is highly effective in removing ozone in the atmosphere. This reaction is the main ozone sink, which determines the background concentration of ozone in the troposphere. Second, when NO_2 concentrations accumulate, the

NO_2 removes the $OH^{\cdot}$ radical and terminates the ozone production reactions (reaction R14). Since $OH^{\cdot}$ radicals are the main molecule that activates the VOC catalysts in the ozone production reactions (reaction R11), when $OH^{\cdot}$ concentrations decrease, it inhibits the production of $RO_2^{\cdot}$ and $HO_2^{\cdot}$ catalysts and lowers the ozone chemical production rate. These two factors together lowered the ambient ozone concentration in high NOx areas, such as Enumclaw and Carus.

It is also interesting to point out that when anthropogenic NOx was completely removed, ozone concentrations at all sites fell to the background level of between 48 and 64 ppbv. This reduction was similar to combined NOx&VOC emission reductions, but different when only anthropogenic VOCs were removed. When anthropogenic VOC emissions were removed, ozone at all six locations remained at elevated levels. This was because NOx is the main reactant, while VOCs only act as catalysts in the production of ozone. When anthropogenic NOx was completely removed, biogenic NOx became the only available reactant in the air to establish background ozone. Since biogenic NOx was at a much lower concentration than anthropogenic NOx, ozone at all sites was lowered. However, the case was different for VOC emissions. When anthropogenic VOCs were removed, biogenic VOCs could still serve as catalysts for ozone production. Since high levels of anthropogenic NOx were still present and VOC required in the ozone production was low, ozone production remained high in all six regions.

2.4.3.3 Ozone Sensitivity by HNO_3/H_2O_2 Ratio

As discussed previously, we can correlate the ozone sensitivity results to the HNO_3/H_2O_2 ratio. Ozone sensitivity depends on both the NOx and VOC concentrations and the reactivity of each VOC compound. Correlating the ozone sensitivity with the HNO_3/H_2O_2 ratio takes both factors into account. This is because HNO_3 is an indirect measure of over production of NO_2 (reaction R12) and H_2O_2 is an indirect measure of over abundance of ozone producing VOCs, regardless of compound reactivities (reaction R13). When the ratio is high, it represents that

NOx is higher than the optimum ozone production level (NOx-rich, VOC sensitive), and the control strategy favors VOC control. When the ratio is low, it shows over abundance of VOC catalyst (NOx sensitive), and the control strategy favors NOx control.

The HNO_3/H_2O_2 ratios for the six locations were calculated from the base-case simulations during high ozone concentration periods. Table 7 lists the ratios for the six regions together with the percentage ozone change from the base-case after changes in anthropogenic VOC and NOx emissions. Enumclaw had the highest value of 3.3 followed by Carus and Tri-cities with 1.9 and 1.4, respectively. Boise, Spokane and Craters of the Moon all had low ratios of less than 1.

The ratio demonstrated to be a good indicator for identifying the NOx-sensitive and VOC-sensitive areas in the six selected sites. Comparing the base-case ratio with the percentage ozone changes from the sensitivity simulation, the ratio corresponded very well to each region's sensitivity towards NOx and VOC emissions. High ratios in Enumclaw, Carus and Tri-cities corresponded to a NOx-rich and VOC-sensitive area, where percentage changes in VOCs caused high percentage changes in ozone. On another hand, low ratios in Boise, Spokane and Craters of the Moon corresponded to the NOx-limited region, where ozone formation was regulated by NOx emissions and was insensitive to changes in VOC emissions. Thus Enumclaw, Carus and Tri-cities were in NOx-rich environments where ozone control favored VOC, and Boise, Spokane and Craters of the Moon were in NOx-limited regions, where ozone control favored NOx emissions. The modeled HNO_3/H_2O_2 ratio in this study compared well with other similar studies in the literature. Sillman et al. (1995), and Chock et al. (1999) used the same ratio to study the ozone behavior in the Lake Michigan region and Southern California, respectively. They estimated the NOx to VOC sensitivity region transitions when the ratio is between 1.8 and 3.0.

Table 7: HNO_3/H_2O_2 ratio and percentage ozone change due to anthropogenic VOC or anthropogenic NOx emission changes for six locations grouped by their emissions sensitivity.

Region	Ozone Sensitivity to Anthropogenic VOC (aVOC) Emission							HNO_3/H_2O_2 Ratio	Ozone Sensitivity to Anthropogenic NOx (aNOx) Emission						
	100%	50%	25%	Base-case	-25%	-50%	-100%		100%	50%	25%	Base-case	-25%	-50%	-100%
Enumclaw	10%	8%	5%	0%	-7%	-17%	-50%	3.3	-34%	-9%	-1%	0%	-5%	-17%	-64%
Carus	8%	5%	3%	0%	-4%	-9%	-33%	1.9	-14%	5%	4%	0%	-7%	-19%	-67%
Tri-cities	6%	4%	2%	0%	-3%	-7%	-20%	1.4	4%	6%	4%	0%	-7%	-17%	-57%
Boise	1%	1%	0%	0%	0%	-1%	-2%	0.9	13%	8%	5%	0%	-5%	-12%	-34%
Spokane	1%	0%	0%	0%	0%	0%	-1%	0.6	18%	10%	6%	0%	-7%	-14%	-34%
Craters of the Moon	0%	0%	0%	0%	0%	0%	0%	0.3	6%	3%	2%	0%	-2%	-4%	-8%

It is also interesting to observe that the ozone sensitivity at six locations did not correlate with base-case ozone concentration, but did correlate closely with the base-case HNO_3/H_2O_2 ratio. Regions with high HNO_3/H_2O_2 ratios showed high ozone sensitivity to changes in precursor emissions, and regions with similar ratio showed similar percentage ozone changes to changes in emissions. Table 7 grouped regions with similar ratios together to show the difference. Although Enumclaw had the second highest ozone levels, it was the most sensitive to VOC and NOx changes. With the highest ratio of 3.3, the same percentage change in VOC and NOx emissions produced the greatest change in ozone over all other regions. Although Carus had the highest ozone level, the ozone sensitivity was less sensitive to VOC and NOx changes than that of Enumclaw. Carus and Tri-cities had the second highest ratio. The ozone sensitivity in Carus was more similar to that of Tri-cities. Although only Carus showed negative ozone sensitivity when NOx emissions were increased, the negative sensitivity was only observed when NOx was increased by 100%. When NOx was increased by only 25% to 50%, ozone in Carus increased, and the degree of change was similar to Tri-cities. Furthermore, ozone in both cities had similar percentage changes to VOC emissions. The similar HNO_3/H_2O_2 ratios in both areas correlated well with their similar ozone sensitivities. The correlation can also extend to other regions. Boise and Spokane had similar HNO_3/H_2O_2 ratios, and their sensitivity results displayed a similar degree of change. Craters of the Moon had the lowest ratio of all six locations, and it displayed the lowest percentage change in ozone to changes with either NOx or VOC emissions.

The correlation of the HNO_3/H_2O_2 ratio and the ozone sensitivity presented in this study demonstrates that the ratio is a good indicator for judging different areas' response to changes in precursor emissions. Further studies, including field measurements, are needed to better understand the correlation, and narrow down the average range of ratios for NOx/VOC-sensitive areas in the Pacific Northwest.

2.4.4 Impact of Emissions on Model Performance

During the model simulation period, several ozone and PM monitoring stations were operating in the domain. The ozone measurements were from the EPA Aerometric Information Retrieval System (AIRS) database and the PM measurements were from the Interagency Monitoring of PROtected Visual Environments (IMPROVE) database. O'Neill et al. (2002) compared the CMAQ base-case results with the monitoring sites and provided a statistical analysis of the model performance. This section compares some of these observational results with sensitivity simulation results for ozone and PM2.5. This addresses the question as to how model performance is affected by uncertainties in the emission inventory.

Four ozone stations and four PM2.5 stations were selected to compare with the modeled sensitivity results. Figure 18 shows the locations of these observation stations. Ozone measurements were hourly averaged values for the entire simulation period. Figure 19a to 19d show the maximum predicted ozone concentrations by emissions scenarios for the period at each of the monitoring sites. The graphs also show maximum observed ozone concentration for simulation period and the percent predicted ozone change from the base-case. The graphs are for stations in Enumclaw, WA, Beacon Hill, WA, Carus, OR and Milwaukie High School, OR respectively. The numerical data for the graphs are listed in Appendix H. The base-case simulation results compared well for the Carus and Milwaukie High School stations, but CMAQ over-predicted maximum ozone for the Enumclaw and Beacon Hill stations.

Figure 18: Selected ozone and PM2.5 observation stations used to compare measurements with simulation results.

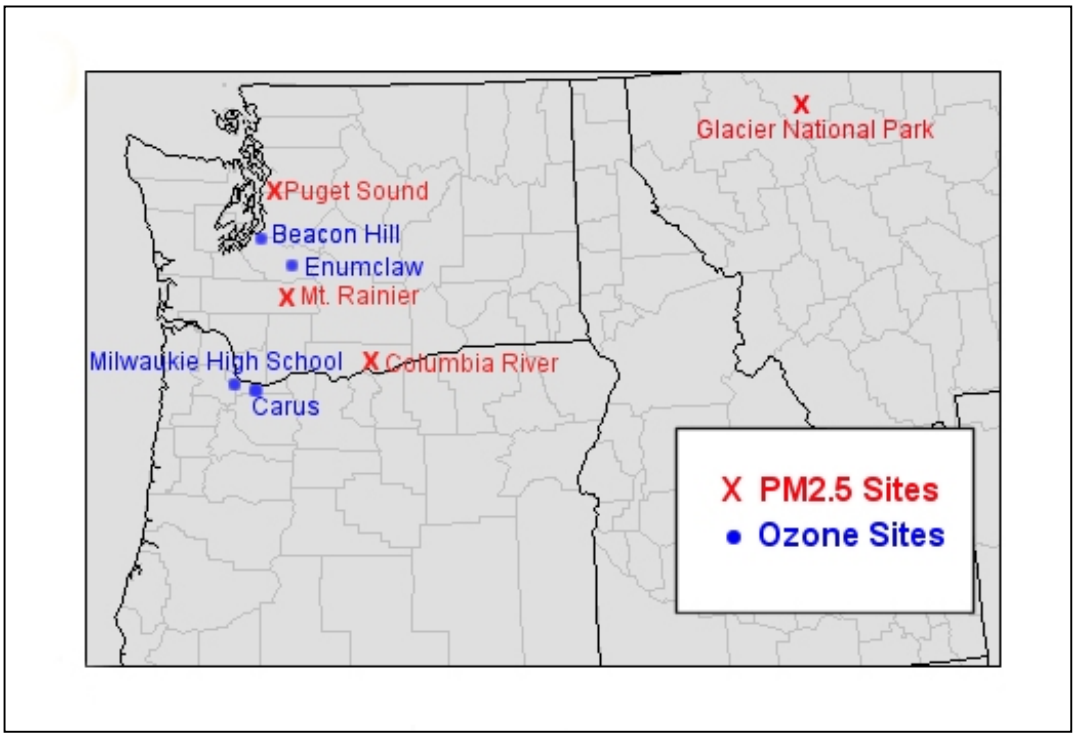

Figure 19a-b: Maximum 1-hour predicted ozone concentrations by emissions scenarios with maximum 1-hour observed ozone concentration for the three-day simulation period. The dotted line shows the percent maximum predicted ozone change from the base-case simulation for different emission scenarios.

(19a) Enumclaw, WA

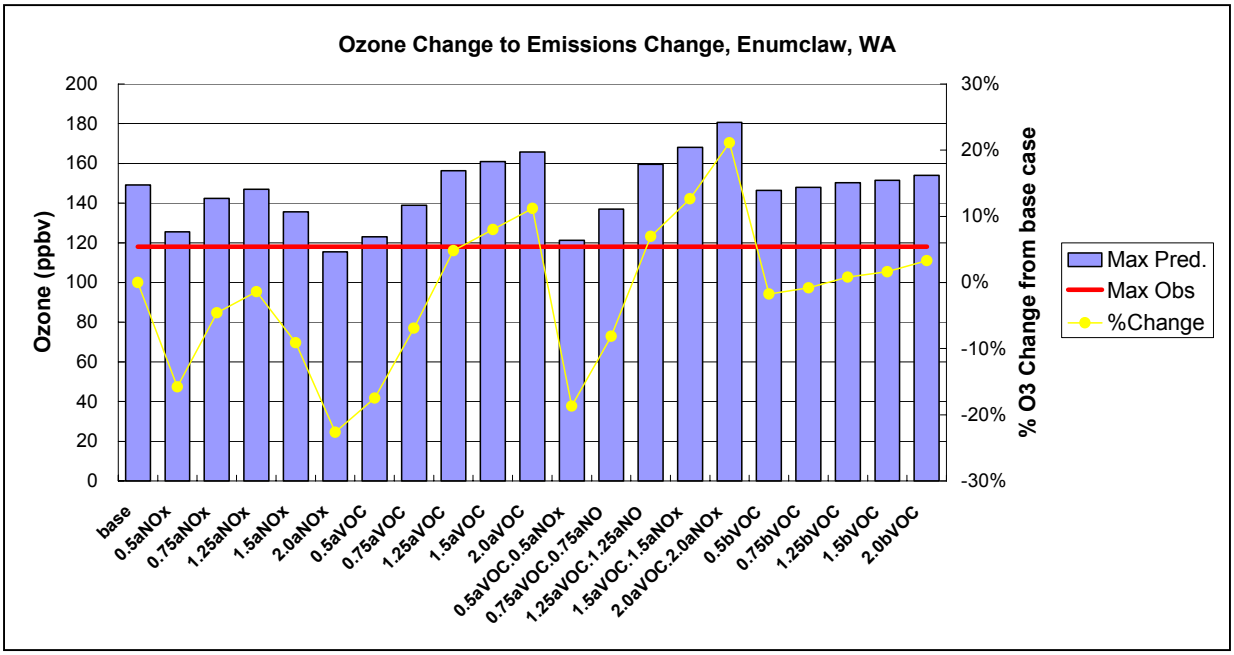

(19b) Beacon Hill, WA

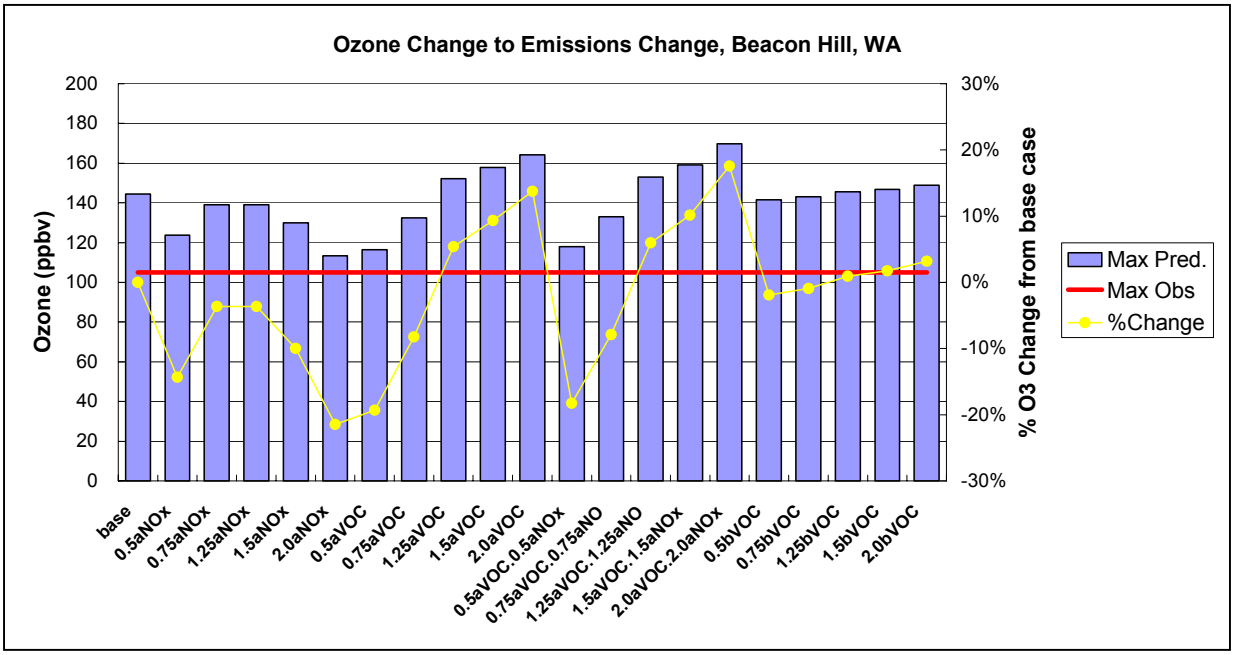

Figure 19c-d: Maximum 1-hour predicted ozone concentrations by emissions scenarios with maximum 1-hour observed ozone concentration for the three-day simulation period. The dotted line shows the percent maximum predicted ozone change from the base-case simulation for different emission scenarios.

(19c) Carus, OR

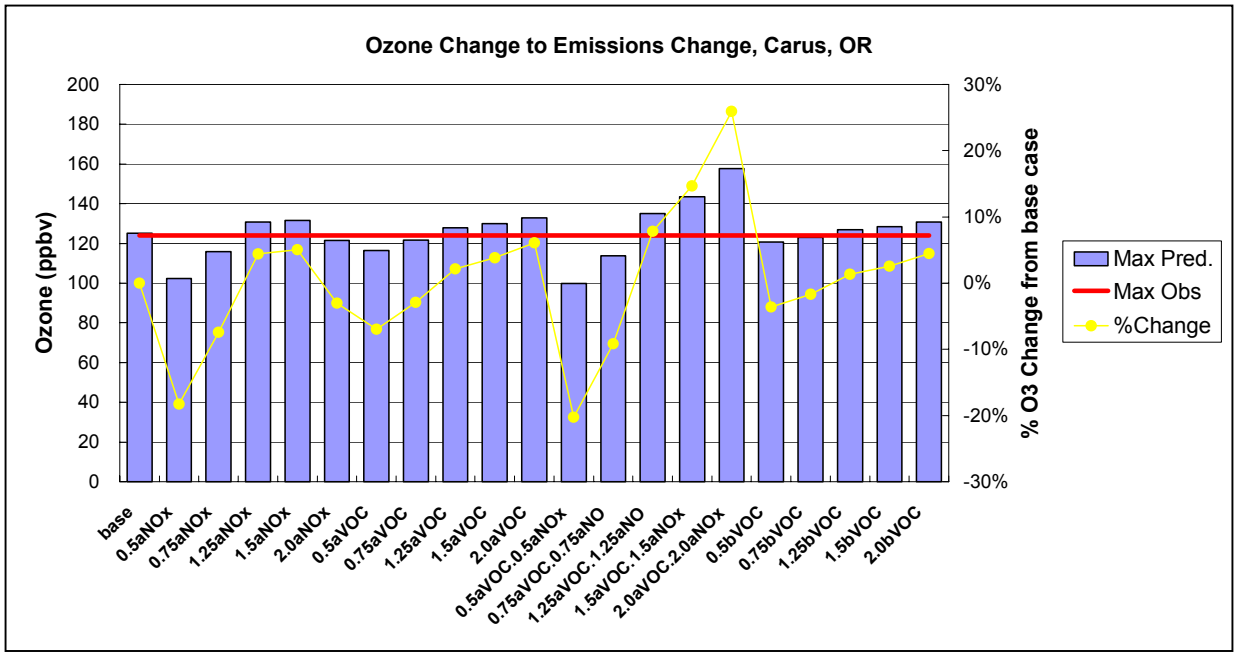

(19d) Milwaukie High School, OR

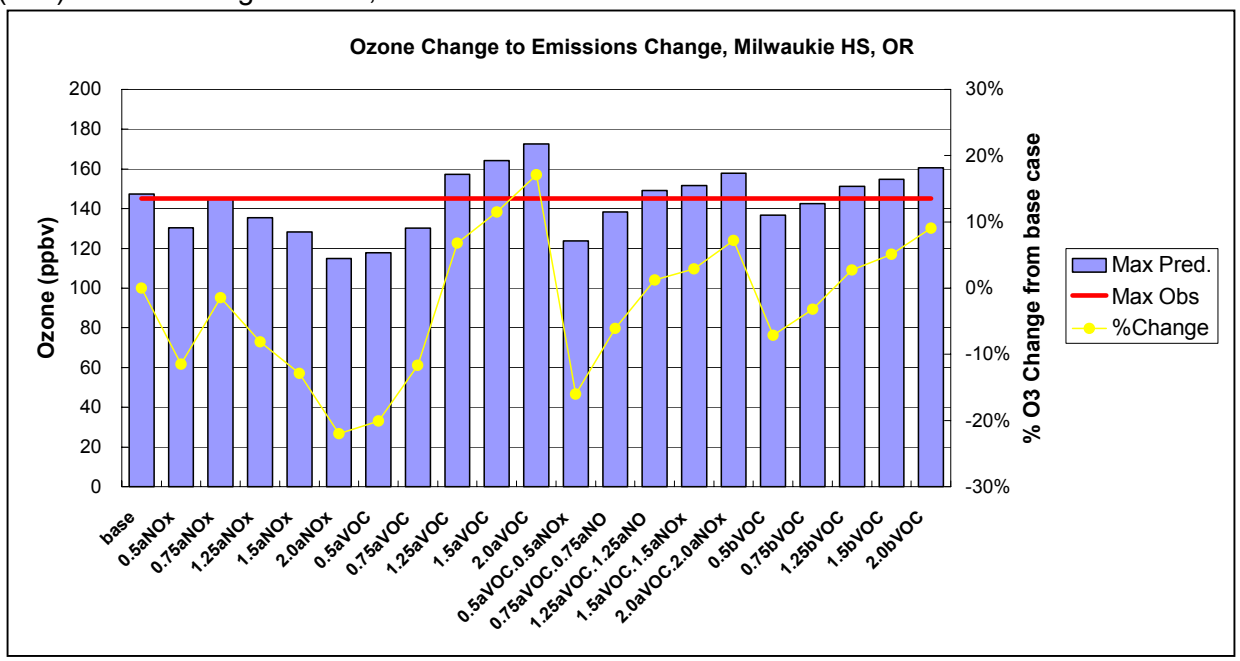

The overall ozone changes from the range of different emission scenarios were similar for all four sites. In general, ozone changed linearly with anthropogenic VOC emissions but non-linearly with anthropogenic NOx emissions. Increasing VOC emissions increases ozone formation, but increasing NOx emissions reduces ozone formation due to enhanced NO titration of ozone. For Enumclaw, Beacon Hill, and Carus, ozone increased by the largest amount when both NOx and VOC emissions were increased together by 100% (2.0aVOC.2.0aNOx). For Milwaukie High School however, the largest ozone increase occurred when anthropogenic VOC emissions were increased by 100% (2.0.aVOC). In terms of largest ozone reductions from the base-case, they were observed for Enumclaw, Beacon Hill and Milwaukie High School when NOx emissions were increased by 100% (2.0aNOx). For Carus, the largest ozone reduction occurred when both NOx and VOC emissions were reduced together by half (0.5aVOC.0.5aNOx). Between the maximum predicted ozone scenarios (2.0aVOC.2.0aNOx at Milwaukie High School) and the minimum predicted ozone scenario (2.0aNOx at Enumclaw), ozone changes range from +26% to -23% of the base-case simulation.

In terms of model performance improvements, at Enumclaw where the maximum ozone was overestimated, better model performance was obtained for the cases when NOx emissions were increased by 100% (2.0aNOx) or when NOx and VOC emissions were both reduced by 50% (0.5aVOC.0.5aNOx). At these emission scenarios, the predicted maximum ozone concentrations reduced from the base-case to -2% and 3% away from the observed level. For the Beacon Hill station, CMAQ performance improved for the case when NOx emissions were increased by 100% (2.0aNOx). At this emission scenario, the maximum predicted ozone level also decreased from the base-case and improves the ozone prediction by 30%. It is also interesting to observe that, in Carus, similar base-case model performance, in terms of predicting maximum ozone level, could be achieved when biogenic VOC was lowered by 25% (0.75bVOC). For Milwaukie High School, similar base-case ozone performance could be achieved when NOx emissions were reduced by 25%.

The four graphs also showed ozone being more sensitive to anthropogenic VOC than biogenic VOC emissions. For all four sites, changing anthropogenic VOC from 50% to 100% changed base-case ozone by an average of -16% to +12%, however when biogenic VOC were changed by the same percentage, ozone only changed by an average of -4% to +5. Among the four ozone observation sites, Milwaukie High School had slightly higher biogenic sensitivity (-7% to 9%) than the rest of the stations.

In terms of PM2.5 sensitivity results with observations, four PM2.5 measurement sites were compared. Since measurements from the IMPROVE database were at 24-hour averaged for July 13, 1996, the predicted PM2.5 concentrations were averaged over the first simulation day for comparisons. Figure 20a to 20d show the predicted PM2.5 concentrations by emissions scenarios with observed PM2.5 concentration, and percent PM2.5 change from the base-case simulation for Puget Sound, WA (PUSO), Mount Rainier national park, WA (MORA), Columbia River Gorge national park, OR (CORI), and Glacier national park, MT (GLAC) respectively. The numerical data are listed in Appendix I. The graphs showed that CMAQ over-predicted PM2.5 for all four locations, the over-prediction is more pronounced for PUSO and CORI sites than MORA and GLAC sites.

Figure 20a-b: 24-hour averaged predicted PM2.5 concentrations by emissions scenarios with 24-hour averaged observed PM2.5 concentrations for July 13, 1996. The dotted line shows the percent predicted PM2.5 change from the base-case simulation.

(20a) Puget Sound, WA

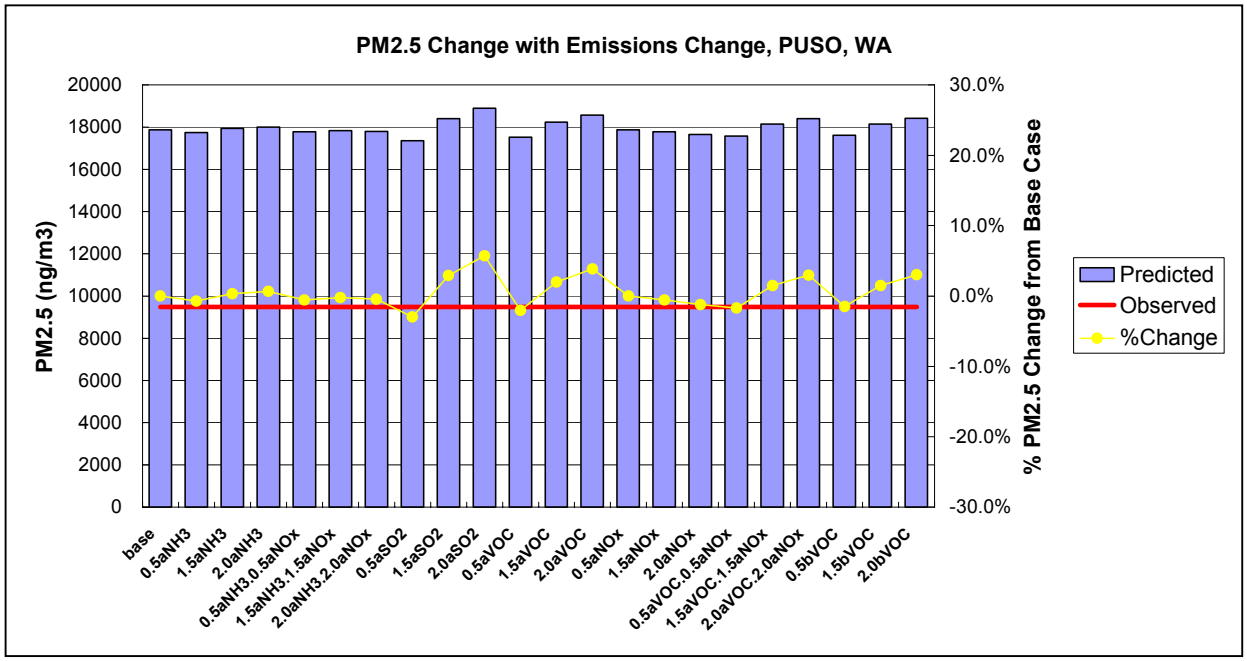

(20b) Mount Rainier, WA

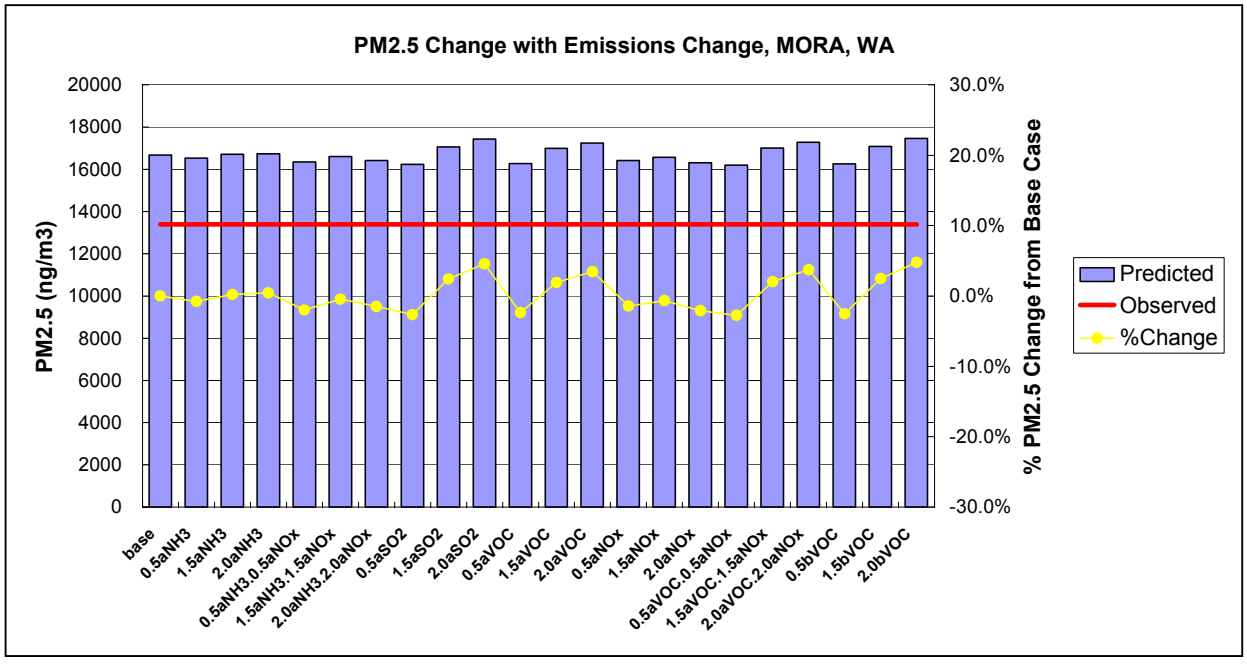

Figure 20c-d: 24-hour averaged predicted PM2.5 concentrations by emissions scenarios with 24-hour averaged observed PM2.5 concentrations for July 13, 1996. The dotted line shows the percent predicted PM2.5 change from the base-case simulation.

(20c) Columbia River Gorge, OR

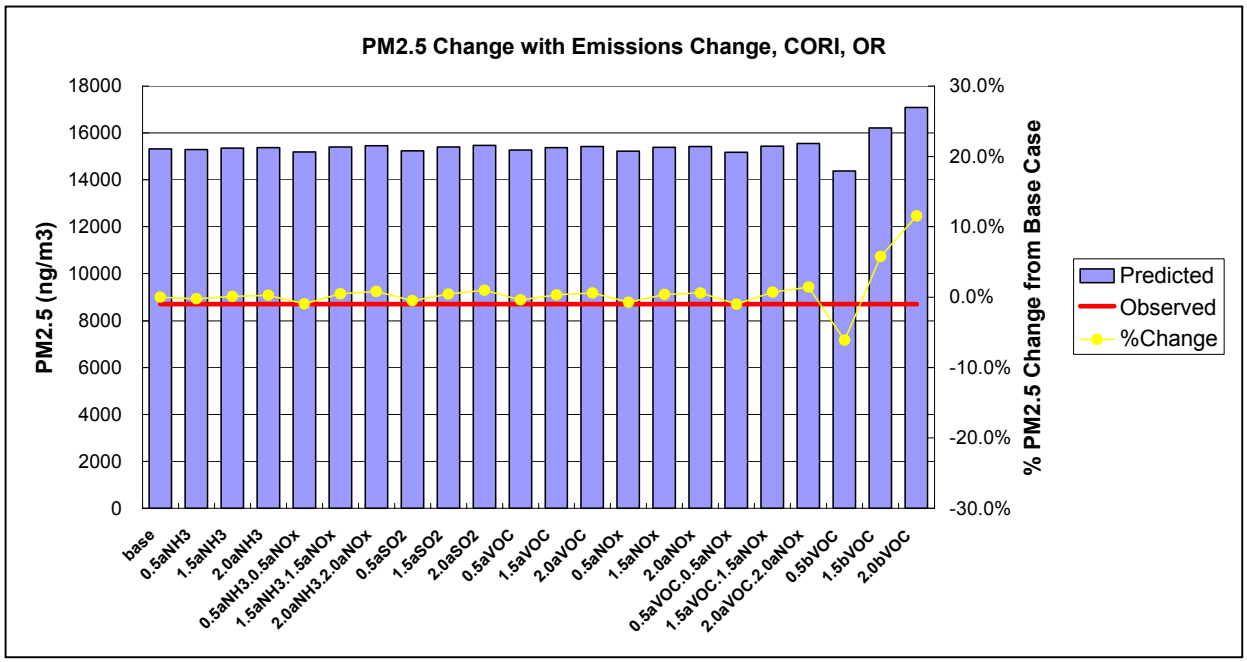

(20d) Glacial National Park, MT

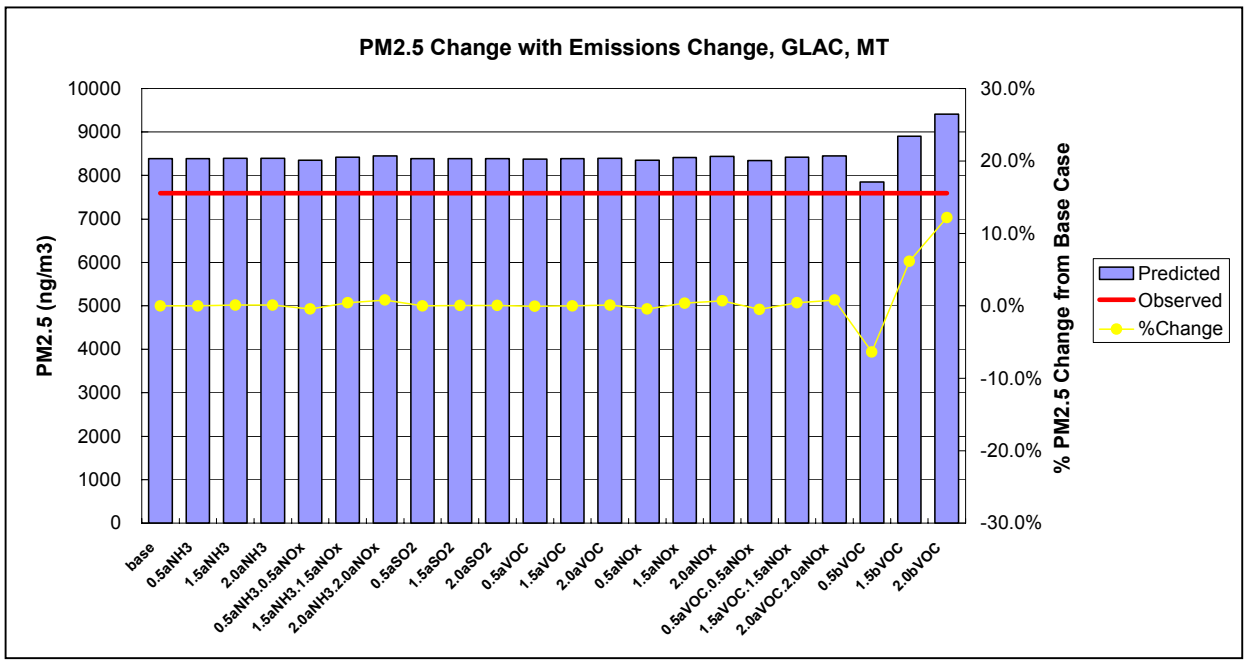

Comparing PM2.5 changes with various emission sensitivity cases, the range of changes were less significant than that of ozone. Changing different PM2.5 precursor emissions did not change the averaged-daily predicted PM2.5 by a big amount, and different emissions scenarios did not suggest improvements on model performance. For CORI and GLAC stations, changing biogenic VOC produce the largest PM2.5 changes compare to other emissions change. For MORA and PUSO stations, changing SO2, anthropogenic VOC and biogenic VOC produced higher PM2.5 changes than other emission changes. Between the maximum predicted PM2.5 scenarios (2.0bVOC at GLAC) and the minimum predicted PM2.5 scenario (0.5bVOC at GLAC) of the four stations, PM2.5 changes range from +12% to -6% of the base-case simulation. This range is much narrower than the changes observed for ozone. However, it is important to recognize that the results presented for the four stations were averaged over 24-hours. The long average time can lessen the percentage change in modeled PM2.5. Furthermore, since the results were obtained from the first-day of a three-day model episode, insufficient model spin-ups may delay the full effects of changing precursor emissions on PM2.5 formation and lessen the degree of PM2.5 sensitivity towards emission changes.

2.5 Summary and Conclusions

The Community Multi-scale Air Quality (CMAQ) Model was employed to perform ozone and aerosol sensitivity analyses over the Pacific Northwest region. The analyses focused on aerosol and ozone responses to domain-wide changes in precursor emissions. The direct emissions change method was employed in this study. Several sensitivity simulations plus a base-case were performed. The base-case simulation had a complete set of biogenic and anthropogenic emissions while the sensitivity runs had step-wise adjustments in various precursor emissions: anthropogenic VOCs, NOx, SO2, NH3, biogenic VOCs, and combined anthropogenic NOx&VOCs and anthropogenic NOx&NH3. The adjustments were made at ±25%, ±50% or ±100% from the base-case emissions. Ozone and PM2.5 results of the sensitivity simulations were compared against the base-case run.

Changes in total PM2.5 were analyzed for changes in SO2, NOx, NH3, VOC precursor emissions and NOx&NH3 combined emissions for four sites in the region. Predicted PM2.5 in different regions responded differently to changes in emissions. Areas with higher predicted base-case PM generally had higher PM2.5 sensitivity (Enumclaw, Carus and CORI), while areas with lower base-case PM had lower PM2.5 changes to precursor emissions (Craters of the Moon).

The individual PM2.5 responses were dependant upon the local total ammonia to sulfate molar ratio ([TNH3]/[TSO4]). In Enumclaw, the ammonia molar concentration was more than twice that of the sulfate molar concentration. Under this ammonia-rich condition, reductions in NOx, NH3 or NH3&NOx were effective in reducing PM2.5 formation, but changes in SO2 emissions did not produce much change to the total PM2.5 concentration. This was mainly due to the high ammonia concentrations that reacted with high HNO3 to produce ammonia nitrate aerosol in the region. On the other hand, Carus and CORI had the base-case total ammonia to sulfate molar concentration ratio less than two. In these ammonia-poor conditions PM2.5 was highly sensitive to changes in SO2 emissions but insensitive to NH3 changes. This was due to the presence of partly neutralized sulfate aerosols that buffer the NH3 emission changes. At rural Craters of the Moon site, there were low base-case precursor emissions and it had the least PM2.5 sensitivity towards emission changes.

One unexpected PM2.5 change was in Carus, where the increases in NOx decreased total PM2.5. This nonlinear PM2.5 to NOx relationship illustrates the coupled aerosol and ozone chemistry in urban regions. When anthropogenic NOx emissions were increased, the already high NOx emissions in the urban area lowered ozone formation in the region. This in turn decreased the oxidant formation through NO titration. As atmospheric oxidant concentrations changed, they led to changes in PM2.5, since secondary aerosols were formed through atmospheric oxidation of precursor gases.

Ozone sensitivity to precursor anthropogenic NOx, VOC, VOC&NOx and biogenic VOC emissions were analyzed for six regions in the domain. It was found that ozone changed linearly with combined NOx&VOC emissions, anthropogenic VOCs and biogenic VOCs. The correlation was strongest for NOx&VOC combined emissions but weakest for biogenic VOC changes.

The large ozone changes to combined VOC&NOx emissions were expected since both VOC and NOx are primary precursors to ozone. During anthropogenic VOC sensitivity simulations, Enumclaw, Carus and Tri-cities had the greatest ozone change, while smaller urban regions and rural areas had little or no ozone change. The differences in ozone change were due to different base-case NOx concentrations in the regions. High NOx in urban areas caused high ozone changes to changes in anthropogenic VOC emissions than rural regions. The ozone sensitivity between urban and rural regions was switched when domain-wide biogenic VOCs were adjusted. Urban areas such as, Enumclaw, Carus and Tri-cities had little ozone sensitivity to biogenic VOC, but the smaller urban areas and rural regions such as, Boise, Spokane and Craters of the Moon, had much larger ozone changes.

For anthropogenic NOx emission changes, ozone changed non-linearly in Carus and Enumclaw but linearly in all other regions. This was because Carus and Enumclaw had high levels of anthropogenic NOx emissions with respect to VOC. Elevated NOx actively removed ozone and inhibited ozone chemical production. In smaller urban and rural regions, ozone changed linearly with NOx emissions. This was because NOx was the limited reagent in ozone production.

The base-case HNO_3/H_2O_2 ratio at six selected sites was also used to correlate ozone sensitivity to NOx and VOC changes. Overall, the HNO_3/H_2O_2 ratio demonstrated to be a good indicator for identifying VOC or NOx sensitive regions. Enumclaw, Carus and Tri-cities had high ratios and they corresponded to NOx-rich and VOC-sensitive areas, while Boise, Spokane and Craters of the Moon had low ratios and they correspond to NOx-limited conditions, where ozone

controls favor NOx. The ratio also suggests how responsive the areas were to changes in precursor emissions. Regions with high ratio showed high ozone sensitivity to NOx and VOC changes, and regions with similar ratios showed similar percentage ozone changes to changes in precursor emissions.

The sensitivity analyses were also used to evaluate model performance as affected by uncertainties in the emission inventory. The results indicated that CMAQ predicted the base-case ozone concentrations well, but over-predicted the 24-hour averaged PM2.5 concentrations. Among the simulated emission scenarios, increase NOx emissions by 100% improved the model performance for ozone at both the Eunmclaw and Beacon Hill observational sites. However, the improvements were not significant for PM2.5. Between the maximum predicted ozone scenarios and the minimum predicted ozone scenario, ozone changes range from +26% to -23% of the base-case simulation. This range was less significant for PM2.5. Changing different PM2.5 precursor emissions only changed the averaged-daily predicted PM2.5 by +12% to -6%. This insensitivity of PM2.5 to emission scenarios may due to the long averaging period and insufficient model spin-up in the simulation results.

This study presents the first model assessment of aerosol sensitivity, and the first instance in correlating ozone sensitivity to the HNO_3/H_2O_2 concentration ratio over the Pacific Norwest region. The results provide some insight to PM2.5 responses to changes in various precursor emissions, and show the direct coupling of aerosol and ozone chemistry in the region. The study also suggests that secondary chemical concentration ratios such as TNH4/TSO4 and HNO_3/H_2O_2 could be good indicators of the behavior of different chemical systems in the area. Although CMAQ is a state-of-science air quality model that includes many physical and chemical aerosol production algorithms, the algorithms are far from perfect. Further investigations, including various field experiments, are necessary to verify and to better understand the chemical relationship between ozone, aerosol, and their corresponding indicator ratios in this beautiful Pacific Northwest.

References

Andreani-Aksoyoglu, Sebnem, Lu, Cheng-Hsuan, Keller, Johannes, Prevot, Andre S. H., and Chang, Julius S., Variability of indicator values for ozone production sensitivity: a model study in Switzerland and San Joaquin Valley (California), *Atmospheric Environment*, 35, 5593-5604, 2001.

Ansari, A. S. and S. N. Pandis, Prediction of Multicomponent Inorganic Atmospheric Aerosol Behavior, *Atmospheric Environment*, 33, 745-757, 1999.

Atkinson, Roger, Atmospheric chemistry of VOCs and NOx, *Atmospheric Environment*, 34, 2063-2101, 2000.

Barna, M., B. Lamb, S. O'neill, H. Westberg, C. Figueroa-Kaminsky, S. Otterson, C. Bowman, and J. Demay, Modeling Ozone Formation and Transport in the Cascadia Region of the Pacific Northwest, *Journal of Applied Meteorology*, 39, 349-366, 2000.

Barna, M., B. Lamb, and H. Westberg, Modeling the Effects of VOC/NOx Emissions on Ozone Synthesis in the Cascadia Airshed of the Pacific Northwest, *Journal of the Air & Waste Management Association*, 51, 1021-1034, 2001.

Binkowski, F. S. and U. Shankar, The Regional Particulate Matter Model .1. Model Description and Preliminary Results, *Journal of Geophysical Research-Atmospheres*, 100, 26191-26209, 1995.

Blanchard, Charles L., Ozone process insights from field experiments - Part III: extent of reaction and ozone formation, *Atmospheric Environment*, 34, 2035-2043, 2000.

Bullock, O. R. and K. A. Brehme, Atmospheric Mercury Simulation Using the CMAQ Model: Formulation Description and Analysis of Wet Deposition Results, *Atmospheric Environment*, 36, 2135-2146, 2002.

Byun, D., Young, J. Gipson G., Godowitch, J., Binkowski, F., Roselle, S., Benjey, B., Pleium, J., Ching, J., Novak, J., Coats, C., Odman, T., Hanna, A., Alapty, K., Mathur, R., McHenry, J., Shakar, U., Fine, S., Ziu, A., and Jang, C. The Environmental Protection Agency third generation air quality modeling system: An overall perspective. 10th Joint Conference on the Applications of Air Pollution Meteorology with the A&WMA. 1998.

Byun, D. W. and Ching, J. K. S. Science Algorithms of the EPA Models-3 Community Multi-scale Air Quality (CMAQ) Modeling System. 1999. Office of Research and Development Washington DC, U.S. Environmental Protection Agency.

Chameides, W. L., R. D. Saylor, and E. B. Cowling, Ozone Pollution in the Rural United States and the New NAAQS, *Science*, 276, 916, 1997.

Chandrasekar, A., Sun, Q., and Gerorgopoulous P.G. A comparative study of prognostic meteorological and of air quality model predictions with NEOPS 1999 observations. Fourth Conference on Atmospheric Chemistry: Urban, Regional and Global-scale Impacts of Air Pollutants. American Meteorological Society 2002.

Chock, David P., Chang, Tai Y., Winkler, Sandra L., and Nance, Barbara I., The impact of an 8 hour ozone air quality standard on ROG and NOx controls in Southern California, *Atmospheric Environment*, 33, 2471-2485, 1999.

Dennis, R. L., D. W. Byun, J. H. Novak, K. J. Galluppi, C. J. Coats, and M. A. Vouk, The next generation of integrated air quality modeling: EPA's Models-3, *Atmospheric Environment*, 30, 1925-1938, 1996.

Griffin, R. J., D. R. Cocker, R. C. Flagan, and J. H. Seinfeld, Organic Aerosol Formation From the Oxidation of Biogenic Hydrocarbons, *Journal of Geophysical Research-Atmospheres*, 104, 3555-3567, 1999.

Guenther, A., C. Geron, T. Pierce, B. Lamb, P. Harley, and R. Fall, Natural Emissions of Non-Methane Volatile Organic Compounds; Carbon Monoxide, and Oxides of Nitrogen From North America, *Atmospheric Environment*, 34, 2205-2230, 2000.

Houyoux, M. and Vukovich, J. Updates to the Sparse Matrix Operator Kernel Emissions (SMOKE) Modeling System and Integration with Models-3. The Emissions Inventory: Regional Strategies for the Future Conference. 1999. Air & Waste Management Association.

Houyoux, M, Vukovich, J, and Brandmeyer, J. Sparse Matrix Operator Kernel Emissions Modeling System User Manual. 2000.

Jacobson, M. Z., Development and Application of a New Air Pollution Modeling System .2. Aerosol Module Structure and Design, *Atmospheric Environment*, 31, 131-144, 1997.

Jiang, G., Photochemical air quality modeling in the Puget Sound region, Ph.D. thesis, Washington State University, Department of Chemistry, Pullman, WA, 2001.

Jiang, W. and Yin, D. Mathematical formulation and consideration for converting CMAQ modal particulate matter results into size-resolved quantities. American Meteorological Society Fourth Conference on Atmospheric Chemistry: Urban, Regional, and Global-Scale Impacts of Air Pollutants. 2002.

Jiang, Weimin, Singleton, Donald L., McLaren, Robert, and Hedley, Mark, Sensitivity of ozone concentrations to rate constants in a modified SAPRC90 chemical mechanism used for Canadian Lower Fraser Valley ozone studies, *Atmospheric Environment*, 31, 1195-1208, 1997.

Lurmann, F. W., A. S. Wexler, S. N. Pandis, S. Musarra, N. Kumar, and J. H. Seinfeld, Modelling Urban and Regional Aerosols .2. Application to California's South Coast Air Basin, *Atmospheric Environment*, 31, 2695-2715, 1997.

Meng, Z., D. Dabdub, and J. H. Seinfeld, Chemical Coupling Between Atmospheric Ozone and Particulate Matter, *Science*, 277, 116-119, 1997.

Meng, Z. Y., D. Dabdub, and J. H. Seinfeld, Size-Resolved and Chemically Resolved Model of Atmospheric Aerosol Dynamics, *Journal of Geophysical Research-Atmospheres*, 103, 3419-3435, 1998.

Middleton, P., Daqm-Simulated Spatial and Temporal Differences Among Visibility, Pm, and Other Air Quality Concerns Under Realistic Emission Change Scenarios, *Journal of the Air & Waste Management Association*, 47, 302-316, 1997.

Milford, J. B., A. G. Russell, G. J. McRae, and G. R. Cass, A New Approach to Photochemical Pollution Control: Implications of Spatial Patterns in Pollutant Responses to Reductions in Nitrogen Oxides and Reactive Organic Gas Emissions, *Environmental Science & Technology,* 23, 1290-1301, 1989.

National Research Council (NRC). Rethinking the ozone problem in urban and regional air pollution. 1991.

Nenes, A., S. N. Pandis, and C. Pilinis, ISORROPIA: a New Thermodynamic Equilibrium Model for Multiphase Multicomponent Inorganic Aerosols, *Aquatic Geochemistry*, 4, 123-152, 1998.

Nguyen, K. and D. Dabdub, NOx and VOC Control and Its Effects on the Formation of Aerosols, *Aerosol Science and Technology*, 36, 560-572, 2002.

Odum, J. R., T. Hoffmann, F. Bowman, D. Collins, R. C. Flagan, and J. H. Seinfeld, Gas/Particle Partitioning and Secondary Organic Aerosol Yields, *Environmental Science & Technology*, 30, 2580-2585, 1996.

Pagowski, M., Chtcherbakov, A., Bloxam, R., Wong, S., Lin, X., Sloan, J., and Soldatenko, S. Evaluation of Models-3/CMAQ performance during a winter high particulate matter episode in February 1998. Fourth Conference on Atmospheric Chemistry: Urban, Regional and Global-scale Impacts of Air Pollutants. American Meteorological Society, 2002.

Pai, P., K. Vijayaraghavan, and C. Seigneur, Particulate Matter Modeling in the Los Angeles Basin Using Saqm-Aero, *Journal of the Air & Waste Management Association*, 50, 32-42, 2000.

Pandis, S. N., R. A. Harley, G. R. Cass, and J. H. Seinfeld, Secondary Organic Aerosol Formation and Transport, *Atmospheric Environment Part a-General Topics*, 26, 2269-2282, 1992.

Pun, B. K. and C. Seigneur, Sensitivity of Particulate Matter Nitrate Formation to Precursor Emissions in the California San Joaquin Valley, *Environmental Science & Technology*, 35, 2979-2987, 2001.

Russell, A. and R. Dennis, Narsto Critical Review of Photochemical Models and Modeling, *Atmospheric Environment*, 34, 2283-2324, 2000.

Saxena, P., A. B. Hudischewskyj, C. Seigneur, and H. J. Seinfeld, A comparative study of equilibrium approaches to the chemical characterization of secondary aerosols, *Atmospheric Environment*, 20, 1471-1483, 1986.

Saylor, Rick D., Chameides, William L., and Chang, Michael E., Demonstrating attainment in Atlanta using urban airshed model simulations: impact of boundary conditions and alternative forms of the NAAQS, *Atmospheric Environment*, 33, 1057-1064, 1999.

Seigneur, C., Current Status of Air Quality Models for Particulate Matter, *Journal of the Air & Waste Management Association*, 51, 1508-1521, 2001.

Seigneur, C., P. Pai, P. K. Hopke, and D. Grosjean, Modeling Atmospheric: Particulate Matter, *Environmental Science & Technology*, 33, 80A-86A, 1999.

Seinfeld, J. H. and S. N. Pandis, Atmospheric chemistry and physics: from air pollution to climate change, John Wiley and Sons Inc., New York: 1998.

Sillman, S., The Use of NOy, H2O2, and HNO3 as Indicators for Ozone-NOx- Hydrocarbon Sensitivity in Urban Locations, *Journal of Geophysical Research-Atmospheres*, 100, 14175-14188, 1995.

Sillman, S., The Relation Between Ozone, Nox and Hydrocarbons in Urban and Polluted Rural Environments, *Atmospheric Environment*, 33, 1821-1845, 1999.

Turpin, B. J., P. Saxena, and E. Andrews, Measuring and Simulating Particulate Organics in the Atmosphere: Problems and Prospects, *Atmospheric Environment*, 34, 2983-3013, 2000.

U.S. Environmental Protection Agency. Biogenic Emissions Inventory System Model. 1998 Available online: http://www.epa.gov/ttn/chief/emch/models/beis/

U.S. Environmental Protection Agency. Community Multi-scale Air Quality (CMAQ) modeling system. 1999a Available online: http://www.epa.gov/asmdnerl/models3/cmaq.html

U.S. Environmental Protection Agency. SPECIATE - Repository of Total Organic Compound (TOC) and Particulate Matter (PM) speciation profiles. 1999b Available online: http://www.epa.gov/ttn/chief/software/speciate/

U.S. Environmental Protection Agency. MOBILE vehicle emission factor model. 2000 Available online: http://www.epa.gov/otaq/mobile.htm

U.S. Environmental Protection Agency. Biogenic Emissions Landcover Database. 2001 Available online: http://www.epa.gov/asmdnerl/biogen.html

Wark, K., C. F. Warner, and W. T. Davis, Air pollution: its origin and control, Addison-Wesley, Menlo Park, Calif.: 1998.

Washington State Department of Ecology, Oregon Department of Environmental Quality, Idaho Department of Environmental Quality, EPA Region 10, Washington State University, University of Washington, and Environment Canada. Regional Technical Center Demonstration Project: Summary Report. 2002.

CHAPTER 3

SUMMARY AND CONCLUSIONS

3.1 Summary

Ozone and aerosol in the troposphere are atmospheric pollutants that pose threats to human health and welfare. Fine aerosols (PM2.5) in the air also scatter light and attribute to visibility degradation. In this study, we applied the CMAQ model to investigate the sensitivity of these secondary pollutants to changes in precursor emissions in the Pacific Northwest.

Sensitivity results for PM2.5 were analyzed for different regions in the domain. Generally regions with higher base-case PM concentrations had higher sensitivity to changes in precursor emissions. Different regions also responded differently to changes in emissions species. The responses were explained by the region's total ammonia to sulfate molar ratio (TNH3/TSO4). Enumclaw, WA, had a high ratio (ammonia rich), and PM2.5 concentrations were highly sensitive to NOx and NH3 emissions, but insensitive to SO2 emissions change. For the Enumclaw area, reducing NH3 or NH3 with NOx emissions is suggested to be a good control option for lowering total PM2.5 concentrations in the region. In areas that had low ratios (ammonia poor) such as Carus, OR and the Columbia River Gorge, the PM2.5 responses were different. Predicted PM2.5 concentrations were highly sensitive to changes in SO2 emissions, but insensitive to NOx and NH3 changes. Lowering SO2 emissions directly lowered the sulfate aerosol and decreased PM2.5, but changing NH3 emissions had little impact on final PM2.5 formation.

The series of sensitivity results also demonstrated that aerosol and ozone chemistry are closely tied to each other. The chemistry between the two is tied through the oxidant production reactions in the atmosphere. High ozone concentrations led to higher atmospheric oxidant production, which in turn, increased aerosol formation. This coupled chemistry led to decreases

in PM2.5 formation with increased NOx emission in Carus, OR, as ozone was titrated by the increased NO emissions.

Ozone sensitivity towards VOC and NOx emissions changes were also analyzed for different regions in the domain. We found that ozone changed linearly in all areas with combined NOx&VOC, anthropogenic VOCs and biogenic VOCs. The sensitivity is stronger in urban regions than rural sites. Different ozone sensitivity was observed when NOx emissions was changed alone. We found ozone changed non-linearly with NOx in urban regions, but linearly with NOx in rural sites. In most high ozone observational sites, the increase of 100% NOx was able to produce the maximum ozone reduction compared to all other sensitivity scenarios. The degrees of ozone sensitivity towards NOx or VOC emissions were correlated with base-case H_2O_2/HNO_3 concentration ratio. This ratio appears to be a good indicator for regions that were sensitive to either NOx or VOC emissions changes, where a large ratio suggests a higher degree of ozone response to changes in precursor emissions.

3.2 Recommendations

Modeling the formation and transport of air pollutants is a complex and difficult task. Although CMAQ is a state-of-science air quality model, the algorithms are far from perfect. Improvements to the chemical transport models that can more realistically represent the chemistry and physics of the atmosphere and are likely to improve model performances. Some of the model improvements suggest for future work include:

- Update the gas-phase chemical mechanism to incorporate more condensable organic species, including their secondary and tertiary oxidized compounds, and their formation kinetics.
- Update the organic aerosol module to include additional aerosol partitioning methods, including, vapor saturation, adsorption, absorption and dissolution.

- Include sea salt (NaCl) chemistry, crustal and carbonate species (K^+, Ca^{+2}, Mg^+, CO_3^{-2}) in the CMAQ inorganic aerosol module.
- Inclusion of heterogeneous chemistries that occur on particle surfaces (eg. ozone reactions on soot particles).

Organic aerosol represents a large fraction of fine PM in the Pacific Northwest region. Having a detailed and updated organic aerosol algorithm can improve the prediction of fine aerosols in the region. Sea salt and crustal species are also important in representing the ionic balance in the costal regions and predicting airborne dust in the inland regions of Washington and Oregon.

In addition, having correct model inputs are necessary to improve model accuracy. The two primary inputs into air quality models are meteorology and emission inventory. In this study, the meteorological inputs were generated from the MM5 model at 12-km resolution. This resolution may not be sufficient to describe the complex wind field caused by the complex terrain in the region. Increasing the meteorological resolution in both horizontal and vertical directions can provide better descriptions of the wind patterns and better descriptions of the mixing layer heights. The detailed meteorological data can improve both the spatial and temporal distribution of the predicted pollutants. In terms of predicting aerosol and gas-phase pollutants together, it is also important to include radiation attenuation routines that account for scattering of short and long wave radiations by particulate matter, which affect the photochemical reaction rates.

Emissions inventory improvement is another critical aspect in improving model results. This is the hardest piece of information to acquire, and the data often contain high degrees of uncertainty. Good emissions inventories need (1) correct amount of emissions from a complete set of source categories, (2) appropriate spatial surrogates that spatially allocate the emissions into gridded model domain, (3) representative temporal profiles that temporally distribute emissions to months/days/hour fractions, and (4) accurate chemical speciation data that speciate inventory chemical species (eg. VOC, PM10, PM25) to modeled species (eg. ALD,

HCHO, PEC, PNO3). The spatial profiles require detailed landuse information, census data and GIS processing, the temporal allocation profiles need field monitoring programs and statistical analysis to generate representative allocation fractions for different sources, and the chemical speciation data requires laboratory work on aerosol and VOC composition examinations.

In terms of inventory species improvements, this study demonstrated that ammonia is an important PM precursor in determining the PM sensitivity at a region. Improvements in ammonia emissions in terms of a dynamic model that uses detailed landuse information and meteorological data are necessary for fine resolution inventory used in air quality models. The current ammonia inventory was estimated based on fixed emission fluxes and did not correct for temperature changes. Generate ammonia emissions from a dynamic model with meteorological data can better estimate the temporal changes in ammonia emissions.

Besides ammonia, additional primary particulate sources are needed to have a more complete aerosol inventory. Some emission categories not in the current NWRMC inventory include wind-blown dust, agriculture field burning and forest fires.

Another important emissions need is in biogenic emission estimates. As seen in Chapter 2, find PM are highly sensitive to changes in biogenic VOCs since terpene emissions contribute to high amounts of condensable organics that form secondary organic aerosols. Different terpene spices have different aerosol forming potential. Improving the predictions of biogenic emissions factors can increase the validity of biogenic emission model and enhance biogenic emissions to the air quality models.

Finally and most impotently is the need for field measurement data. Monitoring data at various locations are necessary to verify the model, provide boundary conditions as model inputs, and to better understand the chemical relationships between ozone, aerosol, and their corresponding indicator ratios. Air quality model are mathematical descriptions of our theoretical understanding of the atmospheric chemistry and physics. Verifying the model results

against observational data and keeping the models updated with new observed relationships are necessary steps in building accurate air quality models.

APPENDIX

Appendix A: Definitions of the CMAQ RADM2 gas and aerosol phase species modeled species used in the mechanism. (Taken from (Byun and Ching, 1999)).

CMAQ RADM2 Specie	Description	
ALD	Acetaldehyde and higher aldehydes	Gas Phase Species
CH4	Methane	
CO	Carbon Monoxide	
CSL	Cresol and other hydroxy substituted aromatics	
ETH	Ethane	
HC3	Alkanes w/2.7x10^-13>kOH<3.4x10^-12	
HC5	Alkanes w/3.4x10^-12>kOH<6.8x10^-12	
HC8	Alkanes w/kOH>6.8x10^-12	
HCHO	Formaldehyde	
H2O2	Hydrogen Peroxide	
HNO3	Nitric acid	
ISO	Isoprene	
KET	Ketones	
NH3	Ammonia	
NO	Nitric oxide	
NO2	Nitrogen dioxide	
O3	Ozone	
OL2	Ethene	
OLI	Internal olefins	
OLT	Terminal olefins	
ORA2	Acetic and higher acids	
SO2	Sulfur dioxide	
SULF	Sulfuric acid	
TERPB	Terpenes	
TOL	Toluene and less reactive aromatics	
XYL	Xylene and more reactive aromatics	
ASO4	Sulfate mass concentration	Aerosol Phase Species
ANH4	Ammonium mass concentration	
ANO3	Nitrate mass concentration	
AORGA	Anthropogenic secondary organic mass concentration	
AORGPA	Primary organic mass concentration	
AORGB	Secondary biogenic organic mass concentration	
AEC	Elemental carbon mass concentration	
A25	Unspecified anthropogenic mass concentration	
AH2O	Water mass concentration	
ACORS	Other unspecified anthropogenic mass concentration	
ASEAS	Marine mass concentration	
ASOIL	Soil-derived mass concentration	
NUMATKN	Aitken mode number concentration	
NUMACC	Accumulation mode number concentration	
NUMCOR	Coarse mode number concentration	
SRFATKN	Aitken mode surface area	
SRFACC	Accumulation mode surface area	

Appendix B: CMAQ Aerosol output species and the corresponding descriptions

Mode	CMAQ Species	Description
Aktken (I) and Accumulation (J) mode Aerosols	ASO4(I/J)	Sulfate mass concentration
	ANH4(I/J)	Ammonium mass concentration
	ANO3(I/J)	Nitrate mass concentration
	AORGA(I/J)	Anthropogenic secondary organic mass concentration
	AORGPA(I/J)	Primary organic mass concentration
	AORGB(I/J)	Secondary biogenic organic mass concentration
	AEC(I/J)	Elemental carbon mass concentration
	A25(I/J)	Unspecified anthropogenic mass concentration
	AH2O(I/J)	Water mass concentration
Coarse Mode Aerosols	ACORS	Other unspecified anthropogenic mass concentration
	ASEAS	Marine mass concentration
	ASOIL	Soil-derived mass concentration

Appendix C: Deliquescence Relative Humidity (DRH) of salts modeled in CMAQ aerosol module. (Taken from (Saxena et al., 1986)).

Compound	Molecular Formula	Deliquescence Relative Humidity (%)
Ammonium Sulfate	$(NH_4)_2SO_4$	80
Letovicite	$(NH_4)_3H(SO_4)_2$	69
Ammonium Bisulfate	NH_4HSO_4	40
Ammonium Nitrate	NH_4NO_3	62

Appendix D1-4: PM2.5 concentrations and PM2.5 percentage changes from the Base-case due to changes in anthropogenic inorganic precursor emissions (NH3, NOx, NH3&NOx, SO2) for Enumclaw, Carus, Columbia River and Craters of the Moon.

D1. Enumclaw, WA															
PM2.5 Concentration ($\mu g/m^3$)								Percentage PM2.5 Concentration Change from Base-case							
	100%	50%	25%	0%	-25%	-50%	-100%		100%	50%	25%	0%	-25%	-50%	-100%
NH3	36	33	31	28	25	23	22	NH3	30%	17%	10%	0%	-10%	-18%	-21%
NOx	30	30	29	28	26	23	18	NOx	7%	5%	4%	0%	-7%	-18%	-36%
NH3&NOx	40	35	32	28	24	21	18	NH3&NOx	42%	23%	13%	0%	-15%	-23%	-37%
SO2	28	28	28	28	28	28	28	SO2	0%	0%	0%	0%	0%	1%	1%

D2. Carus, OR															
PM2.5 Concentration ($\mu g/m^3$)								Percentage PM2.5 Concentration Change from Base-case							
	100%	50%	25%	0%	-25%	-50%	-100%		100%	50%	25%	0%	-25%	-50%	-100%
NH3	28	28	28	28	28	27	28	NH3	1%	0%	0%	0%	-2%	-3%	1%
NOx	26	27	28	28	28	28	23	NOx	-9%	-5%	-2%	0%	0%	-2%	-19%
NH3&NOx	26	27	28	28	28	27	23	NH3&NOx	-8%	-5%	-2%	0%	-1%	-4%	-19%
SO2	31	30	29	28	27	26	24	SO2	10%	5%	3%	0%	-4%	-7%	-15%

D3. Columbia River, WA															
PM2.5 Concentration ($\mu g/m^3$)								Percentage PM2.5 Concentration Change from Base-case							
	100%	50%	25%	0%	-25%	-50%	-100%		100%	50%	25%	0%	-25%	-50%	-100%
NH3	25	24	24	24	24	24	24	NH3	2%	0%	-1%	0%	0%	0%	-1%
NOx	25	25	25	24	23	22	18	NOx	2%	2%	2%	0%	-3%	-8%	-25%
NH3&NOx	25	25	24	24	24	23	18	NH3&NOx	4%	2%	1%	0%	-2%	-7%	-26%
SO2	30	27	26	24	22	21	18	SO2	24%	13%	7%	0%	-8%	-14%	-27%

D4. Craters of the Moon, ID															
PM2.5 Concentration ($\mu g/m^3$)								Percentage PM2.5 Concentration Change from Base-case							
	100%	50%	25%	0%	-25%	-50%	-100%		100%	50%	25%	0%	-25%	-50%	-100%
NH3	11	11	11	11	11	11	11	NH3	0%	0%	0%	0%	0%	0%	0%
NOx	11	11	11	11	11	11	11	NOx	0%	0%	0%	0%	0%	0%	0%
NH3&NOx	11	11	11	11	11	11	11	NH3&NOx	0%	0%	0%	0%	0%	0%	0%
SO2	11	11	11	11	11	11	11	SO2	0%	0%	0%	0%	0%	0%	-1%

Appendix E1: CMAQ Aerosol Sensitivity results for Enumclaw, WA.

Enumclaw: July 15 1996 4am (PST) All units in µg/m3

	ASO4	ANH4	ANO3	AORGA	AORGPA	AORGB	AEC	A25	AH2O	INORG2.5	ORG_2.5	mass_PM2.5
Base-Case	1.98	1.58	2.87	2.24	2.16	8.97	1.03	1.11	5.55	6.44	13.36	28.05
0.0aNH3	2.03	0.13	0.01	2.29	2.21	9.16	1.06	1.14	3.57	2.17	13.65	22.16
0.5aNH3	2.04	0.89	0.42	2.30	2.22	9.23	1.06	1.14	3.19	3.35	13.75	23.07
0.75aNH3	2.02	1.18	1.44	2.28	2.20	9.13	1.05	1.13	4.17	4.63	13.60	25.16
1.25aNH3	1.94	1.96	4.24	2.19	2.11	8.78	1.01	1.08	6.85	8.14	13.07	30.73
1.5aNH3	1.90	2.28	5.39	2.14	2.06	8.57	0.98	1.06	7.94	9.57	12.77	32.89
2.0aNH3	1.82	2.80	7.29	2.05	1.96	8.20	0.94	1.01	9.72	11.90	12.21	36.35
0.0aNH3.0.0aNOx	1.35	0.13	0.00	1.39	2.23	7.62	1.07	1.15	2.17	1.48	11.24	17.68
0.5aNH3.0.5aNOx	1.79	0.73	0.21	2.12	2.23	8.98	1.07	1.15	2.63	2.73	13.33	21.47
0.75aNH3.0.75aNOx	1.92	1.01	1.01	2.22	2.21	9.09	1.06	1.14	3.61	3.94	13.52	23.84
1.27aNH3.1.25aNOx	1.99	2.10	4.64	2.19	2.08	8.73	1.00	1.07	7.32	8.73	13.00	31.69
1.5aNH3.1.5aNOx	1.97	2.54	6.20	2.11	1.99	8.42	0.95	1.02	8.84	10.70	12.52	34.61
2.0aNH3.2.0aNOx	1.86	3.34	9.07	1.91	1.83	7.81	0.88	0.94	11.55	14.26	11.55	39.76
0.0aNOx	1.35	0.52	0.04	1.39	2.24	7.64	1.07	1.15	1.87	1.91	11.27	17.84
0.5aNOx	1.78	0.94	0.93	2.11	2.22	8.92	1.06	1.14	3.33	3.64	13.25	22.99
0.75aNOx	1.90	1.31	2.04	2.20	2.18	8.98	1.05	1.12	4.61	5.25	13.37	25.97
1.25aNOx	2.04	1.71	3.26	2.25	2.13	8.95	1.02	1.10	6.01	7.02	13.34	29.06
1.5aNOx	2.09	1.79	3.45	2.24	2.12	8.94	1.02	1.09	6.27	7.32	13.30	29.57
2.0aNOx	2.12	1.85	3.63	2.18	2.10	8.93	1.01	1.08	6.49	7.60	13.21	29.96
0.0aSO2	1.02	1.57	4.08	2.26	2.16	9.00	1.04	1.11	5.45	6.67	13.42	28.26
0.5aSO2	1.50	1.58	3.49	2.25	2.16	8.99	1.04	1.11	5.51	6.57	13.41	28.21
0.75aSO2	1.74	1.58	3.19	2.24	2.16	8.98	1.03	1.11	5.53	6.51	13.38	28.14
1.25aSO2	2.23	1.58	2.54	2.23	2.15	8.95	1.03	1.11	5.55	6.34	13.33	27.93
1.5aSO2	2.46	1.59	2.27	2.22	2.15	8.93	1.03	1.10	5.60	6.32	13.30	27.93
2.0aSO2	2.93	1.64	1.86	2.20	2.14	8.89	1.02	1.10	5.82	6.42	13.23	28.16
0.0aVOC	2.15	1.60	2.73	0.48	2.12	8.75	1.02	1.09	5.63	6.47	11.35	26.14
0.5aVOC	2.09	1.60	2.81	1.34	2.14	8.88	1.02	1.10	5.64	6.51	12.36	27.21
0.75aVOC	2.04	1.59	2.84	1.79	2.15	8.93	1.03	1.10	5.60	6.48	12.87	27.65
1.25aVOC	1.93	1.57	2.89	2.66	2.16	9.00	1.04	1.11	5.50	6.39	13.82	28.43
1.5aVOC	1.88	1.55	2.90	3.07	2.17	9.03	1.04	1.11	5.44	6.33	14.27	28.77
2.0aVOC	1.79	1.51	2.89	3.85	2.18	9.08	1.04	1.12	5.30	6.19	15.11	29.33
0.0aVOC.0.0aNOx	1.52	0.58	0.03	0.45	2.23	7.78	1.07	1.15	2.08	2.12	10.45	17.44
1.5aVOC.1.5aNOx	1.92	1.02	1.05	1.31	2.20	8.86	1.06	1.13	3.64	3.99	12.37	22.76
0.75aVOC.0.75aNOx	1.96	1.34	2.06	1.78	2.18	8.94	1.04	1.12	4.72	5.37	12.90	25.72
1.25aVOC.1.25aNOx	2.00	1.71	3.30	2.69	2.14	8.99	1.03	1.10	5.99	7.00	13.83	29.52
1.5aVOC.1.5aNOx	2.00	1.78	3.54	3.15	2.13	9.02	1.02	1.10	6.24	7.33	14.30	30.56
2.0aVOC.2.0aNOx	2.01	1.86	3.79	4.06	2.13	9.07	1.02	1.09	6.51	7.66	15.25	32.11
0.0bVOC	1.87	1.57	2.98	2.04	1.89	0.80	0.90	0.97	5.50	6.42	4.72	19.09
1.5bVOC	1.97	1.61	2.98	2.18	2.06	4.84	0.99	1.06	5.64	6.56	9.08	23.89
0.75bVOC	1.98	1.60	2.94	2.22	2.11	6.90	1.01	1.09	5.61	6.52	11.23	26.03
1.25bVOC	1.98	1.55	2.78	2.24	2.18	11.02	1.05	1.12	5.44	6.30	15.45	29.93
1.5bVOC	1.96	1.51	2.67	2.24	2.20	13.06	1.06	1.13	5.32	6.15	17.50	31.73
2.0bVOC	1.92	1.43	2.43	2.21	2.23	17.05	1.07	1.15	5.02	5.78	21.50	35.09

Appendix E2: CMAQ Aerosol Sensitivity results for Carus, OR.

Carus: Jul 14 1pm (PST)

All units in µg/m3

	ASO4	ANH4	ANO3	AORGA	AORGPA	AORGB	AEC	A25	AH2O	INORG2.5	ORG_2.5	mass_PM2.5
Base-Case	4.23	1.56	0.01	4.54	2.89	3.24	2.06	1.79	1.89	5.80	10.67	28.23
0.0aNH3	4.11	0.25	0.03	4.41	2.80	3.15	1.99	1.74	3.90	4.39	10.36	27.40
0.5aNH3	4.24	0.95	0.07	4.55	2.89	3.25	2.06	1.79	1.59	5.26	10.69	27.42
0.75aNH3	4.24	1.28	0.03	4.55	2.89	3.24	2.06	1.79	1.67	5.55	10.69	27.78
1.25aNH3	4.23	1.57	0.03	4.54	2.89	3.24	2.06	1.79	1.90	5.83	10.67	28.26
1.5aNH3	4.23	1.57	0.06	4.54	2.89	3.24	2.06	1.79	1.90	5.86	10.67	28.30
2.0aNH3	4.23	1.59	0.11	4.54	2.89	3.24	2.05	1.79	1.92	5.93	10.66	28.38
0.0aNH3.0.0aNOx	2.79	0.25	0.02	1.86	2.83	3.07	2.01	1.75	2.34	3.05	7.76	22.94
0.5aNH3.0.5aNOx	4.10	0.95	0.05	4.32	2.89	3.23	2.06	1.79	1.54	5.10	10.45	26.96
0.75aNH3.0.75aNOx	4.29	1.28	0.03	4.56	2.89	3.24	2.06	1.79	1.68	5.60	10.70	27.85
1.27aNH3.1.25aNOx	4.01	1.49	0.04	4.30	2.89	3.23	2.06	1.79	1.80	5.54	10.41	27.62
1.5aNH3.1.5aNOx	3.78	1.42	0.08	3.97	2.89	3.22	2.06	1.79	1.71	5.28	10.08	26.94
2.0aNH3.2.0aNOx	3.45	1.32	0.15	3.39	2.88	3.19	2.05	1.79	1.59	4.93	9.47	25.85
0.0aNOx	2.84	1.06	0.00	1.89	2.88	3.13	2.05	1.78	1.28	3.90	7.90	22.93
0.5aNOx	4.09	1.51	0.01	4.31	2.89	3.23	2.06	1.79	1.83	5.60	10.42	27.72
0.75aNOx	4.29	1.58	0.01	4.55	2.89	3.24	2.06	1.79	1.91	5.87	10.68	28.32
1.25aNOx	4.01	1.48	0.01	4.30	2.89	3.23	2.06	1.79	1.79	5.50	10.42	27.58
1.5aNOx	3.78	1.40	0.02	3.97	2.89	3.22	2.06	1.79	1.70	5.21	10.08	26.85
2.0aNOx	3.46	1.29	0.03	3.40	2.89	3.20	2.06	1.79	1.56	4.77	9.48	25.68
0.0aSO2	1.87	0.71	0.03	4.56	2.90	3.25	2.07	1.80	0.86	2.61	10.72	24.07
0.5aSO2	3.07	1.14	0.03	4.56	2.90	3.25	2.06	1.79	1.38	4.24	10.70	26.19
0.75aSO2	3.66	1.35	0.02	4.55	2.89	3.24	2.06	1.79	1.64	5.03	10.68	27.22
1.25aSO2	4.81	1.61	0.02	4.54	2.89	3.24	2.06	1.79	2.02	6.44	10.67	28.98
1.5aSO2	5.38	1.62	0.03	4.54	2.89	3.24	2.06	1.79	2.11	7.02	10.66	29.66
2.0aSO2	6.48	1.62	0.04	4.53	2.88	3.24	2.05	1.79	2.42	8.15	10.65	31.08
0.0aVOC	3.66	1.36	0.02	0.57	2.86	3.17	2.04	1.77	1.64	5.03	6.59	23.10
0.5aVOC	4.00	1.48	0.01	2.41	2.88	3.21	2.05	1.78	1.79	5.49	8.50	25.64
0.75aVOC	4.14	1.53	0.01	3.48	2.88	3.23	2.05	1.79	1.85	5.68	9.59	26.98
1.25aVOC	4.27	1.57	0.01	5.56	2.89	3.25	2.06	1.79	1.90	5.85	11.70	29.32
1.5aVOC	4.26	1.57	0.01	6.53	2.89	3.25	2.06	1.79	1.90	5.83	12.67	30.28
2.0aVOC	4.17	1.54	0.01	8.28	2.90	3.25	2.07	1.80	1.86	5.72	14.43	31.89
0.0aVOC.0.0aNOx	3.04	1.13	0.00	0.55	2.86	3.13	2.04	1.78	1.37	4.18	6.54	21.92
1.5aVOC.1.5aNOx	4.29	1.58	0.00	2.55	2.87	3.22	2.05	1.78	1.92	5.88	8.65	26.29
0.75aVOC.0.75aNOx	4.32	1.59	0.00	3.59	2.88	3.23	2.05	1.79	1.93	5.91	9.70	27.39
1.25aVOC.1.25aNOx	4.12	1.52	0.01	5.40	2.89	3.24	2.06	1.79	1.84	5.65	11.54	28.89
1.5aVOC.1.5aNOx	4.00	1.48	0.02	6.18	2.90	3.24	2.06	1.80	1.79	5.50	12.32	29.48
2.0aVOC.2.0aNOx	3.83	1.42	0.03	7.59	2.90	3.25	2.07	1.80	1.72	5.27	13.73	30.60
0.0bVOC	4.04	1.49	0.01	4.35	2.88	1.24	2.05	1.78	1.81	5.54	8.47	25.67
1.5bVOC	4.16	1.53	0.01	4.47	2.88	2.23	2.05	1.79	1.86	5.70	9.59	27.01
0.75bVOC	4.20	1.55	0.01	4.51	2.89	2.74	2.06	1.79	1.87	5.76	10.13	27.63
1.25bVOC	4.26	1.57	0.01	4.56	2.89	3.75	2.06	1.79	1.90	5.83	11.20	28.80
1.5bVOC	4.27	1.57	0.01	4.58	2.89	4.25	2.06	1.79	1.91	5.85	11.72	29.34
2.0bVOC	4.28	1.58	0.01	4.59	2.89	5.26	2.06	1.79	1.91	5.86	12.74	30.39

Appendix E3: CMAQ Aerosol Sensitivity results for Columbia River, WA.

Carus: Jul 14 9pm (PST)

All units in µg/m3

	ASO4	ANH4	ANO3	AORGA	AORGPA	AORGB	AEC	A25	AH2O	INORG2.5	ORG_2.5	mass_PM2.5
Base-Case	5.20	0.82	0.02	1.34	1.10	4.78	0.43	1.40	4.83	6.04	7.22	24.14
0.0aNH3	4.61	0.18	0.03	1.19	0.97	4.24	0.38	1.24	6.87	4.82	6.40	23.92
0.5aNH3	4.95	0.51	0.00	1.27	1.04	4.55	0.41	1.34	5.96	5.46	6.86	24.23
0.75aNH3	5.08	0.66	0.02	1.31	1.07	4.67	0.42	1.37	5.43	5.76	7.04	24.25
1.25aNH3	5.32	0.99	0.02	1.37	1.12	4.88	0.44	1.43	4.14	6.32	7.37	23.92
1.5aNH3	5.31	1.13	0.02	1.37	1.12	4.88	0.44	1.43	4.20	6.45	7.37	24.11
2.0aNH3	5.28	1.41	0.02	1.36	1.11	4.85	0.44	1.42	4.48	6.71	7.32	24.58
0.0aNH3.0.0aNOx	2.30	0.20	0.00	0.95	1.09	4.24	0.43	1.40	2.93	2.50	6.29	17.76
0.5aNH3.0.5aNOx	4.28	0.53	0.03	1.26	1.08	4.58	0.42	1.38	4.73	4.83	6.91	22.50
0.75aNH3.0.75aNOx	4.82	0.67	0.02	1.30	1.08	4.67	0.43	1.39	4.95	5.51	7.06	23.55
1.27aNH3.1.25aNOx	5.46	0.98	0.02	1.37	1.11	4.90	0.44	1.43	4.43	6.46	7.38	24.36
1.5aNH3.1.5aNOx	5.56	1.13	0.02	1.39	1.12	4.94	0.44	1.43	4.35	6.71	7.45	24.59
2.0aNH3.2.0aNOx	5.47	1.40	0.05	1.39	1.11	4.94	0.44	1.43	4.58	6.92	7.45	25.02
0.0aNOx	2.36	0.81	0.01	0.98	1.13	4.36	0.44	1.45	2.26	3.18	6.47	18.02
0.5aNOx	4.47	0.85	0.02	1.32	1.13	4.79	0.44	1.45	3.43	5.34	7.23	22.11
0.75aNOx	4.94	0.83	0.02	1.33	1.11	4.78	0.44	1.42	4.30	5.79	7.23	23.38
1.25aNOx	5.34	0.82	0.02	1.34	1.09	4.79	0.43	1.40	5.11	6.18	7.22	24.54
1.5aNOx	5.40	0.81	0.02	1.35	1.09	4.80	0.43	1.39	5.24	6.24	7.23	24.74
2.0aNOx	5.36	0.81	0.02	1.36	1.09	4.84	0.43	1.40	5.15	6.19	7.29	24.67
0.0aSO2	1.60	0.60	0.00	1.41	1.15	5.04	0.45	1.48	1.62	2.21	7.60	17.57
0.5aSO2	3.50	0.84	0.02	1.39	1.14	4.97	0.45	1.46	2.87	4.35	7.50	20.84
0.75aSO2	4.43	0.85	0.02	1.38	1.13	4.94	0.45	1.45	3.41	5.29	7.45	22.26
1.25aSO2	5.89	0.80	0.02	1.29	1.06	4.61	0.42	1.35	6.18	6.71	6.96	25.83
1.5aSO2	6.53	0.77	0.02	1.25	1.02	4.45	0.40	1.31	7.39	7.31	6.72	27.34
2.0aSO2	7.68	0.73	0.00	1.17	0.95	4.17	0.38	1.22	9.53	8.41	6.29	30.03
0.0aVOC	5.37	0.80	0.02	0.55	1.07	4.61	0.42	1.37	5.26	6.19	6.23	23.67
0.5aVOC	5.33	0.81	0.02	0.94	1.08	4.69	0.42	1.38	5.13	6.16	6.72	24.02
0.75aVOC	5.27	0.82	0.02	1.14	1.09	4.74	0.43	1.39	4.99	6.11	6.96	24.10
1.25aVOC	5.12	0.83	0.02	1.54	1.10	4.82	0.43	1.41	4.66	5.97	7.47	24.16
1.5aVOC	5.04	0.83	0.02	1.74	1.11	4.86	0.44	1.42	4.48	5.90	7.71	24.16
2.0aVOC	4.87	0.85	0.02	2.14	1.13	4.92	0.44	1.44	4.11	5.73	8.19	24.12
0.0aVOC.0.0aNOx	2.59	0.81	0.01	0.55	1.12	4.37	0.44	1.44	2.37	3.42	6.04	17.92
1.5aVOC.1.5aNOx	4.73	0.83	0.02	0.94	1.11	4.71	0.44	1.42	3.93	5.58	6.77	22.34
0.75aVOC.0.75aNOx	5.03	0.82	0.02	1.14	1.10	4.74	0.43	1.41	4.52	5.88	6.98	23.43
1.25aVOC.1.25aNOx	5.29	0.82	0.02	1.55	1.10	4.82	0.43	1.40	4.99	6.13	7.47	24.64
1.5aVOC.1.5aNOx	5.34	0.82	0.02	1.76	1.10	4.87	0.43	1.41	5.07	6.18	7.73	25.03
2.0aVOC.2.0aNOx	5.38	0.83	0.02	2.19	1.11	4.95	0.44	1.42	5.11	6.23	8.24	25.65
0.0bVOC	5.19	0.73	0.02	1.28	0.99	0.80	0.39	1.27	5.30	5.94	3.06	20.17
1.5bVOC	5.27	0.78	0.02	1.31	1.05	2.74	0.41	1.35	5.15	6.07	5.10	22.29
0.75bVOC	5.25	0.80	0.02	1.33	1.08	3.75	0.42	1.38	5.01	6.07	6.15	23.25
1.25bVOC	5.13	0.84	0.02	1.35	1.11	5.82	0.44	1.43	4.63	5.99	8.28	24.98
1.5bVOC	5.05	0.85	0.02	1.35	1.13	6.87	0.44	1.44	4.41	5.91	9.35	25.78
2.0bVOC	4.84	0.86	0.02	1.35	1.15	8.96	0.45	1.47	3.95	5.73	11.46	27.27

Appendix E4: CMAQ Aerosol Sensitivity results for Craters of the Moon, ID.

Craters of the Moon: Jul 14 5pm (PST)

All units in µg/m3

	ASO4	ANH4	ANO3	AORGA	AORGPA	AORGB	AEC	A25	AH2O	INORG2.5	ORG_2.5	mass_PM2.5
Base-Case	1.80	0.25	0.03	0.76	0.06	1.32	0.13	0.09	0.73	2.08	2.15	11.00
0.0aNH3	1.78	0.22	0.03	0.76	0.06	1.31	0.13	0.09	0.80	2.04	2.13	11.00
0.5aNH3	1.79	0.24	0.03	0.76	0.06	1.32	0.13	0.09	0.77	2.06	2.14	11.00
0.75aNH3	1.80	0.24	0.03	0.76	0.06	1.32	0.13	0.09	0.75	2.07	2.14	11.00
1.25aNH3	1.80	0.25	0.03	0.77	0.06	1.32	0.13	0.09	0.72	2.09	2.15	11.00
1.5aNH3	1.81	0.26	0.03	0.77	0.06	1.33	0.13	0.09	0.70	2.10	2.16	11.00
2.0aNH3	1.81	0.26	0.03	0.77	0.06	1.33	0.13	0.09	0.68	2.11	2.16	10.99
0.0aNH3.0.0aNOx	1.77	0.22	0.03	0.75	0.06	1.31	0.13	0.09	0.79	2.03	2.12	10.98
0.5aNH3.0.5aNOx	1.79	0.24	0.03	0.76	0.06	1.32	0.13	0.09	0.76	2.05	2.14	10.99
0.75aNH3.0.75aNOx	1.79	0.24	0.03	0.76	0.06	1.32	0.13	0.09	0.75	2.07	2.14	10.99
1.27aNH3.1.25aNOx	1.81	0.25	0.03	0.77	0.06	1.33	0.13	0.09	0.72	2.09	2.15	11.00
1.5aNH3.1.5aNOx	1.81	0.26	0.03	0.77	0.06	1.33	0.13	0.09	0.71	2.10	2.16	11.01
2.0aNH3.2.0aNOx	1.82	0.26	0.03	0.77	0.06	1.33	0.13	0.09	0.68	2.12	2.17	11.02
0.0aNOx	1.79	0.25	0.03	0.76	0.06	1.32	0.13	0.09	0.72	2.07	2.14	10.97
0.5aNOx	1.79	0.25	0.03	0.76	0.06	1.32	0.13	0.09	0.73	2.07	2.14	10.99
0.75aNOx	1.80	0.25	0.03	0.76	0.06	1.32	0.13	0.09	0.73	2.08	2.15	10.99
1.25aNOx	1.80	0.25	0.03	0.76	0.06	1.32	0.13	0.09	0.74	2.08	2.15	11.01
1.5aNOx	1.81	0.25	0.03	0.77	0.06	1.32	0.13	0.09	0.74	2.08	2.15	11.01
2.0aNOx	1.81	0.25	0.03	0.77	0.06	1.32	0.13	0.09	0.74	2.09	2.15	11.02
0.0aSO2	1.77	0.25	0.03	0.77	0.06	1.33	0.13	0.09	0.70	2.05	2.15	10.94
0.5aSO2	1.78	0.25	0.03	0.76	0.06	1.32	0.13	0.09	0.72	2.06	2.15	10.97
0.75aSO2	1.79	0.25	0.03	0.76	0.06	1.32	0.13	0.09	0.73	2.07	2.15	10.99
1.25aSO2	1.81	0.25	0.03	0.76	0.06	1.32	0.13	0.09	0.74	2.09	2.15	11.01
1.5aSO2	1.81	0.25	0.03	0.76	0.06	1.32	0.13	0.09	0.75	2.09	2.15	11.03
2.0aSO2	1.83	0.25	0.03	0.76	0.06	1.32	0.13	0.09	0.76	2.11	2.14	11.05
0.0aVOC	1.80	0.25	0.03	0.74	0.06	1.32	0.13	0.09	0.73	2.08	2.12	10.97
0.5aVOC	1.80	0.25	0.03	0.75	0.06	1.32	0.13	0.09	0.73	2.08	2.14	10.99
0.75aVOC	1.80	0.25	0.03	0.76	0.06	1.32	0.13	0.09	0.73	2.08	2.14	10.99
1.25aVOC	1.80	0.25	0.03	0.77	0.06	1.32	0.13	0.09	0.73	2.08	2.15	11.00
1.5aVOC	1.80	0.25	0.03	0.78	0.06	1.32	0.13	0.09	0.73	2.08	2.16	11.01
2.0aVOC	1.80	0.25	0.03	0.79	0.06	1.32	0.13	0.09	0.73	2.08	2.17	11.02
0.0aVOC.0.0aNOx	1.79	0.25	0.03	0.74	0.06	1.32	0.13	0.09	0.72	2.07	2.12	10.95
1.5aVOC.1.5aNOx	1.80	0.25	0.03	0.75	0.06	1.32	0.13	0.09	0.73	2.07	2.13	10.97
0.75aVOC.0.75aNOx	1.80	0.25	0.03	0.76	0.06	1.32	0.13	0.09	0.73	2.08	2.14	10.99
1.25aVOC.1.25aNOx	1.80	0.25	0.03	0.77	0.06	1.32	0.13	0.09	0.74	2.08	2.16	11.01
1.5aVOC.1.5aNOx	1.81	0.25	0.03	0.78	0.06	1.32	0.13	0.09	0.74	2.08	2.16	11.02
2.0aVOC.2.0aNOx	1.81	0.25	0.03	0.79	0.06	1.33	0.13	0.09	0.74	2.09	2.18	11.05
0.0bVOC	1.80	0.24	0.03	0.63	0.06	0.93	0.13	0.09	0.75	2.07	1.62	10.47
1.5bVOC	1.80	0.24	0.03	0.70	0.06	1.12	0.13	0.09	0.74	2.07	1.88	10.73
0.75bVOC	1.80	0.24	0.03	0.73	0.06	1.22	0.13	0.09	0.74	2.08	2.01	10.86
1.25bVOC	1.80	0.25	0.03	0.80	0.06	1.42	0.13	0.09	0.73	2.08	2.28	11.13
1.5bVOC	1.80	0.25	0.03	0.83	0.06	1.52	0.13	0.09	0.73	2.08	2.42	11.27
2.0bVOC	1.81	0.25	0.03	0.89	0.06	1.73	0.13	0.10	0.73	2.09	2.69	11.54

Appendix F1-4: PM2.5 concentrations and PM2.5 percentage changes from the Base-case due to changes in organic precursor emissions (anthropogenic VOC (aVOC), anthropogenic VOC&NOx and biogenic VOC (bVOC)) for Enumclaw, Carus, Columbia River and Craters of the Moon.

F1. Enumclaw, WA															
PM2.5 Concentration (μg/m^3)								Percentage PM2.5 Concentration Change from Base-case							
	100%	50%	25%	0%	-25%	-50%	-100%		100%	50%	25%	0%	-25%	-50%	-100%
aVOC	29	29	28	28	28	27	26	VOC	5%	3%	1%	0%	-1%	-3%	-7%
VOC&NOx	32	31	30	28	26	23	17	VOC&NOx	14%	9%	5%	0%	-8%	-19%	-38%
bVOC	35	32	30	28	26	24	19	bVOC	25%	13%	7%	0%	-7%	-15%	-32%

F2. Carus, OR															
PM2.5 Concentration (μg/m^3)								Percentage PM2.5 Concentration Change from Base-case							
	100%	50%	25%	0%	-25%	-50%	-100%		100%	50%	25%	0%	-25%	-50%	-100%
aVOC	32	30	29	28	27	26	23	aVOC	13%	7%	4%	0%	-4%	-9%	-18%
VOC&NOx	31	29	29	28	27	26	22	VOC&NOx	8%	4%	2%	0%	-3%	-7%	-22%
bVOC	30	29	29	28	28	27	26	bVOC	8%	4%	2%	0%	-2%	-4%	-9%

F3. Columbia River, WA															
PM2.5 Concentration (μg/m^3)								Percentage PM2.5 Concentration Change from Base-case							
	100%	50%	25%	0%	-25%	-50%	-100%		100%	50%	25%	0%	-25%	-50%	-100%
aVOC	24	24	24	24	24	24	24	aVOC	0%	0%	0%	0%	0%	0%	-2%
VOC&NOx	26	25	25	24	23	22	18	VOC&NOx	6%	4%	2%	0%	-3%	-7%	-26%
bVOC	27	26	25	24	23	22	20	bVOC	13%	7%	3%	0%	-4%	-8%	-16%

F4. Craters of the Moon, ID															
PM2.5 Concentration (μg/m^3)								Percentage PM2.5 Concentration Change from Base-case							
	100%	50%	25%	0%	-25%	-50%	-100%		100%	50%	25%	0%	-25%	-50%	-100%
aVOC	11	11	11	11	11	11	11	aVOC	0%	0%	0%	0%	0%	0%	0%
VOC&NOx	11	11	11	11	11	11	11	VOC&NOx	0%	0%	0%	0%	0%	0%	0%
bVOC	12	11	11	11	11	11	10	bVOC	5%	2%	1%	0%	-1%	-2%	-5%

Appendix G1-2: Ozone concentrations and percentage ozone changes from the Base-case due to changes in ozone precursor emissions (anthropogenic VOC and anthropogenic NOx) for Enumclaw, Carus, Columbia River and Craters of the Moon.

G1. Anthropogenic VOC (aVOC) Emission Sensitivity															
Ozone Concentration (ppbv)								Percentage Ozone Change from the Base-case							
	100%	50%	25%	0%	-25%	-50%	-100%		100%	50%	25%	0%	-25%	-50%	-100%
Enumclaw	165	160	156	149	139	123	75	Enumclaw	10%	8%	5%	0%	-7%	-17%	-50%
Carus	198	194	190	184	177	168	124	Carus	8%	5%	3%	0%	-4%	-9%	-33%
Tricities	121	119	118	115	111	107	92	Tricities	6%	4%	2%	0%	-3%	-7%	-20%
Boise	94	93	93	93	92	92	91	Boise	1%	1%	0%	0%	0%	-1%	-2%
Spokane	87	87	86	86	86	86	85	Spokane	1%	0%	0%	0%	0%	0%	-1%
Craters of the Moon	70	70	70	70	70	70	70	Craters of the Moon	0%	0%	0%	0%	0%	0%	0%

G2. Anthropogenic NOx (aNOx) Emission Sensitivity															
Ozone Concentration (ppbv)								Percentage Ozone Change from the Base-case							
	100%	50%	25%	0%	-25%	-50%	-100%		100%	50%	25%	0%	-25%	-50%	-100%
Enumclaw	99	136	147	149	141	124	53	Enumclaw	-34%	-9%	-1%	0%	-5%	-17%	-64%
Carus	158	193	193	184	172	149	60	Carus	-14%	5%	4%	0%	-7%	-19%	-67%
Tricities	120	122	120	115	107	96	50	Tricities	4%	6%	4%	0%	-7%	-17%	-57%
Boise	105	100	97	93	88	82	61	Boise	13%	8%	5%	0%	-5%	-12%	-34%
Spokane	101	95	91	86	81	74	57	Spokane	18%	10%	6%	0%	-7%	-14%	-34%
Craters of the Moon	74	72	71	70	69	67	64	Craters of the Moon	6%	3%	2%	0%	-2%	-4%	-8%

Appendix G3-4: Ozone concentrations and percentage ozone changes from the Base-case due to changes in ozone precursor emissions (anthropogenic NOx and VOC and biogenic VOC) for Enumclaw, Carus, Columbia River and Craters of the Moon.

G3. Anthropogenic NOx and VOC (aVOC&aNOX) Emission Sensitivity															
Ozone Concentration (ppbv)								Percentage Ozone Change from the Base-case							
	100%	50%	25%	0%	-25%	-50%	-100%		100%	50%	25%	0%	-25%	-50%	-100%
Enumclaw	181	168	160	149	137	120	56	Enumclaw	21%	13%	7%	0%	-8%	-19%	-62%
Carus	240	214	199	184	168	146	52	Carus	30%	16%	8%	0%	-9%	-21%	-72%
Tricities	145	131	124	115	105	93	53	Tricities	26%	14%	8%	0%	-9%	-19%	-54%
Boise	108	102	97	93	87	81	62	Boise	17%	10%	5%	0%	-6%	-12%	-34%
Spokane	104	96	91	86	80	74	57	Spokane	20%	11%	6%	0%	-7%	-14%	-34%
Craters of the Moon	74	72	71	70	69	67	64	Craters of the Moon	6%	3%	2%	0%	-2%	-4%	-8%

G4. Biogenic VOC (bVOC) Emission Sensitivity															
Ozone Concentration (ppbv)								Percentage Ozone Change from the Base-case							
	100%	50%	25%	0%	-25%	-50%	-100%		100%	50%	25%	0%	-25%	-50%	-100%
Enumclaw	154	152	150	149	148	147	143	Enumclaw	3%	2%	1%	0%	-1%	-2%	-4%
Carus	194	190	187	184	181	178	172	Carus	5%	3%	2%	0%	-2%	-3%	-7%
Tricities	118	117	116	115	114	113	109	Tricities	2%	1%	1%	0%	-1%	-2%	-5%
Boise	95	94	94	93	91	89	83	Boise	3%	2%	1%	0%	-1%	-4%	-10%
Spokane	87	87	87	86	86	85	81	Spokane	1%	1%	0%	0%	-1%	-1%	-6%
Craters of the Moon	71	70	70	70	69	69	69	Craters of the Moon	2%	0%	0%	0%	-1%	-1%	-1%

Appendix H: Maximum 1-hour predicted ozone concentrations by emissions scenarios with maximum 1-hour observed ozone concentration for the three-day simulation period. The %Change indicates the percent maximum predicted ozone change from the base-case simulation for different emission scenarios. Ozone concentration unit is ppbv.

	Enumclaw, WA			Beacon Hill, WA			Carus, OR			Milwaukie High School, OR		
	Max Obs	Max Pred.	%Change	Max Obs	Max Pred.	%Change	Max Obs	Max Pred.	%Change	Max Obs	Max Pred.	%Change
Base-case	118	149	0%	105	144	0%	124	125	0%	145	147	0%
0.5aNOx	118	126	-16%	105	124	-14%	124	102	-18%	145	130	-11%
0.75aNOx	118	142	-5%	105	139	-4%	124	116	-7%	145	145	-1%
1.25aNOx	118	147	-1%	105	139	-4%	124	131	4%	145	135	-8%
1.5aNOx	118	136	-9%	105	130	-10%	124	132	5%	145	128	-13%
2.0aNOx	118	115	-23%	105	113	-21%	124	121	-3%	145	115	-22%
0.5aVOC	118	123	-17%	105	117	-19%	124	117	-7%	145	118	-20%
0.75aVOC	118	139	-7%	105	133	-8%	124	122	-3%	145	130	-12%
1.25aVOC	118	156	5%	105	152	5%	124	128	2%	145	157	7%
1.5aVOC	118	161	8%	105	158	9%	124	130	4%	145	164	11%
2.0aVOC	118	166	11%	105	164	14%	124	133	6%	145	173	17%
0.5aVOC.0.5aNOx	118	121	-19%	105	118	-18%	124	100	-20%	145	124	-16%
0.75aVOC.0.75aNO	118	137	-8%	105	133	-8%	124	114	-9%	145	138	-6%
1.25aVOC.1.25aNO	118	160	7%	105	153	6%	124	135	8%	145	149	1%
1.5aVOC.1.5aNOx	118	168	13%	105	159	10%	124	144	15%	145	152	3%
2.0aVOC.2.0aNOx	118	181	21%	105	170	18%	124	158	26%	145	158	7%
0.5bVOC	118	147	-2%	105	142	-2%	124	121	-4%	145	137	-7%
0.75bVOC	118	148	-1%	105	143	-1%	124	123	-2%	145	143	-3%
1.25bVOC	118	150	1%	105	146	1%	124	127	1%	145	151	3%
1.5bVOC	118	152	2%	105	147	2%	124	128	3%	145	155	5%
2.0bVOC	118	154	3%	105	149	3%	124	131	4%	145	161	9%

Appendix I: 24-hour averaged predicted PM2.5 concentrations by emissions scenarios with 24-hour averaged observed PM2.5 concentrations for July 13, 1996. The %Change indicates the percent predicted PM2.5 change from the base-case simulation for different emission scenarios. PM2.5 concentration unit is ng/m^3.

	PUSO, WA			MORA, WA			CORI, OR			GLAC, MT		
	Avg Obs	Avg Pred.	%Change	Avg Obs	Avg Pred.	%Change	Avg Obs	Avg Pred.	%Change	Avg Obs	Avg Pred.	%Change
Base-case	9495	17880	0%	13398	16670	0%	8696	15330	0%	7596	8385	0%
0.5aNH3	9495	17750	-1%	13398	16540	-1%	8696	15300	0%	7596	8383	0%
1.5aNH3	9495	17940	0%	13398	16710	0%	8696	15350	0%	7596	8392	0%
2.0aNH3	9495	18000	1%	13398	16740	0%	8696	15370	0%	7596	8395	0%
0.5aNH3.0.5aNOx	9495	17780	-1%	13398	16340	-2%	8696	15190	-1%	7596	8348	0%
1.5aNH3.1.5aNOx	9495	17840	0%	13398	16600	0%	8696	15410	1%	7596	8422	0%
2.0aNH3.2.0aNOx	9495	17800	0%	13398	16420	-1%	8696	15460	1%	7596	8452	1%
0.5aSO2	9495	17350	-3%	13398	16230	-3%	8696	15250	-1%	7596	8384	0%
1.5aSO2	9495	18400	3%	13398	17070	2%	8696	15400	0%	7596	8388	0%
2.0aSO2	9495	18900	6%	13398	17430	5%	8696	15480	1%	7596	8388	0%
0.5aVOC	9495	17520	-2%	13398	16280	-2%	8696	15270	0%	7596	8381	0%
1.5aVOC	9495	18230	2%	13398	16990	2%	8696	15380	0%	7596	8387	0%
2.0aVOC	9495	18570	4%	13398	17250	3%	8696	15420	1%	7596	8394	0%
0.5aNOx	9495	17880	0%	13398	16430	-1%	8696	15220	-1%	7596	8348	0%
1.5aNOx	9495	17780	-1%	13398	16560	-1%	8696	15390	0%	7596	8416	0%
2.0aNOx	9495	17660	-1%	13398	16320	-2%	8696	15420	1%	7596	8442	1%
0.5aVOC.0.5aNOx	9495	17570	-2%	13398	16210	-3%	8696	15180	-1%	7596	8346	0%
1.5aVOC.1.5aNOx	9495	18150	2%	13398	17010	2%	8696	15440	1%	7596	8421	0%
2.0aVOC.2.0aNOx	9495	18410	3%	13398	17290	4%	8696	15550	1%	7596	8452	1%
0.5bVOC	9495	17610	-2%	13398	16250	-3%	8696	14390	-6%	7596	7852	-6%
1.5bVOC	9495	18150	2%	13398	17080	2%	8696	16220	6%	7596	8902	6%
2.0bVOC	9495	18420	3%	13398	17470	5%	8696	17100	12%	7596	9409	12%